

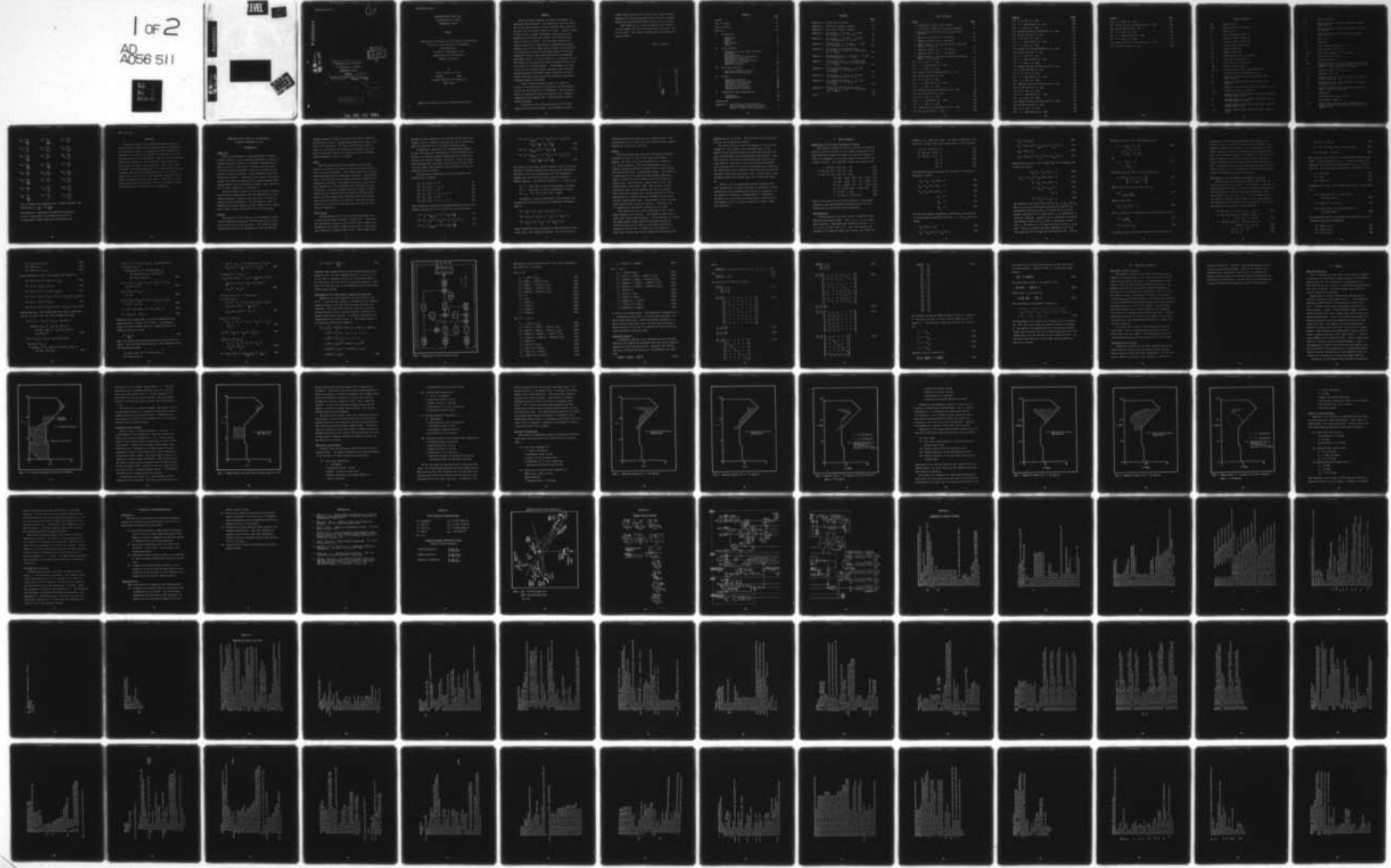
AD-A056 511 AIR FORCE INST OF TECH WRIGHT-PATTERSON AFB OHIO SCH--ETC F/G 1/3
INVESTIGATION OF THE YF-16 IN HIGH ANGLE OF ATTACK ASYMMETRIC F--ETC(U)
MAR 78 E B HOUSE

UNCLASSIFIED

AFIT/GAE/AA/78M-6

NL

1 OF 2
AD
A056 511



AFIT/GAE/AA/78M-6

ADA 056511

AD No. 1
DDC FILE COPY

INVESTIGATION OF THE YF-16
IN HIGH ANGLE OF ATTACK
ASYMMETRIC FLIGHT

THESIS

AFIT/GAE/AA/78M-6 Eric B. House, II
Captain USAF

Masters Thesis

Mar 78

165 p.

This document has been approved
for public release and sale; its
distribution is unlimited.

012 225
78 07 07 006 act

INVESTIGATION OF THE YF-16
IN HIGH ANGLE OF ATTACK
ASYMMETRIC FLIGHT

THESIS

Presented to the Faculty of the School of Engineering
of the Air Force Institute of Technology
Air University
in Partial Fulfillment of the
Requirements for the Degree of
Master of Science

by
Eric B. House II, B.A.E.
Captain USAF
Graduate Aeronautical Engineering
March 1978

Approved for public release; distribution unlimited.

Preface

With the current emphasis of fighter development on sustained high performance, the chances for aircraft losses due to the pilot entering a flight condition from which the aircraft will not recover become very great. Ideally, design of the aircraft includes aerodynamic characteristics or augmentation which make the aircraft free from the possibility of loss of control. For the newer generation of fighters which have a high degree of augmentation already actively part of the flight control system, the possibility of a departure controller being added offers a relatively inexpensive means of improving both aircraft performance and flight safety. It was my intention to determine for the YF-16 where in the alpha-beta control boundary loss of control might be a serious problem. I then hoped to be able to put the uncontrolled motions resulting from pitch and yaw perturbations into small enough categories so that a simple controller could prevent the motions by monitoring a minimum number of variables.

I wish to thank my thesis advisor, Dr. Robert A. Calico, of the Department of Aeronautics and Astronautics of the Air Force Institute of Technology. He was instrumental in helping me tackle this project with a degree of organization and insight that I could not have attained without guidance.

I also would like to thank Tom Chord and the other members of the Aircraft Group, Control Dynamics Branch,

Flight Control Division of the Air Force Flight Dynamics Laboratory who helped me become familiar with the computer simulation program which formed the basis of this study.

Most importantly, I wish to thank my wife, Marilyn, for her support and devotion during this very hectic time in our lives. This thesis is dedicated to her and to our new son, Ryan.

Eric B. House II

ACCESS	SEARCH
N IS	SEARCHED
THIS	SEARCHED
INDEXED	INDEXED
SERIALIZED	SERIALIZED
JULY 1985	
U.S. GOVERNMENT PRINTING OFFICE: 1985 500-100-012	
SPECIAL	
A	

<u>Contents</u>	<u>Page</u>
Preface	ii
List of Figures	vi
List of Symbols	ix
Abstract	xii
I. Introduction	1
Background	1
Purpose	1
Model	2
Data Package	2
Method	5
II. Linear Analysis	7
Development of the Linear Equations of Motion	7
Trim Equations	7
Development of the Unaugmented Perturbation Equations	11
Development of the Longitudinal Augmentation Equations	16
Stability Analysis	19
III. Non-Linear Analysis	24
Non-Linear Computer Program	24
Perturbed Motion Analysis	24
IV. Results	26
Alpha-Beta Envelope	26
Perturbed Motion Analysis	28
Pitch Rate Perturbations	30
Yaw Rate Perturbations	32
Control Surface Analysis	40
Yaw Departure Controller	41
V. Conclusions and Recommendations	42
Conclusions	42
Recommendations	42
Bibliography	44
Appendix A: YF-16 Physical Characteristics, Control Surfaces Deflection Limits, Control Surfaces Sign Convention	45

Contents

	<u>Page</u>
Appendix B: Flight Control System	47
Appendix C: Eigenvalue Computer Program	50
Appendix D: Non-Linear Computer Program	57
Appendix E: Erect Spin, $\alpha = 21$ deg, $\beta = 10$ deg, $q = 20$ deg/sec at $t = 15$ sec	89
Appendix F: Erect Spin, $\alpha = 21$ deg, $\beta = 10$ deg, $r = -20$ deg/sec at $t = 15$ sec	95
Appendix G: Inverted Spin, $\alpha = 23$ deg, $\beta = 13$ deg, $q = 30$ deg/sec at $t = 20$ sec	101
Appendix H: Erect Spin to an Inverted Spin, $\alpha = 19$ deg, $\beta = 4$ deg, $r = -30$ deg/sec at $t = 15$ sec	107
Appendix I: Rolling Departure, $\alpha = 19$ deg, $\beta = 9$ deg, $q = 20$ deg/sec at $t = 15$ sec	113
Appendix J: Rolling Departure to an Inverted Spin, $\alpha = 17$ deg, $\beta = 9$ deg, $q = 20$ deg/sec at $t = 15$ sec	119
Appendix K: No Uncontrolled Motion, $\alpha = 21$ deg, $\beta = 10$ deg, $q = 30$ deg/sec at $t = 15$ sec	125
Appendix L: Erect Spin, $\alpha = 25$ deg, $\beta = 6$ deg, $r = -20$ deg/sec at $t = 15$ sec	131
Appendix M: No Uncontrolled Motion, $\alpha = 25$ deg, $\beta = 6$ deg, $r = -30$ deg/sec at $t = 15$ sec	137
Appendix N: Effects of Departure Controller, $\alpha = 19$ deg, $\beta = 4$ deg, $r = -30$ deg/sec at $t = 15$ sec	143
Vita	149

List of Figures

<u>Figure</u>	<u>Page</u>
1 Longitudinal Flight Control System	17
2 α - β Control Boundary and Stability Boundary	27
3 Regions where the Non-Linear Program could not trim	29
4 Departure Region for $q = 20$ deg/sec	33
5 Departure Region for $q = 30$ deg/sec	34
6 Regions where $q = 20$ deg/sec had more influence than $q = 30$ deg/sec	35
7 Departure Region for $r = -20$ deg/sec	37
8 Departure Region for $r = -30$ deg/sec	38
9 Region where $r = -20$ deg/sec had more influence than $r = -30$ deg/sec	39
E-1 p , q , and r vs. time	90
E-2 α , β , and Velocity vs. time	91
E-3 θ , ϕ , and ψ vs. time	92
E-4 Control Forces and Deflections vs. time	93
E-5 N_z and Altitude vs. time	94
F-1 p , q , and r vs. time	96
F-2 α , β , and Velocity vs. time	97
F-3 θ , ϕ , and ψ vs. time	98
F-4 Control Forces and Deflections vs. time	99
F-5 N_z and Altitude vs. time	100
G-1 p , q , and r vs. time	102
G-2 α , β , and Velocity vs. time	103
G-3 θ , ϕ , and ψ vs. time	104
G-4 Control Forces and Deflections vs. time	105
G-5 N_z and Altitude vs. time	106

<u>Figure</u>	<u>Page</u>
H-1 p, q, and r vs. time	108
H-2 α , β , and Velocity vs. time	109
H-3 θ , ϕ , and ψ vs. time	110
H-4 Control Forces and Deflections vs. time	111
H-5 N_z and Altitude vs. time	112
I-1 p, q, and r vs. time	114
I-2 α , β , and Velocity vs. time	115
I-3 θ , ϕ , and ψ vs. time	116
I-4 Control Forces and Deflections vs. time	117
I-5 N_z and Altitude vs. time	118
J-1 p, q, and r vs. time	120
J-2 α , β , and Velocity vs. time	121
J-3 θ , ϕ , and ψ vs. time	122
J-4 Control Forces and Deflections vs. time	123
J-5 N_z and Altitude vs. time	124
K-1 p, q, and r vs. time	126
K-2 α , β , and Velocity vs. time	127
K-3 θ , ϕ , and ψ vs. time	128
K-4 Control Forces and Deflections vs. time	129
K-5 N_z and Altitude vs. time	130
L-1 p, q, and r vs. time	132
L-2 α , β , and Velocity vs. time	133
L-3 θ , ϕ , and ψ vs. time	134
L-4 Control Forces and Deflections vs. time	135
L-5 N_z and Altitude vs. time	136
M-1 p, q, and r vs. time	138
M-2 α , β , and Velocity vs. time	139

<u>Figure</u>	<u>Page</u>
M-3 θ , ϕ , and ψ vs. time	140
M-4 Control Forces and Deflections vs. time	141
M-5 N_z and Altitude vs. time	142
N-1 p , q , and r vs. time	144
N-2 α , β , and Velocity vs. time	145
N-3 θ , ϕ , and ψ vs. time	146
N-4 Control Forces and Deflections vs. time	147
N-5 N_z and Altitude vs. time	148

List of Symbols

AR	aspect ratio
ARI	aileron-rudder interconnect
b	wing span, ft
\bar{c}	mean aerodynamic chord, ft
c_1	rolling moment coefficient
c_m	pitching moment coefficient
c_n	yawing moment coefficient
c_T	thrust coefficient
c_W	weight coefficient
c_x	longitudinal force coefficient
c_y	side force coefficient
c_z	vertical force coefficient
FCS	flight control system
F_3, F_4	variable gains in the longitudinal FCS
g	acceleration due to gravity, ft/sec^2
I_x	moment of inertia about longitudinal body axis, $\text{slug}\cdot\text{ft}^2$
I_y	moment of inertia about lateral body axis, $\text{slug}\cdot\text{ft}^2$
I_z	moment of inertia about normal body axis, $\text{slug}\cdot\text{ft}^2$
I_{zx}	product of inertia, $\text{slug}\cdot\text{ft}^2$
L	rolling moment acting about x body axis; positive rolling right, ft-lb
M	pitching moment acting about y body axis; positive pitching up, ft-lb
N	yawing moment acting about z body axis; positive yawing right, ft-lb
N_z	normal acceleration; positive in the $-z$ direction

m	mass of aircraft
p	roll rate about x body axis; positive rolling right, deg/sec
q	pitch rate about y body axis; positive pitching up, deg/sec
r	yaw rate about z body axis; positive yawing right, deg/sec
S	wing area, ft^2
T	thrust, lb
T_2	time to double amplitude, sec
t^*	time constant, $\bar{c}/2V_e$, sec
u, v, w	body axis components of V , ft/sec
V	true airspeed, ft/sec
W	aircraft weight, lb
x, y, z	orthogonal body axis system, positive x -axis out nose of aircraft, positive y -axis out right wing, positive z -axis out bottom of aircraft
α	body axis angle of attack, deg
β	sideslip angle, deg
δ_a	aileron deflection, positive when right aileron is deflected down, deg
δ_r	rudder deflection, positive when trailing edge is deflected left, deg
δ_s	stabilator deflection, positive when trailing edge is deflected down, deg
λ	eigenvalue
μ	non-dimensional mass, $2m/\rho_e \bar{c}S$
ρ	air density, slugs/ ft^3
ψ, θ, ϕ	Euler transformation angles representing yaw, pitch, and roll respectively in proper rotation sequence, deg

$$C_{1_p} = \frac{\partial C_1}{\frac{\partial pb}{2V}}$$

$$C_{1_r} = \frac{\partial C_1}{\frac{\partial rb}{2V}}$$

$$C_{1_\alpha} = \frac{\partial C_1}{\partial \alpha}$$

$$C_{1_\beta} = \frac{\partial C_1}{\partial \beta}$$

$$C_{1_{\delta_a}} = \frac{\partial C_1}{\partial \delta_a}$$

$$C_{1_{\delta_r}} = \frac{\partial C_1}{\partial \delta_r}$$

$$C_{m_q} = \frac{\partial C_m}{\frac{\partial qc}{2V}}$$

$$C_{m_\alpha} = \frac{\partial C_m}{\partial \alpha}$$

$$C_{m_{\delta_s}} = \frac{\partial C_m}{\partial \delta_s}$$

$$C_{n_p} = \frac{\partial C_n}{\frac{\partial pb}{2V}}$$

$$C_{n_r} = \frac{\partial C_n}{\frac{\partial rb}{2V}}$$

$$C_{n_\alpha} = \frac{\partial C_n}{\partial \alpha}$$

$$C_{n_\beta} = \frac{\partial C_n}{\partial \beta}$$

$$C_{n_{\delta_a}} = \frac{\partial C_n}{\partial \delta_a}$$

$$C_{n_{\delta_r}} = \frac{\partial C_n}{\partial \delta_r}$$

$$C_{x_q} = \frac{\partial C_x}{\frac{\partial qc}{2V}}$$

$$C_{x_\alpha} = \frac{\partial C_x}{\partial \alpha}$$

$$C_{x_{\delta_s}} = \frac{\partial C_x}{\partial \delta_s}$$

$$C_{y_\beta} = \frac{\partial C_y}{\partial \beta}$$

$$C_{y_{\delta_a}} = \frac{\partial C_y}{\partial \delta_a}$$

$$C_{y_{\delta_r}} = \frac{\partial C_y}{\partial \delta_r}$$

$$C_{z_q} = \frac{\partial C_z}{\frac{\partial qc}{2V}}$$

$$C_{z_\alpha} = \frac{\partial C_z}{\partial \alpha}$$

$$C_{z_{\delta_s}} = \frac{\partial C_z}{\partial \delta_s}$$

Dots or numbers in parentheses over a symbol represent time

derivatives ($\dot{q} = \frac{dq}{dt}$, $\overset{(5)}{q} = \frac{d^5q}{dt^5}$).

The subscript e represents an equilibrium value (V_e).

A hat (^) represents a non-dimensional value (\hat{V}).

A Δ represents a small change from equilibrium ($\Delta\alpha$).

Abstract

A study was made of the theoretical departure modes of the YF-16 due to pitch and yaw perturbations from asymmetrical rectilinear flight. An alpha-beta control boundary was developed, and within that boundary perturbations of 20 deg/sec and 30 deg/sec were introduced. The areas of uncontrolled motions were mapped out and the motions were categorized. Three types of motions were identified: erect spins, inverted spins, and rolling departures. For yaw perturbations only, a simple controller was modelled which had as its inputs alpha, beta, and yaw rate. The controller prevented the aircraft from departing controlled flight. Time traces of the various departure modes and the effects of including a departure controller are presented in the appendices.

INVESTIGATION OF THE YF-16 IN HIGH ANGLE
OF ATTACK ASYMMETRIC FLIGHT

I. Introduction

Background

With the development of a new generation of fighter aircraft capable of ever increasing performance, there is a renewed interest in efforts to eliminate susceptibility to loss of control or spin entry. Attempts have been made to provide design guidelines so that new aircraft will be far more departure-resistant. These guidelines have their limitations, however. Invariably a new fighter, once operational, will have some portion of its flight envelope where through flight tests or analytical studies, spin susceptibility is either experienced or predicted.

The new fighters, because of the high degree of flight control system augmentation, have the possibility of relatively inexpensive modifications being done to correct or enhance overall performance. The task must be, then, to identify potentially dangerous flight regimes and to analyze how a flight control system (FCS) can be used to help.

Purpose

The purpose of this study was to investigate the theoretical departure potential of the YF-16 due to the influence of pitch and yaw perturbations. The resulting uncontrolled motion was to be categorized as much as possible.

Trimmed asymmetric flight was used as the initial condition. The portions of the α - β envelope where departures might occur were to be identified. If results showed regions where a small set of variables were departure producing, then a departure controller which was a function of those variables could be modelled as part of the FCS.

Model

The YF-16 was selected as the model for this study because it represents the newest concept in fighter design, that of static instability. This feature makes the aircraft both highly maneuverable and highly augmented. During flight tests, the YF-16 had certain flight conditions identified as potentially hazardous. Two departures and one actual spin were encountered. The aerodynamic data available was also of interest, as General Dynamics had done studies to incorporate the data obtained from the spin and the departures into a new data package with simplified functional dependencies from the previous data package. The physical characteristics of the YF-16 that were used for this study are listed in Appendix A.

Data Package

The aerodynamic data for the YF-16 was obtained from a study done by General Dynamics in April 1977. This data was used because extensive work had been done to update all aerodynamic coefficients based on the results of the flight test evaluation at Edwards AFB in 1975. This revised data

package not only modelled actual aircraft flight tests more closely, but was expanded to provide data up to ± 120 degrees angle of attack and up to ± 40 degrees sideslip angle.

A significant advantage of the expanded data package is that the functional dependencies of the aerodynamic coefficients are reduced, thereby simplifying the calculations necessary for digital computer simulation. Also, the equations developed for the linear theory portion of this study are more compact than would have been possible with the existing YF-16 data package.

The functional dependencies of the aerodynamic coefficients are as follows:

$$(1) \quad C_x = C_x(\alpha, \delta_s, q) \quad (1)$$

$$(2) \quad C_y = C_y(\alpha, \beta, \delta_a, \delta_r) \quad (2)$$

$$(3) \quad C_z = C_z(\alpha, \delta_s, q) \quad (3)$$

$$(4) \quad C_l = C_l(\alpha, \beta, \delta_a, \delta_r, p, r) \quad (4)$$

$$(5) \quad C_m = C_m(\alpha, \delta_s, q) \quad (5)$$

$$(6) \quad C_n = C_n(\alpha, \beta, \delta_a, \delta_r, p, r) \quad (6)$$

The coefficients obtained from General Dynamics and the independent variables for the coefficients are listed below:

$$(1) \quad C_x = C_{x_{\text{basic}}}(\alpha, \delta_s) + C_{x_q}(\alpha) \frac{qc}{2V} \quad (7)$$

$$(2) \quad C_y = C_{y_\beta}(\alpha) + C_{y_{\delta_a}}(\alpha) \delta_a + C_{y_{\delta_r}}(\alpha) \delta_r \quad (8)$$

$$(3) \quad C_z = C_{z_{\text{basic}}}(\alpha, \delta_s) + C_{z_q}(\alpha) \frac{qc}{2V} \quad (9)$$

$$(4) \quad C_1 = C_{1_{\text{basic}}}(\alpha, \beta) + C_{1_{\delta_a}}(\alpha) \delta_a + C_{1_{\delta_r}}(\alpha) \delta_r \\ + C_{1_p}(\alpha) \frac{pb}{2V} + C_{1_r}(\alpha) \frac{rb}{2V} \quad (10)$$

$$(5) \quad C_m = C_{m_{\text{basic}}}(\alpha, \delta_s) + C_{m_q}(\alpha) \frac{qc}{2V} \quad (11)$$

$$(6) \quad C_n = C_{n_{\text{basic}}}(\alpha, \beta) + C_{n_{\delta_a}}(\alpha) \delta_a + C_{n_{\delta_r}}(\alpha) \delta_r \\ + C_{n_p}(\alpha) \frac{pb}{2V} + C_{n_r}(\alpha) \frac{rb}{2V} \quad (12)$$

The effects of all other control surfaces, such as the automatically scheduled leading edge flaps and the differential horizontal tail, were incorporated into the aerodynamic coefficients for the three primary control surfaces by General Dynamics. The range of values for α , β , and δ_s are:

- (1) α : from -120° to $+120^\circ$ in 5° increments; 49 values
- (2) β : from -40° to $+40^\circ$ in 5° increments; 9 values
- (3) δ_s : -25° , -10° , 0° , $+10^\circ$, $+25^\circ$; 5 values

In addition to these coefficients, the following coefficients were derived using finite differences techniques (Ref 6):

- (1) $C_{x_\alpha}(\alpha, \delta_s)$, $C_{z_\alpha}(\alpha, \delta_s)$, $C_{m_\alpha}(\alpha, \delta_s)$
- (2) $C_{1_\alpha}(\alpha, \beta)$, $C_{1_\beta}(\alpha, \beta)$, $C_{n_\alpha}(\alpha, \beta)$, $C_{n_\beta}(\alpha, \beta)$
- (3) $C_{x_{\delta_s}}(\alpha, \delta_s)$, $C_{z_{\delta_s}}(\alpha, \delta_s)$, $C_{m_{\delta_s}}(\alpha, \delta_s)$

These coefficients were necessary for the perturbation equations used in the eigenvalue problem. All of the data ob-

tained from General Dynamics was for stability axes. The data was converted to body axes since the non-linear computer program was written for body axes.

Method

From the flight tests the areas of potential departure problems in terms of α and β were fairly well known. However, the first step in the analysis was to define an α - β control boundary. This was accomplished by use of a computer program developed by Hawkins (Ref 4) which trimmed the aircraft for level, unaccelerated flight. The values of α ranged from 0° to 29° , which was the maximum attainable angle of attack for level flight for the YF-16 during its flight tests. The values of β ranged from 0° to 40° . The aileron-rudder interconnect (ARI), which serves to help coordinate turns, was not modelled for the trim program. This resulted in slightly more control authority for cross controlling the aircraft than was available for the actual aircraft during flight tests. The solution to the trim equations required that density be constant. Therefore, the α - β boundary was arbitrarily developed for sea level.

The second step was to test each point in the control limits boundary for stability. The linearized equations of motion were used in this analysis. It was necessary to include the longitudinal flight control system when testing for stability since the aircraft was statically unstable for practically all of the α - β region that was considered. A state space approach was used to obtain the eigenvalues and

eigenvectors of the system. The stability of all trim points from the trim program was checked.

The third step was to test the behavior of the aircraft trimmed for level flight and to determine what, if any, adverse flight conditions might be encountered when the aircraft was perturbed from an equilibrium trim position. Since this study was interested in determining what severe situations might be encountered, the sizes of the perturbations were increased until the aircraft experienced such conditions. The equilibrium flight conditions from which the aircraft was disturbed represented slow speed, level, or near level, unaccelerated flight with landing gear and trailing edge flaps up.

Finally, for the uncontrolled flight conditions that were encountered, an analysis was made to determine if these conditions could be grouped into any general categories. It was desired to determine a minimum number of independent variables that could describe regions where loss of control was imminent, and to use these variables to model a departure controller.

II. Linear Analysis

Development of the Linear Equations of Motion

The system of equations used for both the trim analysis and the stability analysis is that found in Reference 3:149. These equations assume the earth as an inertial reference frame, an atmosphere at rest with respect to the earth, and a rigid aircraft. The equations in body axes notation are:

$$X - mg \sin\theta = m(u + qw - rv) \quad (13)$$

$$Y + mg \cos\theta \sin\phi = m(v + ru - pw) \quad (14)$$

$$Z + mg \cos\theta \cos\phi = m(w + pv - qu) \quad (15)$$

$$L = I_x p - I_{zx}(r + pq) - (I_y - I_z)qr \quad (16)$$

$$M = I_y q - I_{zx}(r^2 - p^2) - (I_z - I_x)rp \quad (17)$$

$$N = I_z r - I_{zx}(p - qr) - (I_x - I_y)pq \quad (18)$$

$$\dot{\phi} = p + q \sin\phi \tan\theta + r \cos\phi \tan\theta \quad (19)$$

$$\dot{\theta} = q \cos\phi - r \sin\phi \quad (20)$$

$$\dot{\psi} = (q \sin\phi + r \cos\phi)/\cos\theta \quad (21)$$

This is the system of three force equations, three moment equations, and three kinematic equations which had to be linearized and equilibrium points determined.

Trim Equations

It was desired to have the aircraft trimmed for asymmetrical rectilinear flight. Thus, α_e , β_e , θ_e , ϕ_e , and m were constants. Equilibrium was defined such that p , q , r , u , v , w , p , q , and r were zero. Also, the aircraft was assumed to be symmetric about the xz plane, and thrust was

assumed to act along the x-axis. For these assumptions, equations (13) through (18) reduce respectively to the following:

$$T_e + X_e - mg \sin\theta_e = 0 \quad (22)$$

$$Y_e + mg \cos\theta_e \sin\phi_e = 0 \quad (23)$$

$$Z_e + mg \cos\theta_e \cos\phi_e = 0 \quad (24)$$

$$L_e = 0 \quad (25)$$

$$M_e = 0 \quad (26)$$

$$N_e = 0 \quad (27)$$

Non-dimensionalizing equations (22) through (27) according to Reference 3 yields:

$$C_{T_e} + C_{X_e} - C_{W_e} \sin\theta_e = 0 \quad (28)$$

$$C_{Y_e} + C_{W_e} \cos\theta_e \sin\phi_e = 0 \quad (29)$$

$$C_{Z_e} + C_{W_e} \cos\theta_e \cos\phi_e = 0 \quad (30)$$

$$C_{L_e} = 0 \quad (31)$$

$$C_{M_e} = 0 \quad (32)$$

$$C_{N_e} = 0 \quad (33)$$

The force and moment aerodynamic coefficients are expressed in the following functional forms for α , β , and δ_s being constants:

$$C_{X_e} = C_x(\alpha_e, \delta_s) \quad (34)$$

$$C_{Y_e} = C_{y_{\delta_a}}(\alpha_e) \delta_a + C_{y_{\delta_r}}(\alpha_e) \delta_r \quad (35)$$

$$C_{z_e} = C_z(\alpha_e, \delta_s) \quad (36)$$

$$C_{l_e} = C_l(\alpha_e, \beta_e) + C_{l_{\delta_a}}(\alpha_e) \delta_a + C_{l_{\delta_r}}(\alpha_e) \delta_r \quad (37)$$

$$C_{m_e} = C_m(\alpha_e, \delta_s) \quad (38)$$

$$C_{n_e} = C_n(\alpha_e, \beta_e) + C_{n_{\delta_a}}(\alpha_e) \delta_a + C_{n_{\delta_r}}(\alpha_e) \delta_r \quad (39)$$

Substituting equations (34) through (39) into equations (28) through (33) gives:

$$C_{T_e} + C_x - C_{w_e} \sin \theta_e = 0 \quad (40)$$

$$C_{y_{\delta_a}} \delta_a + C_{y_{\delta_r}} \delta_r + C_{w_e} \cos \theta_e \sin \phi_e = 0 \quad (41)$$

$$C_z + C_{w_e} \cos \theta_e \cos \phi_e = 0 \quad (42)$$

$$C_l + C_{l_{\delta_a}} \delta_a + C_{l_{\delta_r}} \delta_r = 0 \quad (43)$$

$$C_m = 0 \quad (44)$$

$$C_n + C_{n_{\delta_a}} \delta_a + C_{n_{\delta_r}} \delta_r = 0 \quad (45)$$

The unknowns in the above equations are δ_a , δ_r , C_{w_e} , and C_{T_e} . Since δ_s can not be explicitly expressed in terms of the aerodynamic coefficients due to it being one of the independent variables for the coefficients, δ_s is obtained by an iterative technique. Equation (44) is satisfied by scanning the tabulated values for C_m , which is listed for a given α and δ_s . The value of δ_s is found where for a given α , C_m is zero. Once δ_s is known, the other unknowns can be found from equations (40) through (43) and equation (45). Solving

equations (43) and (45) simultaneously gives:

$$\frac{\delta_r = -c_1 c_n \delta_a + c_1 \delta_r c_n}{c_1 \delta_r c_n \delta_a - c_1 \delta_a c_n \delta_r} \quad (46)$$

and

$$\frac{\delta_a = -c_n \delta_r \delta_a - c_n}{c_n \delta_a} \quad (47)$$

Dividing equations (41) by equation (42) gives:

$$\phi_e = \tan^{-1} \left(\frac{-c_y \delta_a + c_y \delta_r}{c_z} \right) \quad (48)$$

Equation (42) can now be solved for c_{w_e} :

$$c_{w_e} = \frac{-c_z}{\cos \theta_e \cos \phi_e} \quad (49)$$

Equation (40) gives:

$$c_{T_e} = c_{w_e} \sin \theta_e - c_x \quad (50)$$

Also, v_e and T_e are calculated from the following relations:

$$v_e = \frac{2W}{\rho_e S c_{w_e}} \quad (51)$$

$$T_e = \frac{1}{2} \rho_e v_e^2 S c_{T_e} \quad (52)$$

A computer program written by Hawkins and revised for the

differences in functional dependency of the data in this study was used to calculate all of the above unknowns. The iterative approach for finding δ_s was a modification for this study. The data from the trim program was then prepared for use in the eigenvalue problem. In addition to this trim program, a comparison of values obtained from the non-linear program (Appendix D) for the same equilibrium conditions was made. Agreement between the two approaches was good with the exception that due to the ARI being in the non-linear program, slight variations of δ_a and δ_r were noted.

Development of the Unaugmented Perturbation Equations

The approach to the stability analysis was to use the linearized equations of motion. As in Hawkins' study (Ref 4), small perturbation theory was used to linearize the equations. An equilibrium of asymmetric rectilinear flight was used. This requires that $p_e = q_e = r_e = 0$. It is assumed that ρ_e is constant, although slight climbs or dives are permitted. The linearization of equations (13) through (21) using small perturbation theory results in the following:

$$\Delta X - mg \cos\theta_e \Delta\theta = m(\Delta u + w_e \Delta q - v_e \Delta r) \quad (53)$$

$$\begin{aligned} \Delta Y + mg \cos\theta_e \cos\phi_e \Delta\phi - mg \sin\theta_e \sin\phi_e \Delta\theta \\ = m(\Delta v + u_e \Delta r - w_e \Delta p) \end{aligned} \quad (54)$$

$$\begin{aligned} \Delta Z - mg \cos\theta_e \sin\phi_e \Delta\phi - mg \sin\theta_e \cos\phi_e \Delta\theta \\ = m(\Delta w + v_e \Delta p - u_e \Delta q) \end{aligned} \quad (55)$$

$$\Delta L = I_x \Delta p - I_{zx} \Delta r \quad (56)$$

$$\Delta M = I_y \Delta q \quad (57)$$

$$\Delta N = I_z \Delta r - I_{zx} \Delta p \quad (58)$$

$$\Delta \phi = \Delta p + \Delta q \sin \phi_e \tan \theta_e + \Delta r \cos \phi_e \tan \theta_e \quad (59)$$

$$\Delta \theta = \Delta q \cos \phi_e - \Delta r \sin \phi_e \quad (60)$$

Eq. 13 is not used since it is uncoupled from the other equations. It was desired to use ΔV , $\Delta \alpha$, and $\Delta \beta$ as state variables for the eigenvalue problem rather than Δu , Δv , and Δw . Therefore, the following relationships are used (Ref 3:117):

$$u = V \cos \alpha \cos \beta \quad (61)$$

$$v = V \sin \beta \quad (62)$$

$$w = V \sin \alpha \cos \beta \quad (63)$$

Linearization of eqs. (61) through (63) results, respectively, in:

$$\begin{aligned} \Delta u &= \cos \alpha_e \cos \beta_e \Delta V - V_e \sin \alpha_e \cos \beta_e \Delta \alpha \\ &\quad - V_e \cos \alpha_e \sin \beta_e \Delta \beta \end{aligned} \quad (64)$$

$$\Delta v = \sin \beta_e \Delta V + V_e \cos \beta_e \Delta \beta \quad (65)$$

$$\begin{aligned} \Delta w &= \sin \alpha_e \cos \beta_e \Delta V + V_e \cos \alpha_e \cos \beta_e \Delta \alpha \\ &\quad - V_e \sin \alpha_e \sin \beta_e \Delta \beta \end{aligned} \quad (66)$$

The aerodynamic forces and moments were assumed to have the following functional dependencies:

$$\Delta X = \Delta X(V, \alpha, q, \delta_s) \quad (67)$$

$$\Delta Y = \Delta Y(\beta, \delta_a, \delta_r) \quad (68)$$

$$\Delta Z = \Delta Z(V, \alpha, q, \delta_s) \quad (69)$$

$$\Delta L = \Delta L(\alpha, \beta, p, r, \delta_a, \delta_r) \quad (70)$$

$$\Delta M = \Delta M(\alpha, q, \delta_s) \quad (71)$$

$$\Delta N = \Delta N(\alpha, \beta, p, r, \delta_a, \delta_r) \quad (72)$$

Linear expansions of eqs. (67) through (72) results in:

$$\Delta X = X_v \Delta V + X_\alpha \Delta \alpha + X_q \Delta q + X_{\delta_s} \Delta \delta_s \quad (73)$$

$$\Delta Y = Y_\beta \Delta \beta + Y_{\delta_a} \Delta \delta_a + Y_{\delta_r} \Delta \delta_r \quad (74)$$

$$\Delta Z = Z_v \Delta V + Z_\alpha \Delta \alpha + Z_q \Delta q + Z_{\delta_s} \Delta \delta_s \quad (75)$$

$$\Delta L = L_\alpha \Delta \alpha + L_\beta \Delta \beta + L_p \Delta p + L_r \Delta r + L_{\delta_a} \Delta \delta_a + L_{\delta_r} \Delta \delta_r \quad (76)$$

$$\Delta M = M_\alpha \Delta \alpha + M_q \Delta q + M_{\delta_s} \Delta \delta_s \quad (77)$$

$$\Delta N = N_\alpha \Delta \alpha + N_\beta \Delta \beta + N_p \Delta p + N_r \Delta r + N_{\delta_a} \Delta \delta_a + N_{\delta_r} \Delta \delta_r \quad (78)$$

Substituting eqs. (64) through (66) and similar expressions for Δu , Δv , and Δw into eqs. (53) through (60) gives:

$$\begin{aligned} X_v \Delta V + X_\alpha \Delta \alpha + X_q \Delta q + X_{\delta_s} \Delta \delta_s - mg \cos \theta_e \Delta \theta \\ = m(\cos \alpha_e \cos \beta_e \Delta V - v_e \sin \alpha_e \cos \beta_e \Delta \alpha \\ - v_e \cos \alpha_e \sin \beta_e \Delta \beta + v_e \sin \alpha_e \cos \beta_e \Delta q \\ - v_e \sin \beta_e \Delta r) \end{aligned} \quad (79)$$

$$\begin{aligned} Y_\beta \Delta \beta + Y_{\delta_a} \Delta \delta_a + Y_{\delta_r} \Delta \delta_r + mg \cos \theta_e \cos \phi_e \Delta \phi \\ - mg \sin \theta_e \sin \phi_e \Delta \theta \\ = m(\sin \beta_e \Delta V + v_e \cos \beta_e \Delta \beta + v_e \cos \alpha_e \cos \beta_e \Delta r \\ - v_e \sin \alpha_e \cos \beta_e \Delta p) \end{aligned} \quad (80)$$

$$\begin{aligned}
Z_v \Delta V + Z_\alpha \Delta \alpha + Z_q \Delta q + Z_{\delta_s} \Delta \delta_s - mg \cos \theta_e \sin \phi_e \Delta \phi \\
- mg \sin \theta_e \cos \phi_e \Delta \theta \\
= m(\sin \alpha_e \cos \beta_e \Delta V + v_e \cos \alpha_e \cos \beta_e \Delta \alpha \\
- v_e \sin \alpha_e \sin \beta_e \Delta \beta + v_e \sin \beta_e \Delta p \\
- v_e \cos \alpha_e \cos \beta_e \Delta q) \tag{81}
\end{aligned}$$

$$\begin{aligned}
L_\alpha \Delta \alpha + L_\beta \Delta \beta + L_p \Delta p + L_r \Delta r + L_{\delta_a} \Delta \delta_a + L_{\delta_r} \Delta \delta_r \\
= I_x \Delta p - I_{zx} \Delta r \tag{82}
\end{aligned}$$

$$\begin{aligned}
M_\alpha \Delta \alpha + M_q \Delta q + M_{\delta_s} \Delta \delta \\
= I_y \Delta q \tag{83}
\end{aligned}$$

$$\begin{aligned}
N_\alpha \Delta \alpha + N_\beta \Delta \beta + N_p \Delta p + N_r \Delta r + N_{\delta_a} \Delta \delta_a + N_{\delta_r} \Delta \delta_r \\
= I_z \Delta r - I_{zx} \Delta p \tag{84}
\end{aligned}$$

$$\Delta \phi = \Delta p + \sin \phi_e \tan \theta_e \Delta q + \cos \phi_e \tan \theta_e \Delta r \tag{85}$$

$$\Delta \theta = \cos \phi_e \Delta q - \sin \phi_e \Delta r \tag{86}$$

Equations (79) through (86) are then non-dimensionalized using Reference 2, except for $\dot{\Delta \beta}$ terms. As in Hawkins' study, to avoid confusion with the coupled equations, the following relation is used:

$$\dot{\Delta \beta} = \frac{\bar{c}}{2V_e} \dot{\Delta \beta} \tag{87}$$

Thus, all terms are non-dimensionalized in time by the same factor. The non-dimensional equations, after combining terms and rearranging become:

$$\begin{aligned}
& - 2\mu \cos \alpha_e \cos \beta_e \dot{\Delta V} + 2\mu \sin \alpha_e \cos \beta_e \dot{\Delta \alpha} \\
& + 2\mu \cos \alpha_e \sin \beta_e \dot{\Delta \beta}
\end{aligned}$$

$$\begin{aligned}
&= -2C_x \Delta \hat{V} - C_{x_\alpha} \Delta \hat{\alpha} + (2\mu \sin \alpha_e \cos \beta_e - C_{x_q} \Delta \hat{q}) \\
&\quad + C_{w_e} \cos \theta_e \Delta \hat{\theta} - \frac{2\mu}{AR} \sin \beta_e \Delta \hat{r} - C_{x_{\delta_s}} \Delta \hat{\delta}_s
\end{aligned} \tag{88}$$

$$\begin{aligned}
&- 2\mu \sin \beta_e \Delta \dot{\hat{V}} - 2\mu \cos \beta_e \Delta \dot{\hat{\beta}} \\
&= C_{w_e} \sin \theta_e \sin \phi_e \Delta \hat{\theta} - C_{y_\beta} \Delta \hat{\beta} + \frac{2\mu}{AR} \cos \alpha_e \cos \beta_e \Delta \hat{r} \\
&\quad - \frac{2\mu}{AR} \sin \alpha_e \cos \beta_e \Delta \hat{p} - C_{w_e} \cos \theta_e \cos \phi_e \Delta \hat{\phi} \\
&\quad - C_{y_{\delta_a}} \Delta \hat{\delta}_a - C_{y_{\delta_a}} \Delta \hat{\delta}_r
\end{aligned} \tag{89}$$

$$\begin{aligned}
&- 2\mu \sin \alpha_e \cos \beta_e \Delta \dot{\hat{V}} - 2\mu \cos \alpha_e \cos \beta_e \Delta \dot{\hat{\alpha}} \\
&+ 2\mu \sin \alpha_e \sin \beta_e \Delta \dot{\hat{\beta}} \\
&= -2C_z \Delta \hat{V} - C_{z_\alpha} \Delta \hat{\alpha} - (2\mu \cos \alpha_e \cos \beta_e + C_{z_q} \Delta \hat{q}) \\
&\quad + C_{w_e} \sin \theta_e \cos \phi_e \Delta \hat{\theta} + \frac{2\mu}{AR} \sin \beta_e \Delta \hat{p} \\
&\quad + C_{w_e} \cos \theta_e \sin \phi_e \Delta \hat{\phi} - C_{z_{\delta_s}} \Delta \hat{\delta}_s
\end{aligned} \tag{90}$$

$$\begin{aligned}
&AR \hat{I}_{zx} \Delta \dot{\hat{r}} - AR \hat{I}_x \Delta \dot{\hat{p}} \\
&= -C_{1_\alpha} \Delta \hat{\alpha} - C_{1_\beta} \Delta \hat{\beta} - C_{1_r} \Delta \hat{r} - C_{1_p} \Delta \hat{p} - C_{1_{\delta_a}} \Delta \hat{\delta}_a \\
&\quad - C_{1_{\delta_r}} \Delta \hat{\delta}_r
\end{aligned} \tag{91}$$

$$-\hat{I}_y \Delta \dot{\hat{q}} = -C_{m_\alpha} \Delta \hat{\alpha} - C_{m_q} \Delta \hat{q} - C_{m_{\delta_s}} \Delta \hat{\delta}_s \tag{92}$$

$$\begin{aligned}
&- AR \hat{I}_z \Delta \dot{\hat{r}} + AR \hat{I}_{zx} \Delta \dot{\hat{p}} \\
&= -C_{n_\alpha} \Delta \hat{\alpha} - C_{n_\beta} \Delta \hat{\beta} - C_{n_r} \Delta \hat{r} - C_{n_p} \Delta \hat{p} \\
&\quad - C_{n_{\delta_a}} \Delta \hat{\delta}_a - C_{n_{\delta_r}} \Delta \hat{\delta}_r
\end{aligned} \tag{93}$$

$$\Delta \dot{\hat{\phi}} = \sin \phi_e \tan \theta_e \Delta \hat{q} + \frac{\cos \phi_e \tan \theta_e}{AR} \Delta \hat{r} + \frac{1}{AR} \Delta \hat{p} \tag{94}$$

$$\dot{\Delta\theta} = \cos\phi_e \Delta\hat{q} - \frac{\sin\phi_e}{AR} \Delta\hat{r} \quad (95)$$

Equations (88) through (95) are eight non-dimensional linear equations with the eight unknowns being $\Delta\hat{V}$, $\Delta\hat{\alpha}$, $\Delta\hat{q}$, $\Delta\hat{\theta}$, $\Delta\hat{\beta}$, $\Delta\hat{r}$, $\Delta\hat{p}$, and $\Delta\hat{\phi}$. Analysis of this set of equations alone is not sufficient since the YF-16 is statically unstable. Therefore, the equations have to be supplemented with the aircraft flight control system.

Development of the Longitudinal Augmentation Equations

Appendix B is the diagram for the entire FCS for the YF-16. It was desired, however, to include for the stability analysis purposes only that portion of the FCS which was essential. The longitudinal FCS was required to give the aircraft positive static stability and was, therefore, included in the linear analysis. A simplified diagram of the longitudinal FCS is shown in Fig. 1. The system reduces to the following differential equation:

$$\begin{aligned}
 & \frac{(6)}{\delta_s} + 61 \frac{(5)}{\delta_s} + 1385 \frac{(4)}{\delta_s} + 14075 \frac{(3)}{\delta_s} + 57750 \frac{(2)}{\delta_s} + 45000 \frac{(1)}{\delta_s} \\
 & = b_1 \frac{(5)}{\alpha} + b_2 \frac{(4)}{\alpha} + b_3 \frac{(3)}{\alpha} + b_4 \frac{(2)}{\alpha} + b_5 \frac{(1)}{\alpha} + b_6 \alpha \\
 & + c_1 \frac{(5)}{q} + c_2 \frac{(4)}{q} + c_3 \frac{(3)}{q} + c_4 \frac{(2)}{q} + c_5 \frac{(1)}{q} \\
 & + (1125 F_3 V_e/g) \frac{(5)}{\theta} + (23625 F_3 V_e/g) \frac{(4)}{\theta} \\
 & + (163125 F_3 V_e/g) \frac{(3)}{\theta} + (421875 F_3 V_e/g) \frac{(2)}{\theta} \\
 & + (281250 F_3 V_e/g) \frac{(1)}{\theta} \quad (96)
 \end{aligned}$$

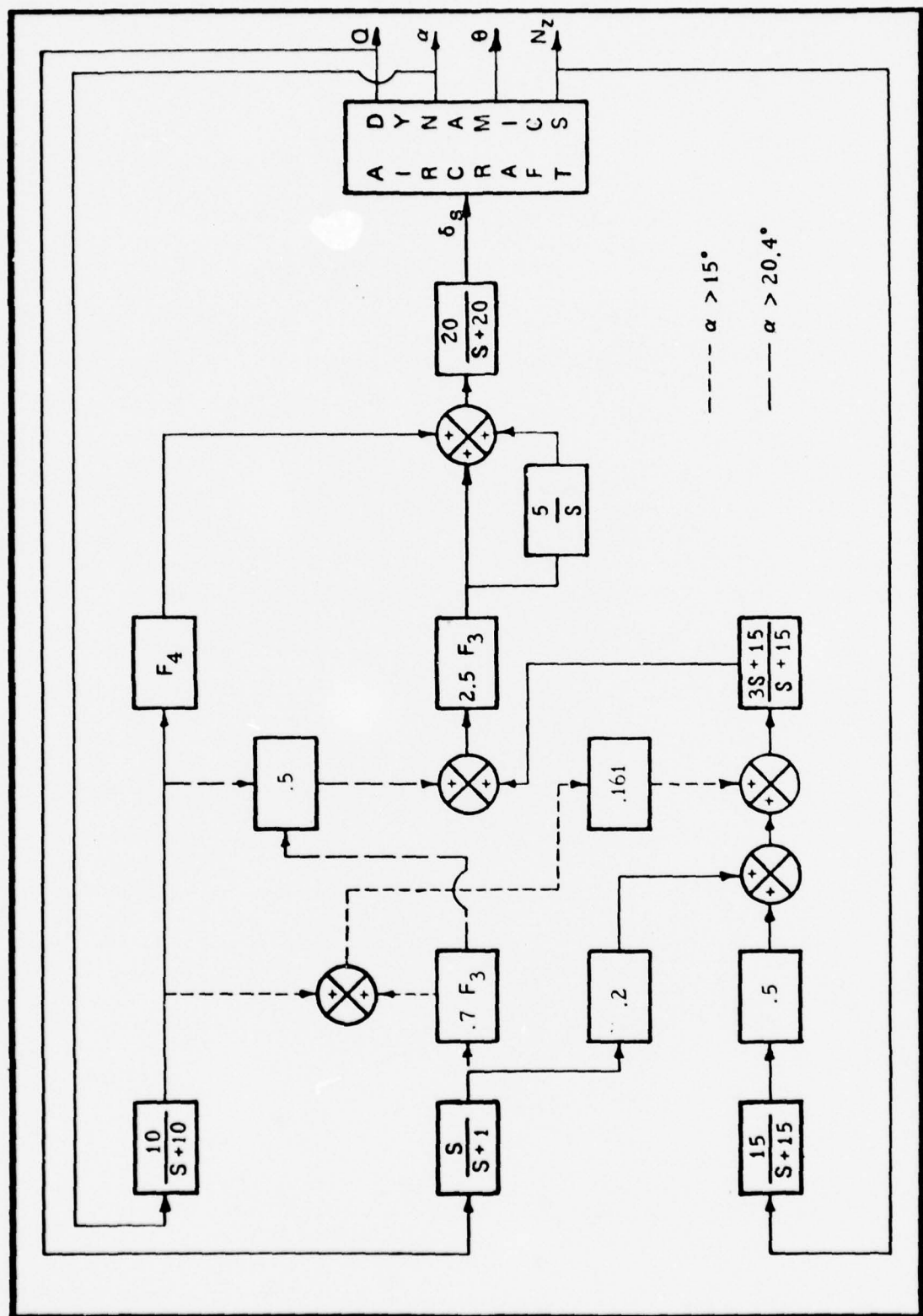


Fig. 1 Longitudinal Flight Control System

The values of the coefficients for α and q vary according to the values of α as follows:

For $\alpha \leq 15^\circ$:

$$b_1 = -1125 F V_e/g \quad (97)$$

$$b_2 = 200 F_4 - 23625 F_3 V_e/g \quad (98)$$

$$b_3 = 6200 F_4 - 163125 F_3 V_e/g \quad (99)$$

$$b_4 = 51000 F_4 - 421875 F_3 V_e/g \quad (100)$$

$$b_5 = 45000 F_4 - 281250 F_3 V_e/g \quad (101)$$

$$b_6 = 0 \quad (102)$$

$$c_1 = 30 F_3 \quad (103)$$

$$c_2 = 1050 F_3 \quad (104)$$

$$c_3 = 12750 F_3 \quad (105)$$

$$c_4 = 63750 F_3 \quad (106)$$

$$c_5 = 112500 F_3 \quad (107)$$

For $15^\circ < \alpha \leq 20.4^\circ$:

$$b_1 = -1125 F_3 V_e/g \quad (108)$$

$$b_2 = 241.5 F_3 + 200 F_4 - 23625 F_3 V_e/g \quad (109)$$

$$b_3 = 6279 F_3 + 6200 F_4 - 163125 F_3 V_e/g \quad (110)$$

$$b_4 = 48300 F_3 + 51000 F_4 - 421875 F_3 V_e/g \quad (111)$$

$$b_5 = 132825 F_3 + 45000 F_4 - 281250 F_3 V_e/g \quad (112)$$

$$b_6 = 9056.5 F_3 \quad (113)$$

$$c_1 = 16.9 F_3^2 + 30 F_3 \quad (114)$$

$$c_2 = 591.5 F_3^2 + 1050 F_3 \quad (115)$$

$$c_3 = 7182.5 F_3^2 + 12750 F_3 \quad (116)$$

$$c_4 = 35912.5 F_3^2 + 63750 F_3 \quad (117)$$

$$c_5 = 63375 F_3^2 + 112500 F_3 \quad (118)$$

For $\alpha > 20.4^\circ$:

$$b_1 = -1125 F_3 V_e/g \quad (119)$$

$$b_2 = 491.5 F_3 + 200 F_4 - 23625 F_3 V_e/g \quad (120)$$

$$b_3 = 15279 F_3 + 6200 F_4 - 163125 F_3 V_e/g \quad (121)$$

$$b_4 = 150800 F_3 + 51000 F_4 - 421875 F_3 V_e/g \quad (122)$$

$$b_5 = 507825 F_3 + 45000 F_4 - 281250 F_3 V_e/g \quad (123)$$

$$b_6 = 371812.5 F_3 \quad (124)$$

$$c_1 = 34.4 F_3^2 + 30 F_3 \quad (125)$$

$$c_2 = 1379 F_3^2 + 1050 F_3 \quad (126)$$

$$c_3 = 19869.5 F_3^2 + 12750 F_3 \quad (127)$$

$$c_4 = 121225 F_3^2 + 63750 F_3 \quad (128)$$

$$c_5 = 260250 F_3^2 + 112500 F_3 \quad (129)$$

F_3 and F_4 are variable gains. (See Appendix B and Appendix C.)

Using Ogata (Ref 5:675) this differential equation was put in state space form. Since the forcing functions (α , q , and θ) involve derivative terms, the form that guarantees a unique solution is the last six equations of the set of equations described by equation (130).

Stability Analysis

A stability analysis of the equilibrium points obtained from the trim program was performed using the linear equations coupled with the longitudinal FCS. Equations (88) through (95) were reordered and written in the following state space form:

$$[A][\dot{\bar{X}}] = [B][\bar{X}] + [C][\bar{U}] \quad (130)$$

where

$$[\bar{X}^T] = [\Delta \hat{V} \quad \Delta \hat{\alpha} \quad \Delta \hat{q} \quad \Delta \hat{\theta} \quad \Delta \hat{\beta} \quad \Delta \hat{r} \quad \Delta \hat{p} \quad \Delta \hat{\phi} \quad \Delta \hat{\delta}_1 \quad \Delta \hat{\delta}_2 \quad \Delta \hat{\delta}_3 \quad \Delta \hat{\delta}_4 \quad \Delta \hat{\delta}_5 \quad \Delta \hat{\delta}_6]$$

and (131)

$$[\bar{U}^T] = [\Delta \hat{\delta}_a \quad \Delta \hat{\delta}_r]$$

(132)

The matrices are defined as follows:

$$[A] = \left[\begin{array}{c|cc} A_{11} & A_{12} \\ \hline A_{21} & A_{22} \end{array} \right]$$

(133)

$$[A_{11}] = \left[\begin{array}{ccccccc} a_{11} & a_{12} & 0 & 0 & a_{15} & 0 & 0 & 0 \\ a_{21} & a_{22} & 0 & 0 & a_{25} & 0 & 0 & 0 \\ 0 & 0 & a_{33} & 0 & 0 & 0 & 0 & 0 \\ 0 & 0 & 0 & a_{44} & 0 & 0 & 0 & 0 \\ a_{51} & 0 & 0 & 0 & a_{55} & 0 & 0 & 0 \\ 0 & 0 & 0 & 0 & 0 & a_{66} & a_{67} & 0 \\ 0 & 0 & 0 & 0 & 0 & a_{76} & a_{77} & 0 \\ 0 & 0 & 0 & 0 & 0 & 0 & 0 & a_{88} \end{array} \right]$$

(134)

$$[A_{12}] = [0]$$

(135)

$$[A_{21}] = [0]$$

(136)

$$[A_{22}] = \left[\begin{array}{cccccc} a_{99} & 0 & 0 & 0 & 0 & 0 \\ 0 & a_{1010} & 0 & 0 & 0 & 0 \\ 0 & 0 & a_{1111} & 0 & 0 & 0 \\ 0 & 0 & 0 & a_{1212} & 0 & 0 \\ 0 & 0 & 0 & 0 & a_{1313} & 0 \\ 0 & 0 & 0 & 0 & 0 & a_{1414} \end{array} \right]$$

(137)

$$[B] = \begin{bmatrix} B_{11} & B_{12} \\ B_{21} & B_{22} \end{bmatrix} \quad (138)$$

$$[B_{11}] = \begin{bmatrix} b_{11} & b_{12} & b_{13} & b_{14} & b_{15} & b_{16} & 0 & 0 \\ b_{21} & b_{22} & b_{23} & b_{24} & b_{25} & 0 & b_{27} & b_{28} \\ 0 & b_{32} & b_{33} & 0 & b_{35} & 0 & 0 & 0 \\ 0 & 0 & b_{43} & 0 & 0 & b_{46} & 0 & 0 \\ b_{51} & b_{52} & 0 & b_{54} & b_{55} & b_{56} & b_{57} & b_{58} \\ 0 & b_{62} & 0 & 0 & b_{65} & b_{66} & b_{67} & 0 \\ 0 & b_{72} & 0 & 0 & b_{75} & b_{76} & b_{77} & 0 \\ 0 & 0 & b_{83} & 0 & 0 & b_{86} & b_{87} & 0 \end{bmatrix} \quad (139)$$

$$[B_{12}] = [0] \quad (140)$$

$$[B_{21}] = \begin{bmatrix} 0 & b_{92} & b_{93} & b_{94} & 0 & 0 & 0 & 0 \\ 0 & b_{102} & b_{103} & b_{104} & 0 & 0 & 0 & 0 \\ 0 & b_{112} & b_{113} & b_{114} & 0 & 0 & 0 & 0 \\ 0 & b_{122} & b_{123} & b_{124} & 0 & 0 & 0 & 0 \\ 0 & b_{132} & b_{133} & b_{134} & 0 & 0 & 0 & 0 \\ 0 & b_{142} & b_{143} & b_{144} & 0 & 0 & 0 & 0 \end{bmatrix} \quad (141)$$

$$[B_{22}] = \begin{bmatrix} 0 & b_{910} & 0 & 0 & 0 & 0 \\ 0 & 0 & b_{1011} & 0 & 0 & 0 \\ 0 & 0 & 0 & b_{1112} & 0 & 0 \\ 0 & 0 & 0 & 0 & b_{1213} & 0 \\ 0 & 0 & 0 & 0 & 0 & b_{1314} \\ 0 & b_{1410} & b_{1411} & b_{1412} & b_{1413} & b_{1414} \end{bmatrix} \quad (142)$$

$$[C] = \begin{bmatrix} 0 & 0 \\ 0 & 0 \\ 0 & 0 \\ 0 & 0 \\ c_{51} & c_{52} \\ c_{61} & c_{62} \\ c_{71} & c_{72} \\ 0 & 0 \\ 0 & 0 \\ 0 & 0 \\ 0 & 0 \\ 0 & 0 \\ 0 & 0 \\ 0 & 0 \\ 0 & 0 \end{bmatrix} \quad (143)$$

The elements for matrices $[A]$ and $[B]$ are listed in Appendix D. Note that the last six rows of matrix $[B]$ vary for the range of α . The $[C]$ matrix terms are valid for all values of α .

$$c_{51} = -c_{y\delta_a} \quad (144)$$

$$c_{52} = -c_{y\delta_r} \quad (145)$$

$$c_{61} = -c_{n\delta_a} \quad (146)$$

$$c_{62} = -c_{n\delta_r} \quad (147)$$

Equation (130) is rewritten as:

$$[\dot{X}] = [A^{-1}][B][X] + [A^{-1}][C][U] \quad (148)$$

The stability of each equilibrium position was checked with no control inputs. Therefore, $[\bar{U}] = 0$, and equation (148) becomes:

$$[\bar{X}] = [A^{-1}][B][\bar{X}] \quad (149)$$

The eigenvalue problem to be solved is then:

$$[A^{-1}[B] - \lambda[I]] [\bar{X}] = 0 \quad (150)$$

which leads to the condition:

$$\text{Det} [A^{-1}[B] - \lambda[I]] = 0 \quad (151)$$

This solution is a polynomial of degree 14:

$$\begin{aligned} & \lambda^{14} + m_1 \lambda^{13} + m_2 \lambda^{12} + m_3 \lambda^{11} + m_4 \lambda^{10} + m_5 \lambda^9 \\ & + m_6 \lambda^8 + m_7 \lambda^7 + m_8 \lambda^6 + m_9 \lambda^5 + m_{10} \lambda^4 + m_{11} \lambda^3 \\ & + m_{12} \lambda^2 + m_{13} \lambda + m_{14} = 0 \end{aligned} \quad (152)$$

For the system to be stable, all 14 roots had to be negative. Eq. (152) was solved using the computer program in Appendix D. In addition, the eigenvectors for the associated eigenvalues were calculated for use in identifying the eight roots traditionally used to describe aircraft characteristics. The six other roots were due to the flight control system and were of no interest.

III. Non-linear Analysis

Non-linear Computer Program

The computer program used for the non-linear analysis (Appendix D) was developed by the Aircraft Group of the Air Force Flight Dynamics Laboratory. It was modified for this study so that the updated data package could be used. The program contained the entire FCS as shown in Appendix B. The inputs for the program were designed to be pilot forces for aileron, rudder, and elevator. However, for purposes of determining perturbation effects, the program was modified so that perturbations of one-half second could be artificially introduced once the aircraft was trimmed. Control forces were held constant once trimmed conditions were achieved. Trim times of 15 seconds and 20 seconds were used. Although maintaining constant trim forces was somewhat of an artificial situation, this approach was necessary to isolate the aircraft's behavior.

To verify the accuracy of both the data and the computer model, several simulations were made with control force pulses and step inputs. The simulations matched the corresponding maneuver from the flight tests very closely.

Perturbed Motion Analysis

During this portion of the study, emphasis was on what severe aircraft motions were encountered and if recovery from the motions could have been accomplished. In the interest of computer resources, it was decided to use only one

lateral perturbation. Therefore, yaw perturbations were used as well as pitch perturbations. Only one perturbation was introduced per simulation in order to try to separate what motions could be expected from longitudinal perturbations and from lateral perturbations. For the case of yaw perturbations, a simple controller was modelled to control yaw divergence.

IV. Results

Alpha-Beta Envelope

The α - β envelope for which the aircraft could be trimmed at sea level for rectilinear flight using the relationships derived from eqs. (22) through (27) is depicted in Fig. 2. This envelope does not account for restricted control deflections due to the ARI. It merely defines where sufficient control authority is available.

Within the α - β control envelope the linearly-derived stability envelope is also shown in Fig. 2. The eigenvalue computer program provided 14 eigenvalues for each given β and α . Of these values eight represented traditional aircraft behavior. Except at large sideslip angles, the short period, phugoid, dutch roll, spiral mode, and roll mode were easily distinguished. Values of the dutch roll natural frequencies calculated from the eigenvalues agreed well with flight test data. The damping ratios were approximately one-half of flight test values for α up to about 20 degrees. However, these damping ratios were within Category B and C, Level 1 handling qualities. The region below $\alpha = 7^\circ$ was unstable largely due to the spiral mode. Time to double amplitude (T_2), however, was well within Category A, Level 1. Discrepancies in lateral characteristics were expected since the lateral FCS was not modelled in the eigenvalue problem. Since no lateral instabilities of any importance were discovered, not including the lateral FCS seemed justified.

Instability in the phugoid mode primarily accounted for

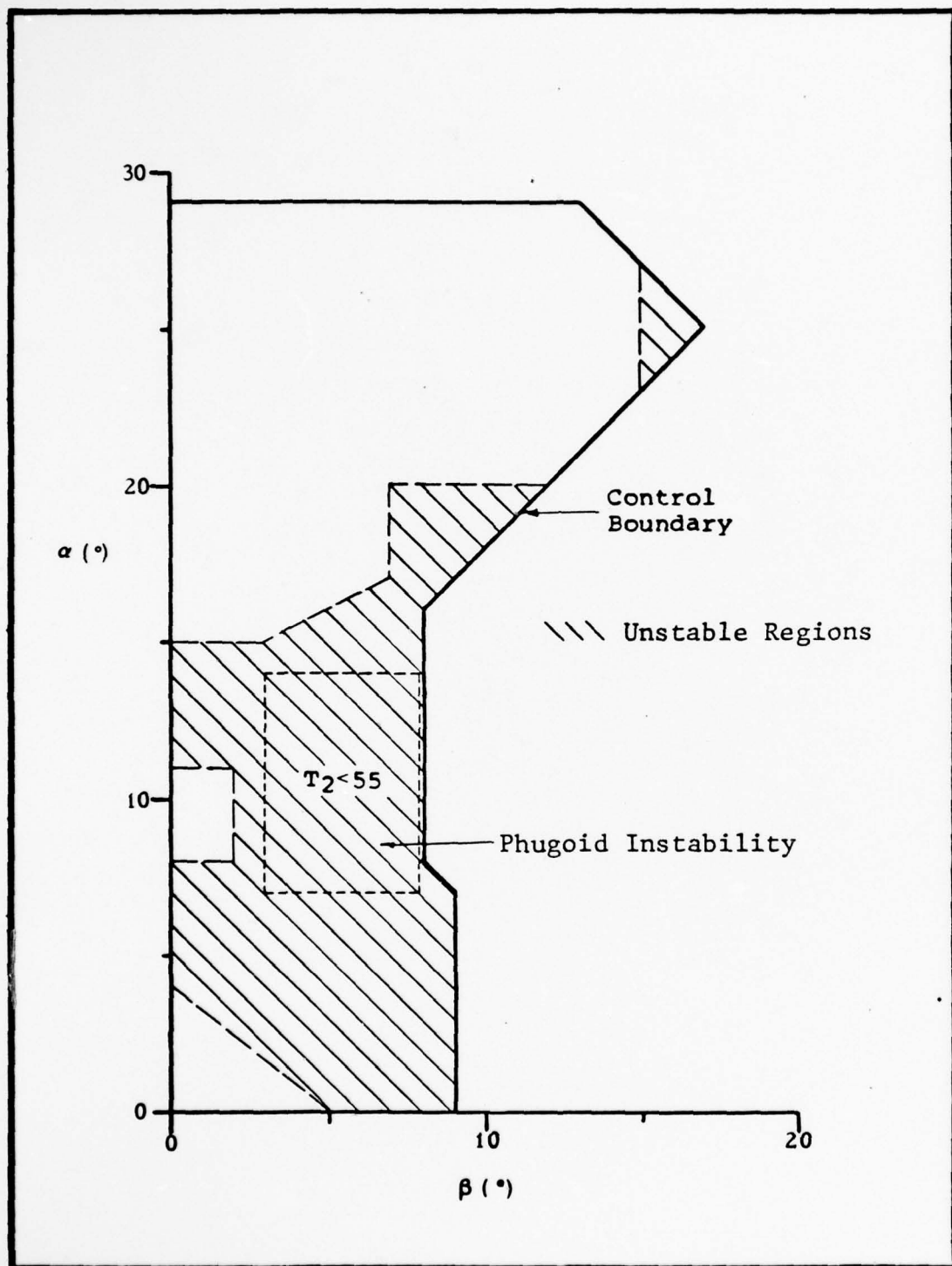


Fig. 2 α - β Control Boundary and Stability Boundary

the portion of the unstable region above $\alpha = 7^\circ$. The only area where Level 3 handling qualities were not satisfied was in the area noted in Fig. 2. In this region T_2 was calculated to be as low as ten seconds. The only region that was of concern for this study was above approximately $\alpha = 10^\circ$.

The linearized α - β control boundary and stability boundary provided guidelines as to where the non-linear computer program should give stable trim points. Information was also gained as to where in the boundary one or more control surfaces should become saturated.

Perturbed Motion Analysis

Points in the α - β boundary between $\alpha = 10^\circ$ and $\alpha = 25^\circ$ in increments of two degrees were tested for dynamic stability with various perturbations. Fig. 3 shows regions where the non-linear computer program was not able to trim the aircraft. Analysis of the lower region showed β was maintained, but α wandered to the upper region and never decreased in value. This supported the linear analysis of an unstable phugoid region. The upper region seemed to be limited by control surface deflection. Some restriction in the control boundary was anticipated since the ARI was part of the non-linear model. Except for the two regions noted, the rest of the α - β control boundary above $\alpha = 10^\circ$ predicted accurately where trimmed flight was possible.

As mentioned in Section III, only pitch and yaw perturbations were introduced. The size of perturbations that

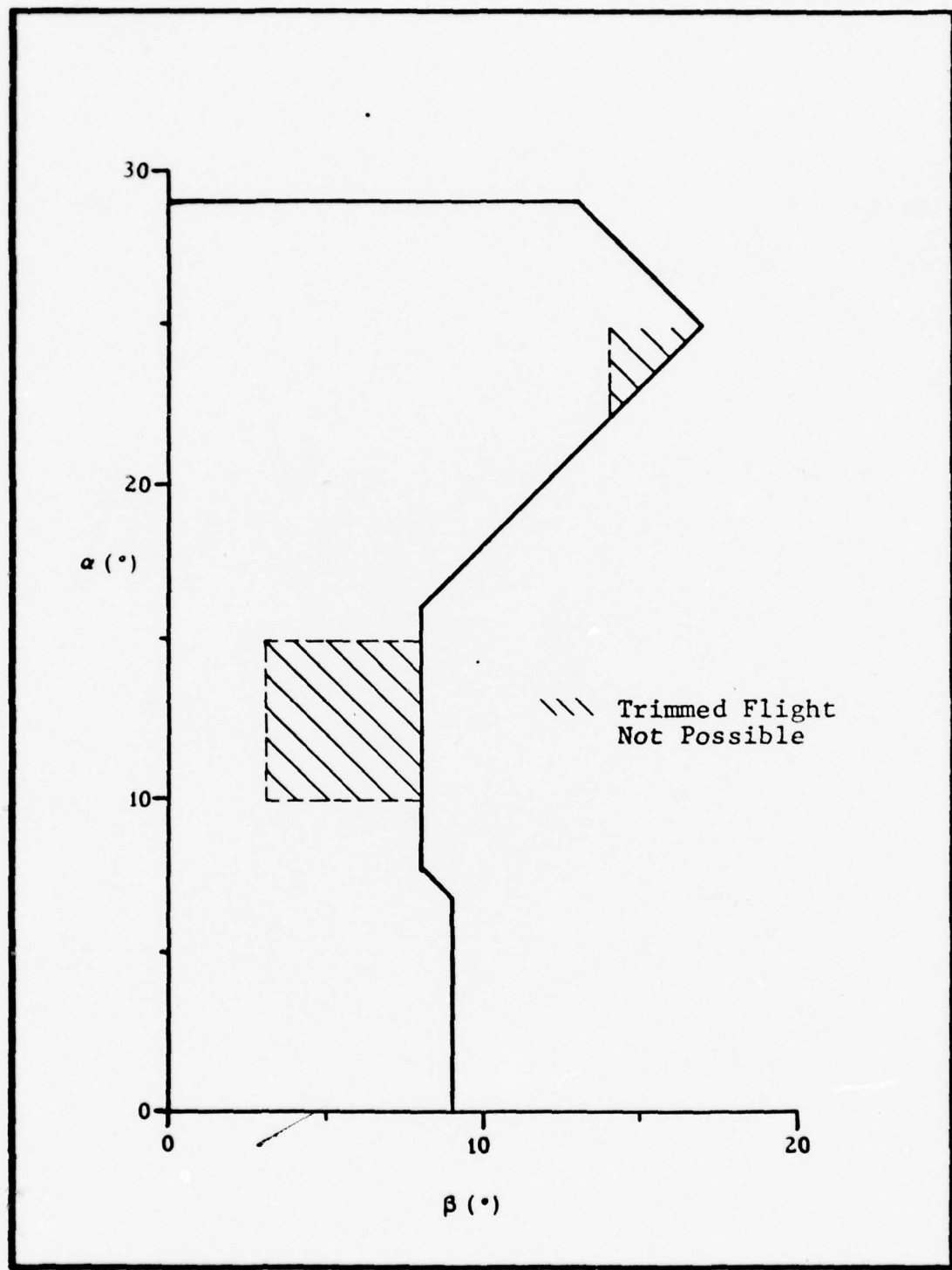


Fig. 3 Regions where the Non-Linear Program could not trim

caused uncontrolled aircraft motion were 20 deg/sec and 30 deg/sec. These were rates that could be generated by the pilot as he begins a variety of maneuvers from trimmed flight. Lesser perturbations resulted in at worst roll rates of 40 deg/sec or merely a negative θ with α and β remaining constant. In all cases with perturbation rates below 20 deg/sec, no control surfaces were saturated, and recovery would have been easily obtained.

The areas shown in Figs. 4 and 5 for pitch perturbations and in Figs. 7 and 8 for yaw perturbations represent equilibrium conditions from which the aircraft was perturbed and the resulting motion was highly uncontrollable. Uncontrollable for purposes of this study means a condition where the resulting motion was very erratic and disorienting, with one or more control surfaces reaching the limits of travel and not affecting a recovery.

Pitch Rate Perturbations

The pitch rate perturbations caused four types of uncontrolled motion. The types of motion and the average behavior of the aircraft for these motions are listed below:

(1) Erect Spin (Appendix E):

$r \approx -60$ deg/sec

θ oscillated around -70 deg

ϕ within ± 30 deg of wings level

q highly oscillatory and ranged between 3.6 and 4.2 sec/cycle

α diverged oscillating around 60 deg

(2) Inverted Spin (Appendix G):

$r \approx -50$ to -70 deg/sec

θ oscillated around -70 deg

ϕ within ± 20 deg of -150 deg

q oscillated at 3.0 to 4.5 sec/cycle

α oscillated around -50 deg

(3) Rolling Departure (Appendix I):

$p \approx 160$ deg/sec

r oscillated from -20 to -60 deg/sec

θ oscillated around -70 deg

α, β diverged to negative values

q oscillated at 2.5 sec/cycle

(4) Rolling Departure to an Inverted Spin (Appendix J):

r diverged beyond -110 deg/sec

θ oscillated around -20 deg

ϕ within ± 20 deg of -160 deg

q oscillated at 2.5 sec/cycle

α oscillated around -20 deg while rolling and

oscillated around -50 deg while inverted.

Of the four types of departures due to pitch perturbations, the rolling departures were the most abrupt motions. The inverted spins that developed from rolling departures had yaw rates three times greater than yaw rates of spins encountered from any other type entry. In addition, the

pitch oscillations were twice those from other spins. Variations between $q = 30$ deg/sec and $q = 20$ deg/sec had little effect on the resulting motion. Both pitch rates produced the same four types of motion. Each rate had a slightly different region of influence on the $\alpha-\beta$ boundary (Figs. 4 and 5). Fig. 6 shows the lines which separate where the controllable motions and the uncontrollable motions occurred for both pitch rates. The cross-hatched regions are of interest because these regions are where $q = 20$ deg/sec caused uncontrolled motion while $q = 30$ deg/sec caused only small roll rates (30 to 40 deg/sec). Appendix E and Appendix K compare a trim point where this occurred.

Yaw Rate Perturbations

Two classes of departures resulted from yaw perturbations, erect spins and erect spins that transitioned to inverted spins.

(1) Erect Spin (Appendix F):

$r \approx -40$ to -80 deg/sec

θ oscillated around -30 deg

ϕ within ± 30 deg of wings level

q oscillated at 3.0 to 4.5 sec/cycle

α diverged oscillating around 60 deg

(2) Erect Spin to Inverted Spin (Appendix H):

While erect, same as above

While inverted:

r diverged beyond -50 deg/sec

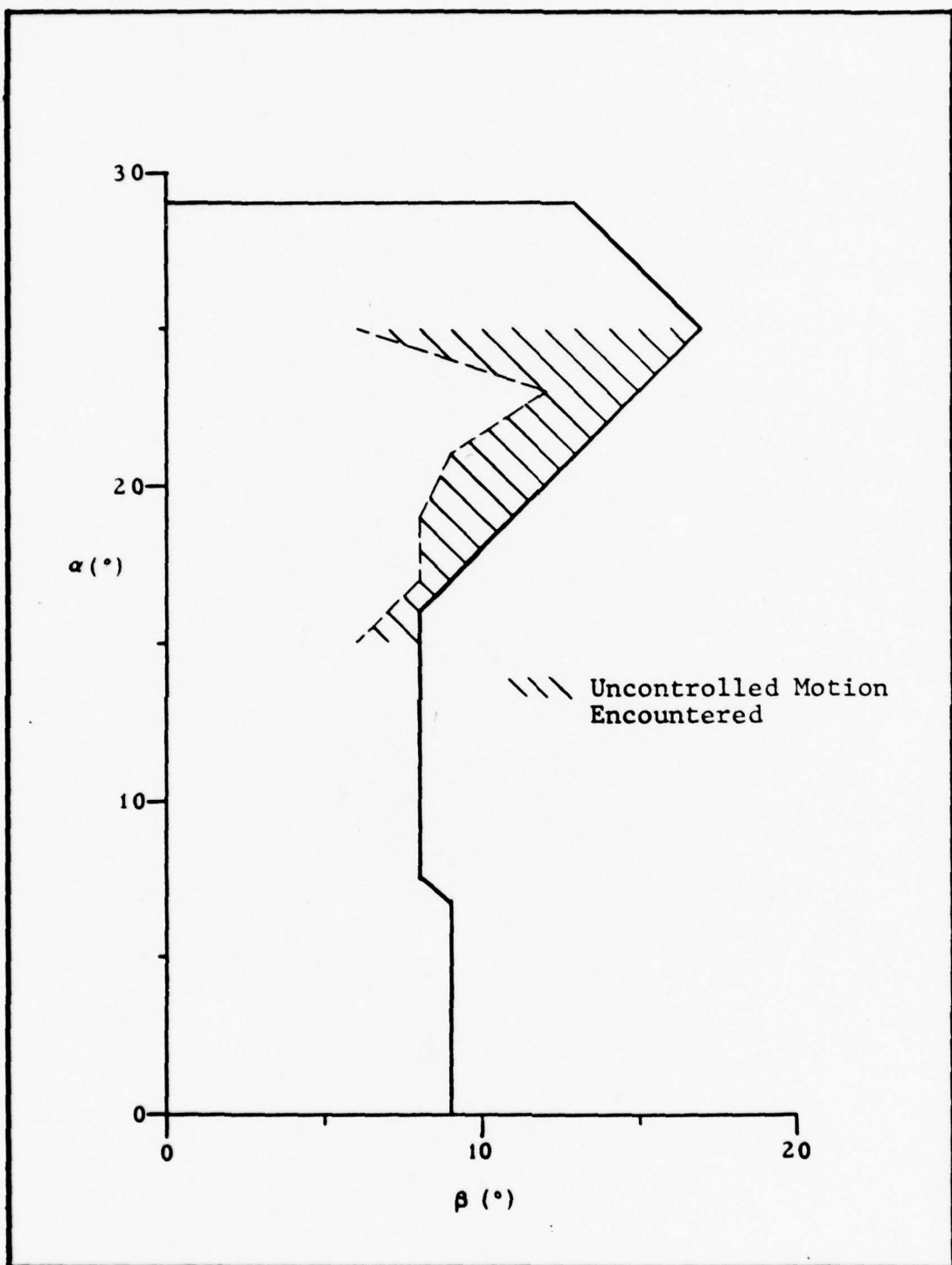


Fig. 4 Departure Region for $q = 20 \text{ deg/sec}$

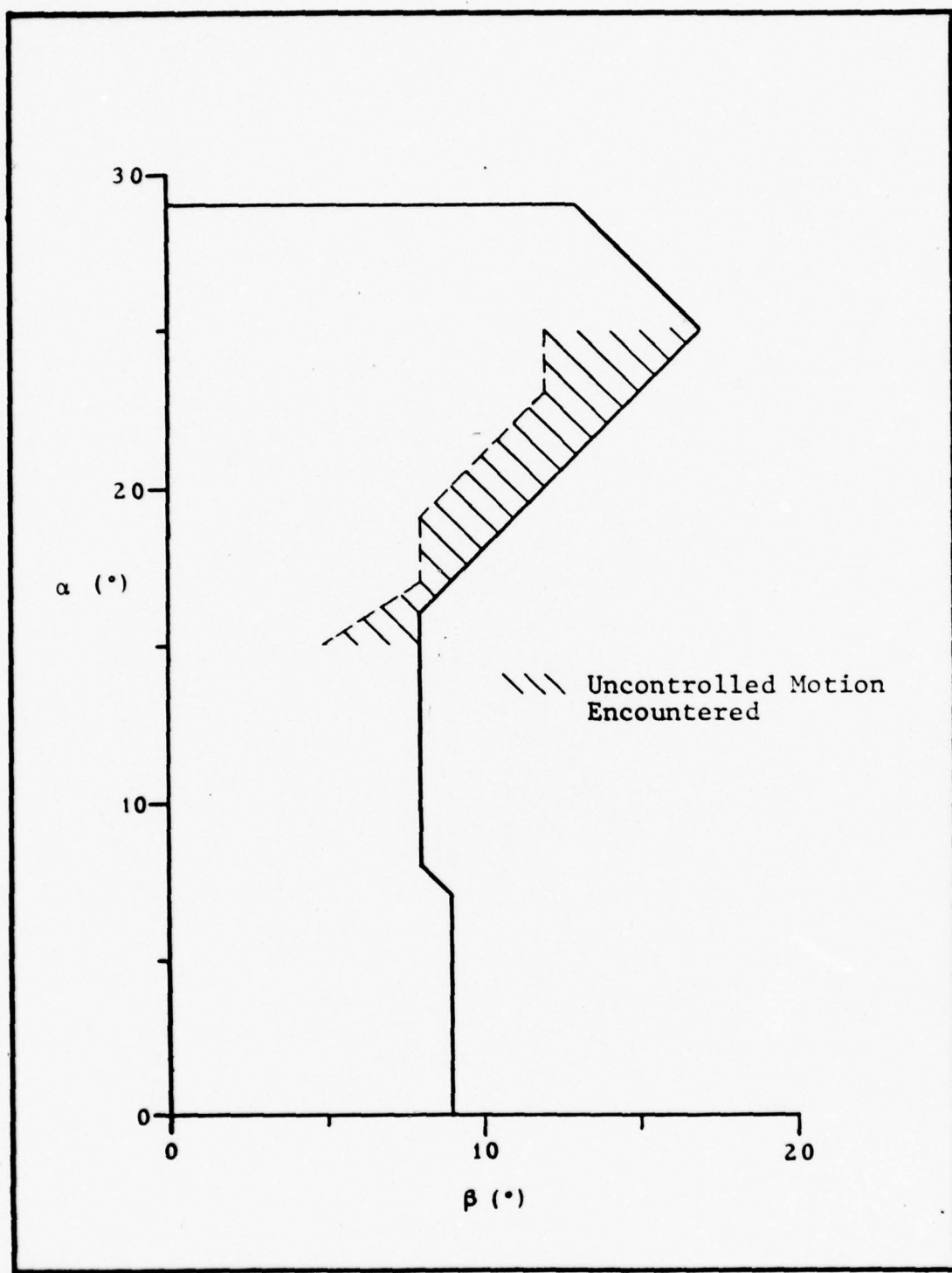


Fig. 5 Departure Region for $q = 30 \text{ deg/sec}$

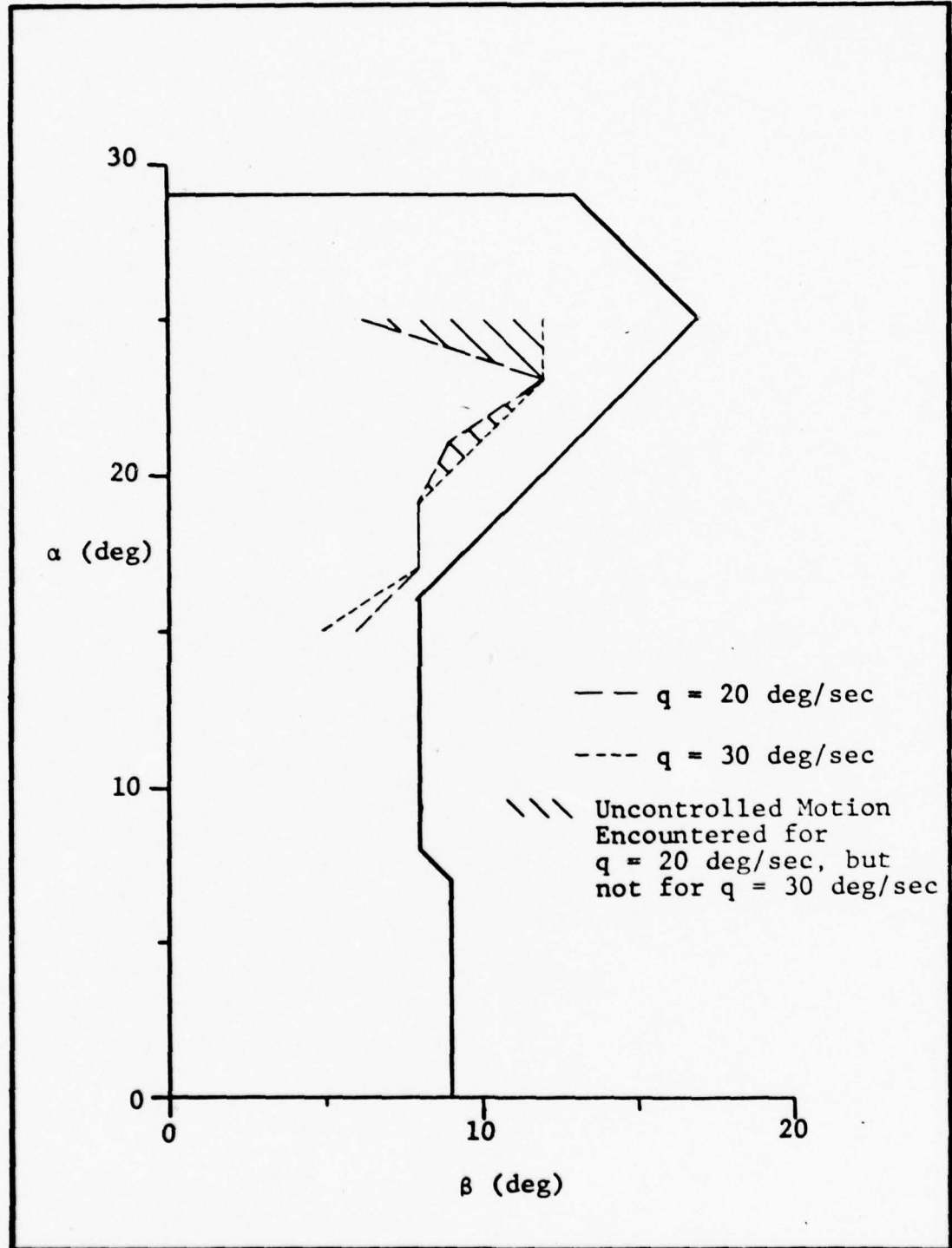


Fig. 6 Regions where $q = 20 \text{ deg/sec}$ had more influence
than $q = 30 \text{ deg/sec}$

θ oscillated around -40 deg
 ϕ within ± 20 deg of -160 deg
 q oscillated at 4 sec/cycle
 α oscillated around -50 deg while inverted

Varying yaw perturbations produced the same sort of results as varying pitch perturbations. The $\alpha-\beta$ region influenced by $r = -30$ deg/sec was about twice that for $r = -20$ deg/sec. Fig. 9 shows a region where the lesser rate caused uncontrolled motion while the larger rate resulted in only slow rolls (30 to 50 deg/sec). Appendix F and Appendix K compare a point where this occurred.

Comparison of the uncontrolled motions produced by pitch and yaw perturbations revealed five basic types of motion:

- (1) Erect Spin
- (2) Erect Spin transitioning to Inverted Spin (yaw perturbations only)
- (3) Inverted Spin (pitch perturbations only)
- (4) Rolling Departure (pitch perturbations only)
- (5) Rolling Departure to Inverted Spin (pitch perturbations only)

Regardless of the type perturbation that caused the out of control motion, all erect spins and all inverted spins were very similar in behavior.

As a basis for comparing the erect spins described by this study, the one actual erect spin that the YF-16 encountered during its flight tests is described below (Ref 1:234):

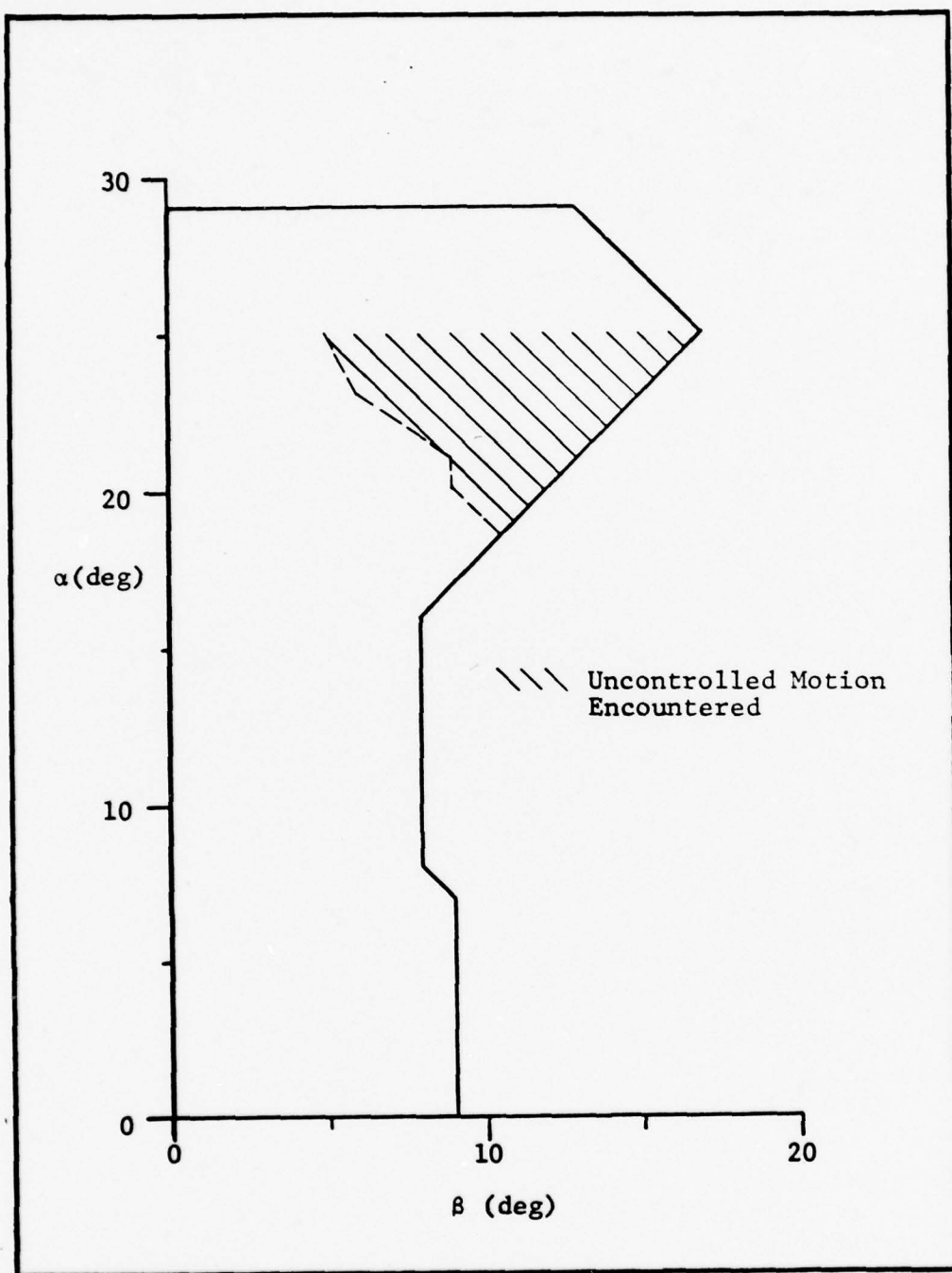


Fig. 7 Departure Region for $r = 20$ deg/sec

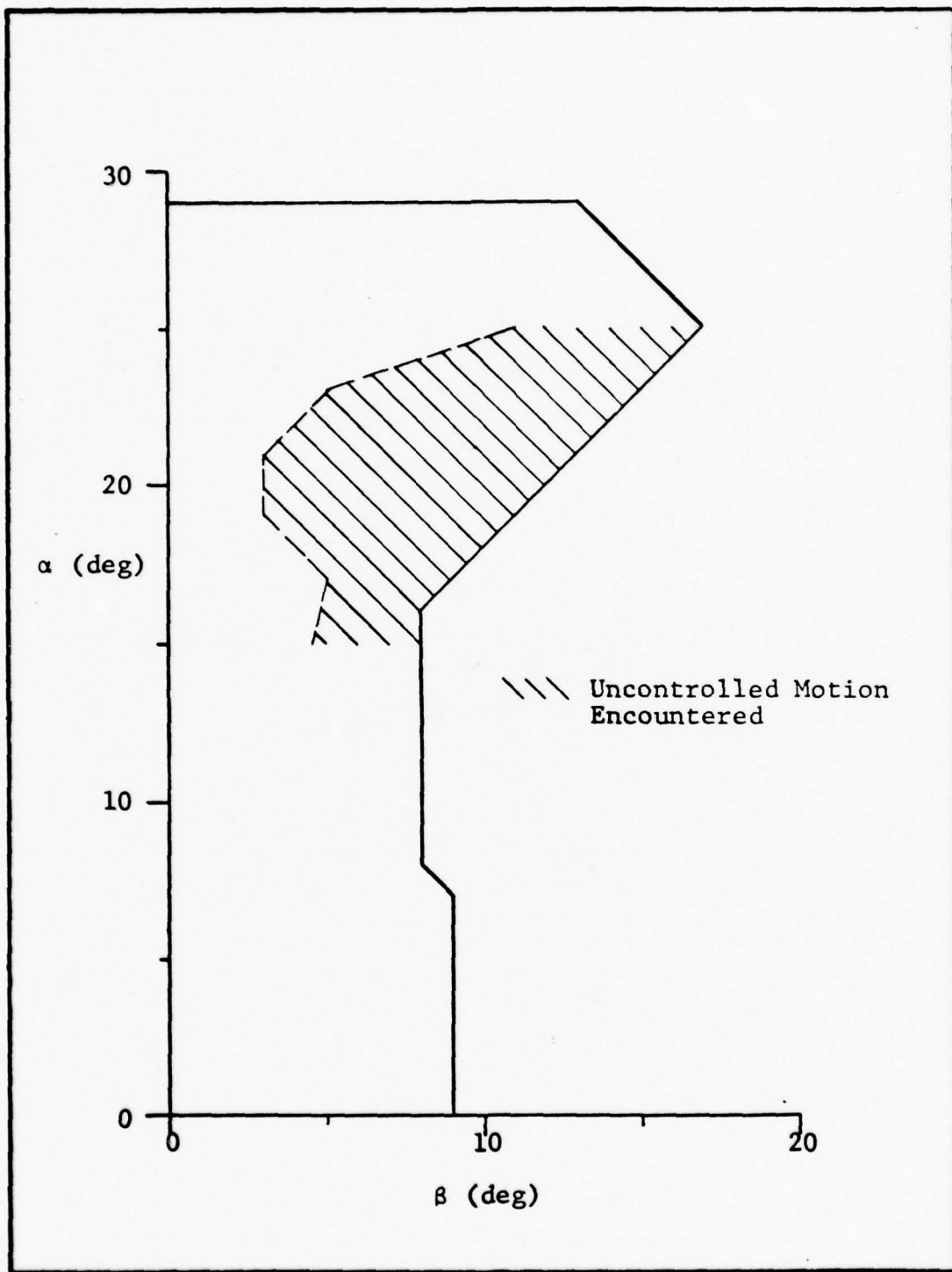


Fig. 8 Departure Region for $r = 30 \text{ deg/sec}$

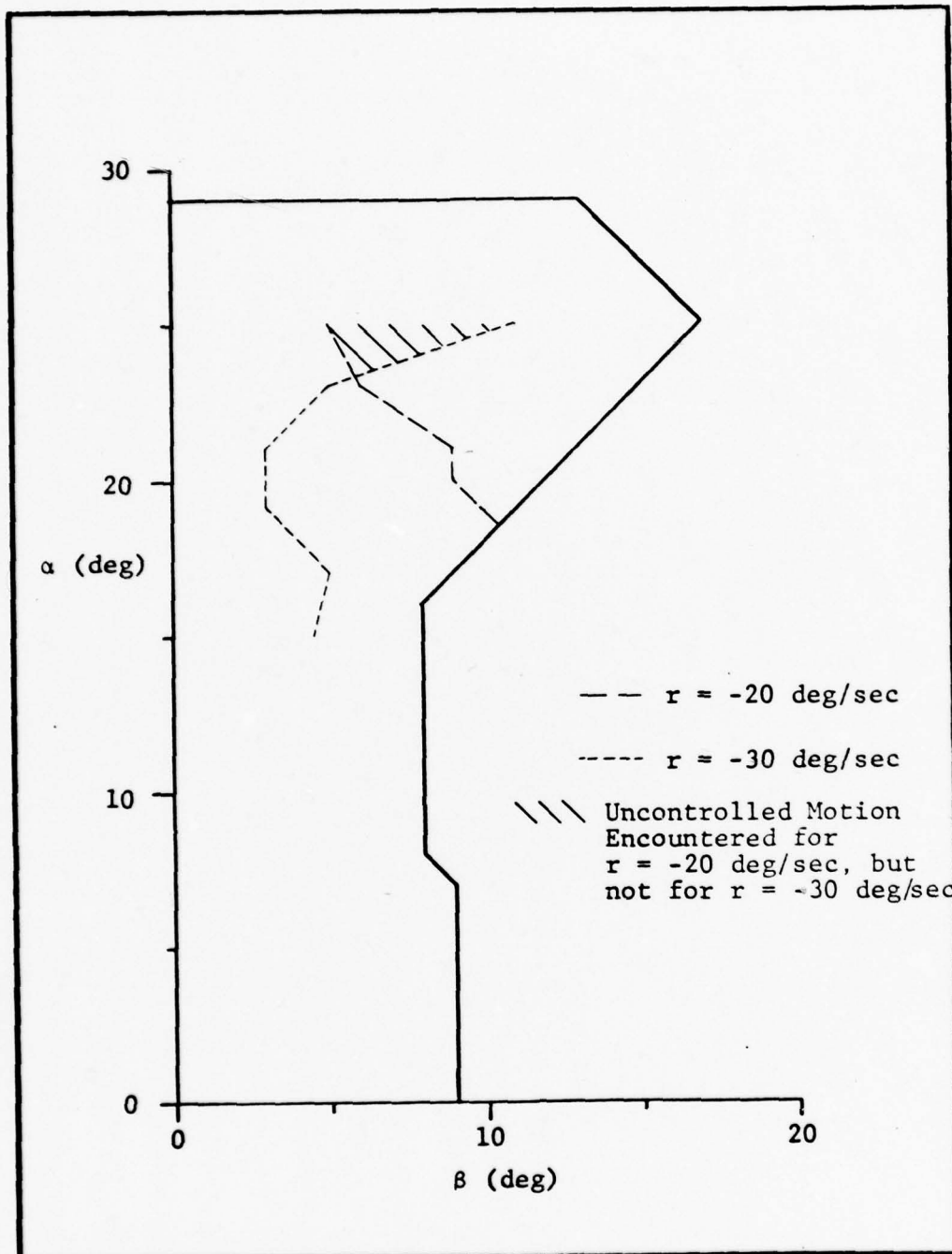


Fig. 9 Region where $r = -20 \text{ deg/sec}$ had more influence
 than $r = -30 \text{ deg/sec}$

$r \approx -10$ to -50 deg/sec

$\theta \approx -75$ deg

ϕ within ± 30 deg of wings level

q the primary oscillatory motion at 4.2 sec/cycle

δ_s oscillated from -25 to $+25$ deg

α was above 30 deg

Control Surfaces Analysis

Analysis of the aircraft's uncontrolled motions leads to three modes that could be prevented: erect spins, inverted spins, and rolling departures. Average control surface deflections during these motions were as follows:

(1) Erect Spin (left turns):

δ_r oscillated 0 to 25 deg

$\delta_s \approx 25$ deg

δ_a oscillated -5 to -20 deg

(2) Inverted Spin (right turns):

$\delta_r \approx 25$ to 30 deg

$\delta_s \approx \pm 5$ deg of neutral

$\delta_a \approx 5$ to -20 deg

(3) Rolling Departure (right rolls):

$\delta_r \approx 30$ deg

$\delta_s \approx -25$ deg

$\delta_a \approx -10$ to 10 deg

The stabilator in all cases of erect spins was fully deflected in order to try to reduce α . However, low dynamic

pressure apparently prevented the stabilator from being effective. This was the case in the actual departures and the spin which the aircraft encountered in flight tests. For the erect and inverted spins, rudder was being held in the direction of the spin. A controller that commanded at least neutral rudder, or possibly opposite rudder once the spin has developed would be seemingly warranted.

The rolling departures appear to be the most difficult departures to control. The rudder is already deflected so as to oppose the resulting roll direction. Sufficient ailerons seem to be available to stop the roll, however. Rolling departures resulted exclusively from pitch perturbations and occurred within two degrees of the right side of the α - β control boundary for $\alpha < 21$ deg. It appears that a controller which prevents the aircraft from entering that region would be warranted.

Yaw Departure Controller

A simple yaw departure controller was modelled which used α , β , and yaw rate as its inputs. The regions of Figs. 7 and 8 were written for β as a function of α . When yaw rates greater than 20 deg/sec or 30 deg/sec were generated and the aircraft was in the appropriate α - β region, rudder was commanded to counteract any increase in β . The controller was effective in keeping the aircraft from entering a spin (Appendix N). The FCS was able to control α once the lateral motion damped out. In all cases the controller was needed for less than one-half second.

V. Conclusions and Recommendations

Conclusions

The results of pitch and yaw perturbations analysis provide the following conclusions based on the YF-16 computer model as described in this study:

- (1) The aircraft exhibits a high degree of susceptibility to loss of control when operating at high angles of attack in asymmetric flight when exposed to moderate pitch and yaw perturbations.
- (2) The uncontrolled motions fall into three basic categories: erect spins, inverted spins, and rolling departures.
- (3) Sufficient control authority seems to be available to stop the primary undesirable motions of yaw and roll.
- (4) A departure controller that monitors α , β and changes in pitch rate and yaw rate appears to be warranted if the aircraft is to be allowed to maneuver with full control surface authority.

Recommendations

This study should be extended in the following ways:

- (1) A departure controller should be investigated for incorporation into the FCS. Once the obvious undesirable aircraft motions are controlled, an analysis of any limitations imposed by the con-

troller should be made.

- (2) The aircraft should be analyzed at various altitudes to determine if the sea level α - β boundary and corresponding areas of uncontrolled motion are representative of all altitudes.
- (3) Asymmetrical flight should be investigated in the landing configuration. This area provides the greatest safety threat since any uncontrolled motion would have extremely limited time and altitude for recovery.
- (4) Turning flight should be investigated for divergence problems.

Bibliography

1. AFFTC-TR-75-15. Flying Qualities Evaluation of the YF-16 Prototype Lightweight Fighter. California: Department of the Air Force, July 1975.
2. Blakelock, John H. Automatic Control of Aircraft and Missiles. New York: Wiley and Sons, 1965.
3. Etkin, Bernard. Dynamics of Atmospheric Flight. New York: Wiley and Sons, 1972.
4. Hawkins, Max L. An Investigation of the Departure Modes of a F-4D Aircraft From a Steady Sideslip Flight Condition. Thesis, GAE/MC/74-6, Ohio: U.S. Air Force Institute of Technology, December 1974.
5. Ogata, Katsuhiko. Modern Control Engineering. New Jersey: Prentice-Hall, 1970.
6. Salvadori, M. G. and Baror, M. L. Numerical Methods in Engineering. New York: Prentice-Hall, 1952.
7. Thelander, J. A. Aircraft Motion Analysis. Ohio: Air Force Flight Dynamics Laboratory, March 1965.
8. Withers, Douglas R. The Influence of Roll, Pitch, and Yaw Rate Perturbations of the $\alpha-\beta$ Stability Envelope of the F-4D Aircraft. Thesis, GAE/MC/75D-10, Ohio: U.S. Air Force Institute of Technology, January 1976.

Appendix A

YF-16 Physical Characteristics

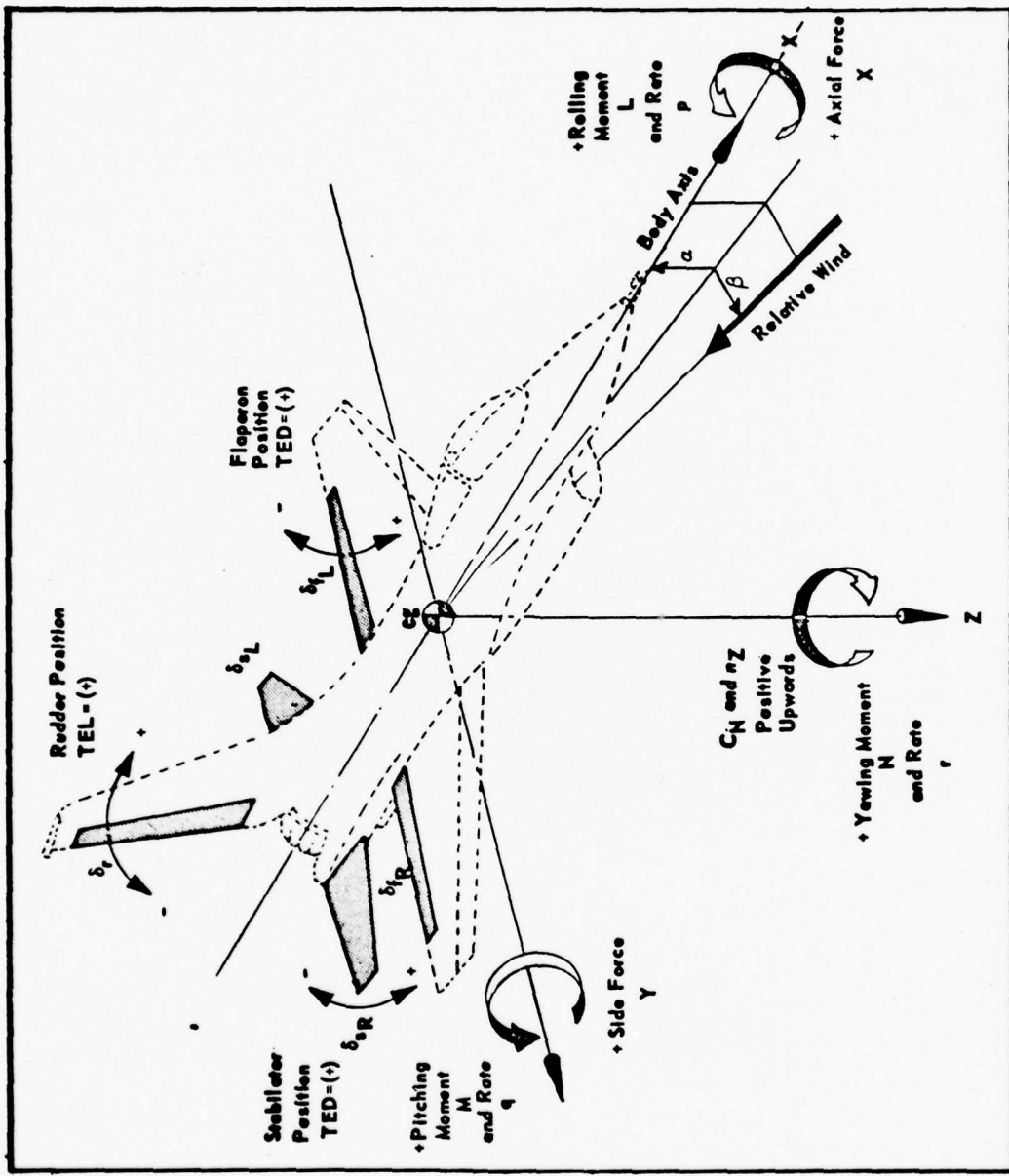
$W = 20,860 \text{ lb}$	$I_x = 6,100 \text{ slugs-ft}^2$
$S = 283 \text{ ft}^2$	$I_y = 51,400 \text{ slugs-ft}^2$
$\bar{c} = 10.94 \text{ ft}$	$I_z = 57,000 \text{ slugs-ft}^2$
$b = 29 \text{ ft}$	$I_{zx} = 160 \text{ slugs-ft}^2$
$AR = 3.0$	

Control Surfaces Deflection Limits

(Primary Control Surfaces)

Aileron Deflection	20 deg up 20 deg down
Rudder Deflection	30 deg left 30 deg right
Stabilator Deflection	25 deg up 25 deg down

Control Surfaces Sign Convention



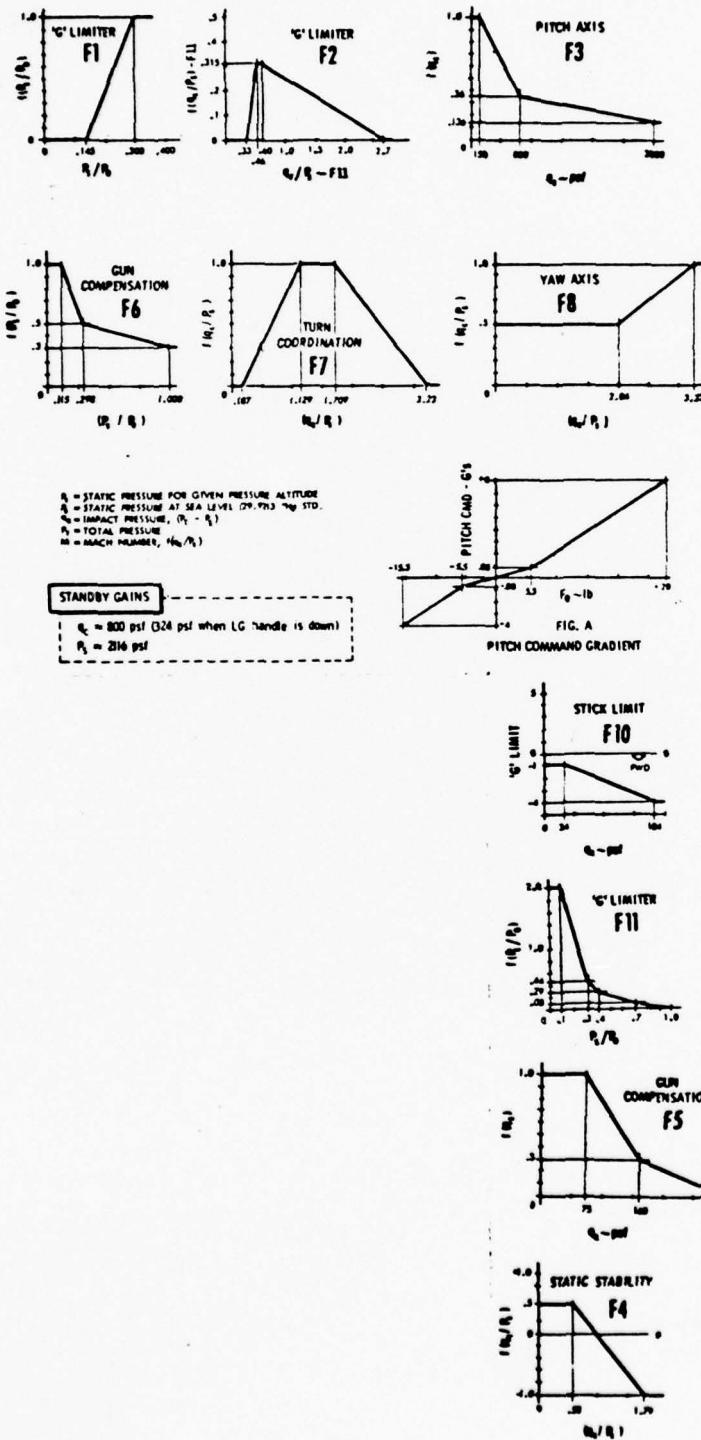
Note: TEL = Trailing Edge Left

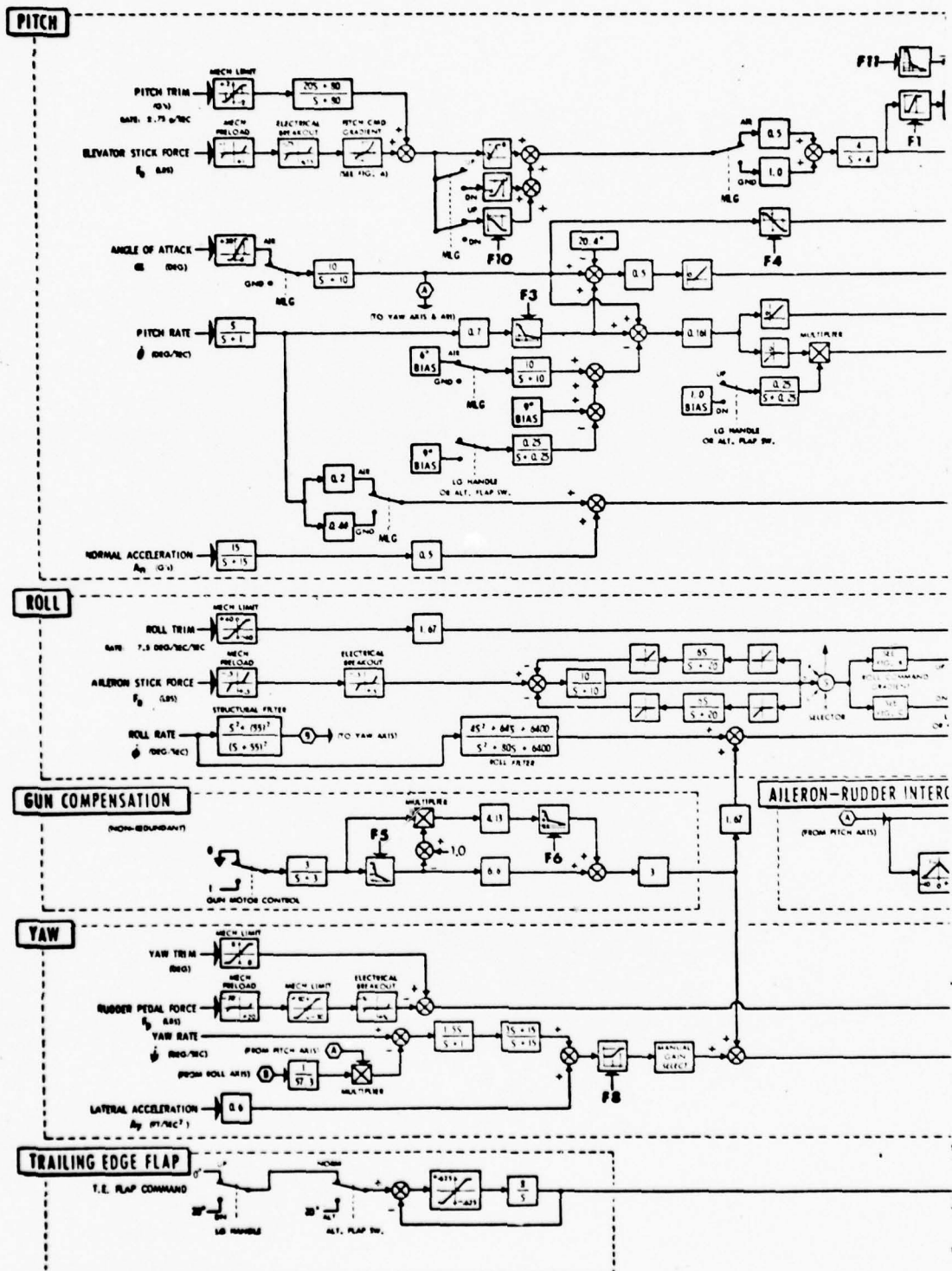
TED = Trailing Edge Down

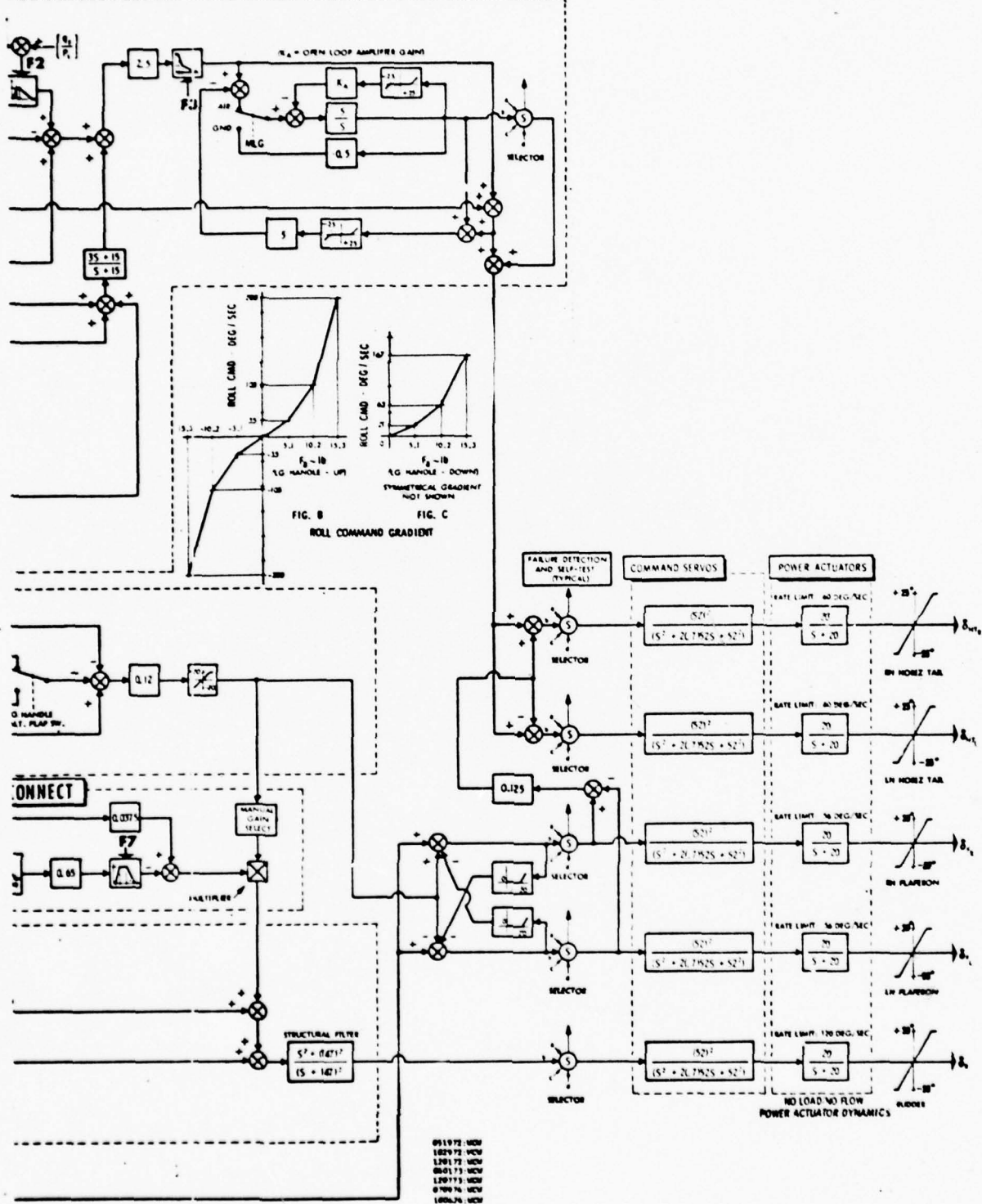
$$\delta_f = \delta_a$$

Appendix B

Flight Control System







Appendix C

Eigenvalue Computer Program

```
PROGRAM EIG(INPUT,OUTPUT,TAPE4=INPUT,TAPE6=OUTPUT)
REAL A(14,14),B(14,14),F(14,14),G(14,14),IX,IY,IZ,IZX,MU
REAL WORK(28)
COMPLEX EIGVAL(14),EIGVEC(14,14)

COMPLEX DFIGVAL(14)
READ(4,1) ALPHA,BETA,ELE,RUN,A1L,THE,PHI,CW,W,CT,T,V, CX,CZ,
1CL,CN,CLP,CLP,CNP,CNP,C4Q,CXDS,C7DS,CMDS,CYDA,C
2LDA,CNDA,CNDR,CYDP,CLDR,CXAL,CMAL,CZAL,CZ0,
3CYBE,CAL,CLE,CNAL,CNRE,CX0
1 FORMAT(8E10.4)
1 IF (EOF(4)) 190,160
160 CXAL=CXAL+57.29
CZAL=CZAL+57.29
CLAL=CLAL+57.29
CMAL=CMAL+57.29
CNAL=CNAL+57.29
CYRE=CYRE+57.29
CLBE=CLBE+57.29
CNBE=CNBE+57.29
CXDS=CXDS+57.29
CZDS=CZDS+57.29
CMDS=CMDS+57.29
AS=5.47/V
MU=176. $IX=2.97 $IY=466.66 $I7=27.78 $IZX=.078 $AR=3.
XG=32.2
PS=2116.33
ROH=.002378
RVR2=ROH*V*V
Q=RVR2/2.
OOP=0/PS
IF(0.LE.1E0.) F3=1.
IF(0.GE.3E0.) F3=.136
IF(0.GT.1E0..AND..0.LE.800.) F3=.1476923-.00098462*Q
IF(0.GT.800..AND..0.LT.3000.) F3=.4414545-.00010182*Q
IF(OOP.LE..53) F4=.5
```

```

IF(10P.GE.1.79) F4=-1.
IF(QOP.GT..53.AND.QOP.LT.1.79) F4=1.130952-1.190476*QOP
ALPHA=ALPHA/57.2958  QETA=QETA/57.2958
DO 2 I=1,14
DO 2 J=1,14
A(I,J)=0.
B(I,J)=0.
CONTINUE
2
A(1,1)=-2*MU*COS(ALPHA)*COS(BETA)
A(1,2)=2*MU*SIN(ALPHA)*COS(BETA)
A(1,5)=2*MU*COS(ALPHA)*SIN(BETA)
A(2,1)=-2*MU*SIN(ALPHA)*COS(BETA)
A(2,2)=-2*MU*COS(ALPHA)*COS(BETA)
A(2,5)=2*MU*SIN(ALPHA)*SIN(BETA)
A(3,3)=-IY
A(4,4)=1.
A(5,1)=-2*MU*SIN(BETA)
A(5,5)=-2*MU*COS(BETA)
A(5,6)=-AP*IZ
A(6,7)=AR*I7X
A(7,6)=AR*I7X
A(7,7)=-AP*I8X
A(8,8)=1.
A(9,9)=A(11,10)=A(11,11)=A(12,12)=A(13,13)=A(14,14)=1./AS
B(1,1)=-2*CX
B(1,2)=-CYAL
B(1,3)=+2*MU*SIN(ALPHA)*COS(BETA)-CXQ
B(1,4)=CW*COS(TH)
B(1,6)=-(2*MU*SIN(BETA))/AR
B(1,9)=-CXQS
B(2,1)=-2*CZ
B(2,2)=-C71L
B(2,3)=-2*MU*COS(ALPHA)*COS(BETA) -CZQ
B(2,4)=CW*SIN(TH)*ROS(PHI)

```

```

B(2,7)=2*MU*SIN(BETA)/AR
B(2,8)=CW*COS(THE)*SIN(PHI)
B(2,9)=-C70S
B(3,2)=-CMAL
B(3,3)=-CMQ
B(3,9)=-CMDS
B(4,3)=COS(PHI)
B(4,6)=-SIN(PHI)/AR
B(5,4)=CW*SIN(PHI)*SIN(THE)
B(5,5)=-CYRF
B(5,6)=(2*MU*COS(ALPHA)*COS(BETA)/AR)
B(5,7)=-(2*MU*SIN(ALPHA)*COS(BETA)/AR)
B(5,8)=-CH*COS(THE)*COS(PHI)
B(6,2)=-CNAL
B(6,5)=-CH3F
B(6,6)=-CHR
B(6,7)=-CMAL
B(7,2)=-CLAL
B(7,5)=-CL3F
B(7,6)=-CLR
B(7,7)=-CLP
B(8,3)=SIN(PHI)*TAN(THE)
B(8,6)=COS(PHI)*TAN(THE)/AR
B(8,7)=1/AR
B(9,2)=(-1125.*F3*V/XG)/57.3
B(9,10)=B(10,11)=B(11,12)=B(12,13)=B(13,14)=1.
B(9,4)=(1125.*F3*V/XG)/57.3
B(10,4)=(-4500.*F3*V/XG)/57.3
B(11,4)=(1350)00.*F3*V/XG)/57.3
B(12,4)=(-35437500.*F3*V/XG)/57.3
B(13,4)=(8.0625E08.*F3*V/XG)/57.3
B(14,4)=(-1937012500.*F3*V/XG)/57.3
***** USE THESE CARDS FOR ALPHA < OR = 15 DEGREES.
B(9,3)=(
    30.*F3)/AS

```

B(10,2) =

B(10,3) = (-780.*F3)/AS
B(11,2) = -6000.*E4-(1250000.*F3*V/XG)/57.3
B(11,3) = 18780.*F3/AS
B(12,2) = 140000.*F4+(25437500.*F3*V/XG)/57.3
B(12,3) = -L23780.*F3)/AS
B(13,2) = -3.E06*F4-(8.50625E08*F3*V/XG)/57.3
B(13,3) = 919879C.*F3)/AS
B(14,2) = 5.2E07*F4+(19870312500.*F3*V/XG)/57.3
B(14,3) = -194823780.*F3)/AS

C

USE THESE CARDS FOR 15 < ALPHA < OR = 20.4 DEGREES.

B(9,3) = (16.9*F3*F3+30.*F3)/AS
B(10,2) = 261.5*F3+200.*F4+(45000.*F3*V/XG)/57.3
P(10,3) = (-439.4*F3*F3-79)*F3)/AS
B(11,2) = -9452.5*F3-6300.*F4-(1350000.*F3*V/XG)/57.3
B(11,3) = (11579.**F3+F3*F3+13780.*F3)/AS
B(12,2) = 223425.0*F7+140005.*E4+(25437500.*F3*V/XG)/57.3
B(12,3) = (-238722.*F3+F3-423760.*F3)/AS
B(13,2) = -5.545E06*F3-3.F06*F4-(8.60625E08*F3*V/XG)/57.3
B(13,3) = (5181979.4*F2+F2*919879C.*F3)/AS
B(14,2) = 126187750.0*F3+5.2E17*F4+(19870312500.*F3*V/XG)/57.3
B(14,3) = (-10975079.4*F3+F3*F3-194923780.*F3)/AS

C

USE THESE CARDS FOR ALPHA > 20.4 DEGREES.

R(9,3) = (3L.4*F3*F3+70.*F3)/AS
B(10,2) = 491.5*F2+200.*F4+(45000.*F3*V/XG)/57.3
B(10,3) = (-719.4*F3*F3-79).*F3)/AS
B(11,2) = -14702.5*F3-6000.*F4-(125000.*F3*V/XG)/57.3
B(11,3) = (16108.7*F3+F3+13760.*F3)/AS
B(12,2) = 3E6925.-F3+14000.*F4+(25437500.*F3*V/XG)/57.3
B(12,3) = (-349229.9*F3*F3-423780.*F3)/AS
B(13,2) = -8.6295E06*F3-3.705*E4-(8.60625E08*F3*V/XG)/57.3
B(13,3) = (739134.4*F3+F3+919879C.*F3)/AS
B(14,2) = 1849233770.0*F3+6.2F07*F4+(19870312500.*F3*V/XG)/57.3

```

***** B(14,3)=(-153925216.4*F3*-3-194823780.*F3)/AS ****
***** B(14,10)=-450000.
***** B(14,11)=-57750.
***** B(14,12)=-14075.
***** B(14,13)=-1385.
***** B(14,14)=-51.
N=14

      IF(J=1
      CALL MINV(A,F,N)
      CALL MULT(F,N,G,14,14,14)
      CALL RGEIG(14,14,G,IND,EIGVAL,EIGVEC,WORK)
      DO 205 J=1,N
      DEIGVAL(J)=(V/5.47)*EIGVAL(J)
205  CONTINUE
      WRITE(6,10) ALPHA,RETAD
10    FORMAT(//10X,"ALPHA = ",E10.4,5X,"BETA = ",E10.4)
      WRITE(6,15) (EIGVAL(I),I=1,N)
15    FORMAT(60X,"EIGENVALUES"/4((2E12.4,10X)/))
      WRITE(6,1F) (DEIGVAL(I),I=1,N)
1F    FORMAT(48X,"TIME DOMAIN EIGENVALUES"/4((2E12.4,10X)/))
      DO 206 J=1,N
      WRITE(6,2F) J
206  FORMAT(59Y,"EIGENVECTOR(1,","12,")")
      WRITE(6,3G) EIGVEC(1,J),EIGVEC(2,J),EIGVEC(3,J),EIGVEC(4,J)
      FORMAT(3X,"VEL = ",2E12.4,2X,"ALPHA = ",2E12.4,2X
      1,"THETA = ",2E12.4)
      WRITE(6,35) EIGVEC(5,J),EIGVEC(6,J),EIGVEC(7,J),EIGVEC(8,J)
35    FORMAT(2X,"BETA = ",2E12.4,6X,"R = ",2E12.4,5X,"P = ",2E12.4,4X,"P
      1H = ",2E12.4)
      WRITE(6,37) EIGVEC(9,J),EIGVEC(10,J),EIGVEC(11,J),
      CEIGVEC(12,J)
37    FORMAT(4X,"Y1 = ",2F12.4,5X,"X2 = ",2E12.4,4X,"X3 = ",2E12.4,
      C5X,"X4 = ",2E12.4)
      WRITE(6,38) EIGVEC(13,J),EIGVEC(14,J)

```

38 FORMAT(4X,"X5 = ",2E12.4,5X,"X6 = ",2E12.4)
206 CONTINUE
GO TO 901
190 STOP

```
SUBROUTINE MULT(X,Y,Z,N,M)
REAL X(14,14),Y(14,14),Z(14,14)
DO 250 I=1,M
   DO 250 J=1,N
      SUM=0.0
      DO 250 K=1,N
         SUM=SUM+X(I,K)*Y(K,J)
         Z(I,J)=SUM
      250 CONTINUE
      RETURN
   END
```

Appendix D

Non-Linear Computer Program

```

PROGRAM TIMEH(INPUT, OUTPUT, TAPE2, TAPE5=INPUT, TAPE6=OUTPUT, PLOT)
DIMENSION X(7),Z(7),W(7),X3(7),Y3(7)
DIMENSION DEF(502),DAFD(502),DRFP(502)
DIMENSION Y(30),YD(30),AL>AJ(502),RETAD(502),VFL(502),P(502),
10(502),R(502),ALT(502),THETA(502),PHI(502),PSI(502),YO(7),
2TIME(502),DIST(502),TRAY(502),AX(502),AY(502),AZ(502),DELE(502),
3DELA(502),DELP(502),TGV(502),THRST(502),N7(502)

COMMON/TIME/CYCLE
COMMON/PARAM/FCH(49,5),FCND(49),ECC(49,5),ECC0(49,5),ECMO(49,5),
1ECM0(49),FCLB(49,9),ECLDF(49),ECLDR(49),EFLP(49),ECLR(49),
2ECN3(49,9),FCNDF(49),ECNR(49),ECNP(49),FCYB(49),
3ECYDF(49),ECYDR(49)
COMMON/GEOM/MASS,C,B,THRUS,CG
COMMON/OTHER/IX,IY,IZ,IX?,S
COMMON/REST/A1,A2,A3,A4,A1,92,93,94,C1,C2,C3,C4,D1,AV,
1FUDGE,CERS,SEPS,STHE,CTHE,SFE,CFE,RVR2,ROH,G,VR,THE,FE,SIGH,
2ALPHA,BETA,DP,DE,DF,DH,NLFE,DEC,DRC,DFC,DHC
COMMON/CHECK/SUMCX,SUMCM,CN,CNQ,CC,CCQ,CMD,CMQ
COMMON/CHECK2/C1B,C1R,CNP,CNOR,CND1,CNDF,CLOH,CLP,CLR,
CCLDR,CLB
COMMON/TRTM/BED,GAMAD,AL,EN, SUMCY,PLIFT,XCY,TCONST,GCONST
C,THEO,SIGH0,FF0
COMMON/RIAS/AC,AA,AB,91,93,97,98,TH
COMMON/STICK/DET,DAT,DRT,DEF,DAF,DRF,FB1,FB2
COMMON/STICKF/ DAFT(93),DRFT(93),DEFT(93)
COMMON/THRUSTT/SOSFS(9),TMILT(9,11)
C,TSAVE
COMMON/FLY/FFNO
EXTERNAL GYRATES
REAL IX,IY,IZ,IXZ,MASS,N7
NAMELIST/FFPO/ECN,ECNO,ECC0,ECMO,ECLB,ECLDF,ECLDR,ECLP,
1ECLP,ECN3,ECNDF,ECNDR,ECNP,ECNR,ECIP,ECYB,ECYDF,ECYDR
NAMELIST/FOPC/DAFT,DEFT,DRFT
NAMELIST/GEO/IX,IY,I7,IX7,MASS,S,C,B,THRUS,CG,YO,SIGH0,THE0,FF0,
1EPS

```

```

NAMELIST/ENGNTH/SOSFS,TMILT
READ AERO
READ(5,GEO)
READ(5,ENGNTH)
43 CONTINUE
READ(5,FORCE)
***** PROGRAM CONSTANTS *****
G=32.2
AV=57.295779513
EN=1.
AL=25./AV$ REND=15.
Y0(7)=9000.
BEDO=BED
THEO=AL
WHITE FORCE
A1=(IY-IZ)/IX
A2=IXZ/IX
A3=S*R/(2.*IX)
A4=R/2.
C4=A4
B1=(IZ-IX)/IY
B2=IXZ/IY
B3=S*C/(2.*IY)
B4=C/2.
C1=(IX-IY)/IZ
C2=IZ/IZ
C3=S*B/(2.*IZ)
D1=S/(2.*MASS)
SEPS=SIN(FPS)
CEPS=COS(FPS)
PI=3.14159274TOP1=2.*PI
DO 61 I=1,7
YP(I)=0.5Y(I)=Y0(I)
61 CONTINUE
CALL TURNTRM(Y,YP,Y0)

```

```

TSAVE=THRUS
D060 J=1,7
YP(J)=0.0
Y(J)=Y0(J)
IF(ABS(DE).LT..0001) DE=.0001
T=0.
Q=RVQR2/2. $ PS=2116.33*((1.-.0C00006875*Y(7))**5.2561)
P0=2116.2 $ PS0P0=PS/P0
OOP=Q/PS
RKA=10000.
Y(14)=AL*AV
IF(Y(14).GT.30.) Y(14)=30.
IF( Y(14).LT.-5.) Y(14)=-5.
CALL CONTPOL(T)
Y(15)=YP(5)*AV
Y(16)=CTHF*CFE-1.
Y(16)=Y(16)+(Y(1)*Y(5)-Y(2)*Y(4))/G
F3=1.
IF(0.GT.150.) F3=1.-(0-150.)/650.*.64
IF(0.GT.800.) F3=.36-.224*(0-800.)/2200.
IF(0.GT.3000.) F3=.136
O1=Y(15)*.7*F3
S2=Y(14)-15.+01*IF(S2.LT.0.) S2=0.
Y(17)=Y(16)/2.+S2*.161
Y(17)=Y(17)+2*Y(15)
S4=Y(14)-20.4+013*IF(S4.LT.0.) S4=0.
F4=.5
IF(OOP.GT..53) F4=.5-(OOP-.53)/1.26*1.5
IF(OOP.GT.1.79) F4=-1.
F2=Y(14)*F4
Y(18)=DE-F2
IF(APS(Y(18)).GT.25.) Y(18)=Y(18)/(1.+.RKA*(1.-25./A9S(Y(18))))
S6P=APS(DF)-25.*$1F(S6P.LT.0.) S6P=0.
S7P=A9S(Y(18))-25.*$1F(S7P.LT.0.) S7P=0.
S6=RKA+S7P*Y(18)/A9S(Y(18))

```

```

03=S6+5.*S6P*DE/ABS(DE)
S5=Q3/2.5/F3
PILOT=S5-Y(17)-S4/2.
IF(ABS(DEF).LT.1.75) DEF=0.
IF(ABS(DEF).GE.1.75) DEF=DEF/5.5*.88
IF(ABS(DEF).GT.5.) DEF=(.89+ABS(DEF-.5))/22.5*7.12)*DEF/ABS(DEF)
F11=2.
IF(PSOP0.GT..1.AND.PSOP0.LT..3) F11=-7.8*(PSOP0-1.)*2.
IF(PSOP0.GE..3.AND.PSOP0.LT..4) F11=-1.5*(PSOP0-.3)*44
IF(PSOP0.GE..4.AND.PSOP0.LT..7) F11=-.7*(PSOP0-.4)*29
IF(PSOP0.GE..7.AND.PSOP0.LT.1.) F11=-(.08/.3)*(PSOP0-.7)*.06
IF(PSOP0.GE.1.) F11=0.

GLF1=0.
IF(PSOP0.GT..145.AND.PSOP0.LT..3) GLF1=(PSOP0-.145)/.155
IF(PSOP0.GE..3) GLF1=1.

GLF2I=00P-F11
GLF2N=0.
IF(GLF2I.GT..33.AND.GLF2I.LT..46) GLF2N=.315*(GLF2I-.33)/.13
IF(GLF2I.GF..46.AND.GLF2I.LT..5) GLF2N=.315
IF(GLF2I.GE..6.AND.GLF2I.LT..2.7) GLF2N=-.315*(GLF2I-.6)/2.1+.315
IF(GLF2I.GF..2.7) GLF2N=0.

FUNC=GLF1*GLF2N
T2=2.*PILOT/(FUNC-1.)
Y(26)=T2/2.
FLMT=-1.
IF(0.GE.-34.) FLMT=-1.-(0-34.)/50.
IF(0.GE.184.) FLMT=-4.

T1=T2
IF(T1.GT.7.5) T1=7.5
IF(T1.LT.FLMT) T1=FLMT
DET=T1-DEF
CA=DF
Y(19)=Y(20)=C
Y(25)=DR*Y(23)=DA*Y(24)=DA*Y(21)=DE+DA/4.*$Y(22)=DE-DA/4.
PEAK=10.-ARS(Y(14))/10.*SF(ARS(Y(14)).*GT.10.)PEAK=0.

```

```

F7=0.*$IF(QOP.GT..187) F7=(JOP-.187)/.942
IF(QOP.GT.1.129) F7=1.
IF(QOP.GT.1.709.AND.QOP.LT.3.23) F7=1.- (QOP-1.709)/1.521
F8=.5$IF(QOP.GT.2.84)F8=(QOP-2.84)/.78+.5$IF(QOP.GT.3.23)F8=1.
S11=.0375*Y(14)-PEAK*.654=7$P2=S11*DA
AYT =((YP(2)-Y(3)*Y(4)+Y(1)*Y(6))/32.2)-CTHE*SFE
S13=.6*AYT*6+J.3PILOTR=DR-P2-S13*F8
PILOTA=-DA/.12+Y(4)*AV
ADRF=0.*$IF(ABS(NRF).GT.15.)ADRF=DRF-DRF/ABS(DRF)*15.*$DPT=PILOTR+AD
CRF$DAT=-PILOTA/1.67
DAT=-DAT
WRITE(6,206) DAT,DRT
206 FORMAT(* AILERON TRIM = *,F5.1,* Rudder TRIM = *,F5.1)
Y(27)=0.
F91=FR2=Y(28)=Y(29)=0.
Y(30)=1.6*(.5*Y(15)+Y(14)-2.)
IF ((Y(30)*GT.25.) Y(30)=25.
IF (Y(30).LT.0.) Y(30)=0.
Y(23)=DA$Y(22)=NE-DA/4.*3Y(24)=-DA$Y(21)=DE+DA/4.*3Y(25)=DR
IF (ABS(DET).GT.2.4) WRITE(6,205)
205 FORMAT (* JFLTA TRIM GREATER THAN 2.4 *)
WRITE(6,203) DET
203 FORMAT (* DELTA ELEVATOR TRIM IS = *,F5.1)
U1=THEO/2.
U2=SIGH0/2.
U3=FEO/2.
U4=COS(U1)
U5=SIN(U1)
U6=COS(U2)
U7=SIN(U2)
U8=COS(U3)
U9=SIN(U3)
FUDGE=91.*AV
***** INITIAL CONDITIONS FOR AIRCRAFT STATES *****
YP(8)=0.

```

```

YP(10)=0.
1F(T.LT.0.)GOTO24
Y(8)=U6*U4*U8+U5*U7*U9
Y(9)=U6*U4*U9-U5*U7*U8
Y(10)=U6*U5*U8+U7*U4*U9
Y(13)=0.

GO TO 25
24 Y(8)=THE0$Y(9)=SIGHO$Y(10)=FEO
25 CONTINUE
Y(11)=0.
Y(12)=0.
Y(13)=U7*U4*U8-U6*U5*U9
AL=ATAN2(Y(3),Y(1))
ALPHA=AL*AV
THE0=THFD*AV
FE0D=FE0*AV
SIGHO=SIGH*AV
P(J)=Y(4)*AV
Q(J)=Y(5)*AV
R(J)=Y(6)*AV
WRITE(6,197)
WRITE(6,198)
WRITE(6,199)
197 FORMAT(*1*,3X,*T*,6X,*U*,9X,*P*,8X,*THETA*,5X,*UDOT*,6X,*PDOT*,6X,
C*V2*,9X,*AX*,6X,*DF*,8X,*JH*,8X,*JAF*)
198 FORMAT(11Y,*V*,9X,*0*,8X,*PHI*,7X,*VDOT*,6X,*QDOT*,6X,*BETA*,7X,
C*AY*,8X,*NE*,8X,*NLEFF*,6X,*DEF*)
199 FORMAT(11Y,*W*,9X,*R*,8X,*PSI*,7X,*WDOT*,6X,*RDOT*,6X,*ALPHA*,6X,
C*A7*,8X,*DR*,8X,*NZ*,8X,*JRF*,//)
C *** "100" = EVERY .5 SECONDS
100$0.05=0.5
LTIMF=50
LOOP=2*LTIME
DO 77 J=1,LOOP
XL=J
RIT=XL/10.

```

```

IT=RIT
PERT=RIT-IT
IF (PERT.EQ.0.) WRITE(6,197)
IF (PERT.FN.0.) WRITE(6,199)
IF (PERT.E0.0.) WRITE(6,199)
DO 75 JFK=1,100
IF (T.LT..005)
CWRITE(6,200) T,Y(1),Y(4),THETA(J),YP(1),VR,AX(J),DF,DH,DAF
CWRITE(6,2(1) Y(2),Y(5),PHI(J),YP(2),YP(5),BETA,AY(J),DE,DLEF,DEF
IF (T.LT..005)
CWRITE(6,2(2) Y(3),Y(6),PSI(J),YP(3),YP(6),ALPHA,AZ(J),DR,NZ(J),DRC
C,Y(7)
CALL CONTROL(T)
CALL RKXYZ(T,Y,YP,30,.005,1.000005,GYRATES)
IF(Y(18).GT.100.) Y(18)=100.
IF(Y(19).LT.-100.) Y(18)=-100.
76 CONTINUE
***** STOPAGE OF PARAMETERS FOR PLOTTING *****
AX(J)=((YP(1)-Y(2)*Y(6)+Y(3)*Y(5))/32.2)+STHE
AY(J)=((YP(2)-Y(3)*Y(4)+Y(1)*Y(6))/32.2)-CTHE*SFE
AZ(J)=((YP(3)-Y(1)*Y(5)+Y(2)*Y(4))/32.2)-CTHE*CFE
NZ(J)=-A7(J)
DEFP(J)=DEF
DAFP(J)=DAF
DRFP(J)=DRF
DELE(J)=DE
DELR(J)=DR
DELA(J)=DF
THRST(J)=THRUS
***** TURNS ABOUT THE GRAVITY VECTOR
TGV(J)=SIGH*AV
IF (SIGH.LT.-PI) SIGH=SIGH+TOP1
IF (SIGH.GT.PI) SIGH=SIGH-TOP1
DIST(J)=Y(11)

```

```

TRAV(J)=Y(12)
BETAD(J)=BETA
VEL(J)=VR
P(J)=Y(4)*AV
Q(J)=Y(5)*AV
R(J)=Y(6)*AV
ALT(J)=Y(7)
THETA(J)=TH *AV
PSI(J)=SINH*AV
PHI(J)= FE*AV
ALPHAD(J)=ALPHA
IF( FE.LT.-PI) FE= FE+TOP1
IF( FE.GT.PI) FE= FE-TOP1
TIME(J)=T
CALL SECOND(CPTM)
IF(CPTM.GT.300.)GOT0618
WRITE(6,20J) T,Y(1),P(J),THETA(J),YP(1),YP(4),VR,AX(J),NF,DH,DAF
WRITE(6,21J) Y(2),O(J),PHI(J),YP(2),YP(5),BETA,AY(J),NE,DLEF,DEF
WRITE(6,22J) Y(3),R(J),PSI(J),YP(3),YP(6),ALPHA,AZ(J),OR,NZ(J),DRF
C,ALT(J)
200 FORMAT(1X,F4.1,2X,1C(F7.2,3X))
201 FORMAT(7X,10(F7.2,3X))
202 FORMAT(7X,11(F7.2,3X),//)
77 CONTINUE
GO TO 616
618 LOOP=J-1
619 CONTINUE
C *** PLACE STOP CARD HERE TO STOP PLOT ROUTINE
CALL PLOT(0.,-12.,-3)
CALL PLOT(J.*1.,-3)
CALL SCALF(TIME,5.,LOOP,1)
CALL SCALF(ALPHAD,2.,LOOP,1)
CALL SCALE(BETA,2.,LOOP,1)
CALL SCALF(VEL,2.,LOOP,1)
CALL SCALF(P,2.,LOOP,1)

```

```

CALL SCALE(0,2.,LOOP,1)
CALL SCALE(P,2.,LOOP,1)
CALL SCALE(THETA,2.,LOOP,1)
CALL SCALE(PSI,2.,LOOP,1)
CALL SCALE(DEFP,2.,LOOP,1)
CALL SCALE(DAEP,2.,LOOP,1)
CALL SCALE(DDFP,2.,LOOP,1)
CALL SCALF(NELF,2.,LOOP,1)
CALL SCALF(NELR,2.,LOOP,1)
CALL SCALE(DELTA,2.,LOOP,1)
CALL SCALE(MZ,2.,LOOP,1)
CALL SCALE(ALT,2.,LOOP,1)
L=LOOP+1
M=LOOP+2
PHI(L)=TCV(L)=-180.
PHI(M)=TCV(M)=180.
CALL AXIS(0.,0.,10H TIME - SEC,-10,5.,0.,TIME(L),TIME(M))
CALL AXIS(0.,0.,17H VELOCITY - FT/SEC,17,2.,90.,VEL(L),VEL(M))
CALL LINE(TIME,VEL,LOOP,1,0,75)
CALL PLOT(0.,3.0,-3)
CALL AXIS(0.,0.,10H TIME - SEC,-10,5.,0.,TIME(L),TIME(M))
CALL AXIS(0.,0.,10H BETA - DEG,10,2.,90.,BETAD(L),BETAD(M))
CALL LINE(TIME,BETAD,LOOP,1,0,75)
CALL PLOT(0.,3.0,-3)
CALL AXIS(0.,0.,10H TIME - SEC,-10,5.,0.,TIME(L),TIME(M))
CALL AXIS(0.,0.,11H ALPHA - DEG,11,2.,90.,ALPHAD(L),ALPHAD(M))
CALL LINE(TIME,ALPHAD,LOOP,1,0,75)
CALL PLOT(16.,-15.,-3)
CALL PLOT(0.,1.5,-3)
CALL AXIS(0.,0.,12H TIME - SEC,-10,5.,0.,TIME(L),TIME(M))
CALL AXIS(0.,0.,11H - DEG/SEC,11,2.,90.,P(L),P(M))
CALL LINE(TIME,P,LOOP,1,0,75)
CALL PLOT(0.,3.0,-3)
CALL AXIS(0.,0.,10H TIME - SEC,-10,5.,0.,TIME(L),TIME(M))
CALL AXIS(0.,0.,11H - DEG/SEC,11,2.,90.,Q(L),Q(M))

```

```

CALL LINE(TIME,0,LOOP,1,0,75)
CALL PLOT(0.,3,C,0,-3)
CALL AXIS(0.,0.,10H TIME - SEC, -10,5,0,TIME(L),TIME(M))
CALL AXIS(0.,0.,11HP - DEG/SEC,11,2,90.,R(CL),R(M))
CALL LINE(TIME,P,LOOP,1,0,75)
CALL PLOT(16.,2,-15.,0,-3)
CALL PLOT(0.,1.5,-3)
CALL AXIS(0.,0.,10H TIME - SEC, -10,5,0,TIME(L),TIME(M))
CALL AXIS(0.,0.,11HTHETA - DFG,11,2,90.,THETA(L),THETA(M))
CALL LINE(TIME,THETA,LOOP,1,0,75)
CALL PLOT(0.,3.0,-3)
CALL AXIS(0.,0.,10H TIME - SEC, -10,5,0,TIME(L),TIME(M))
CALL AXIS(0.,0.,9H PHI - DEG,9,2,90.,PHI(L),PHI(M))
CALL PLOT(0.,1.0,-3)
DO27 J=1,LOOP
XX=TIME(J)/TIME(M)
YY=PHI(J)/PHI(M)
27 CALL PLOT(XY,YY,2)
CALL PLOT(C.,2.0,-3)
CALL AXIS(0.,0.,10H TIME - SEC, -10,5,0,TIME(L),TIME(M))
CALL AXIS(0.,0.,9H PSI - DEG,9,2,90.,PSI(L),PSI(M))
CALL LINE(TIME,PSI,LOOP,1,0,75)
CALL PLOT(16.,-12.,-3)
CALL PLOT(0.,1.5,-3)
CALL AXIS(0.,0.,10H TIME - SEC, -10,5,0,TIME(L),TIME(M))
CALL AXIS(0.,0.,18HAIRERON DISP - DEG,18,2,90.,DELA(L),DELA(M))
CALL AXIS(-5.,0.,17HAIRERON FORCE-LBS,17,2,90.,DAFP(L),DAFP(M))
CALL LINE(TIME,DAFP,LOOP,1,10,5)
CALL LINE(TIME,DELA,LOOP,1,0,75)
CALL PLOT(0.,2.0,-3)
CALL AXIS(0.,0.,10H TIME - SEC, -10,5,0,TIME(L),TIME(M))
CALL AXIS(0.,0.,19HELEVATOR DISP - DEG,19,2,90.,DELE(L),DELE(M))
CALL AXIS(-5.,0.,18HELEVATOR FORCE-LBS,18,2,90.,DEFP(L),DEFP(M))
CALL LINE(TIME,DEFP,LOOP,1,10,5)
CALL LINE(TIME,DELE,LOOP,1,0,75)

```

```

CALL PLOT(0., 3.0, -3)
CALL AXIS(0., 0., 10H TIME - SEC, -10, 5., 0., TIME(L), TIME(M))
CALL AXIS(0., 0., 17H RUDDER DISP - DEG, 17, 2., 90., DELR(L), DELR(M))
CALL AXIS(-.5, 0., 16H RUDDER FORCE-LRS, 16, 2., 90., DRFP(L), DRFP(M))
CALL LINE(TIME, DRFP, LOOP, 1, 10, 5)
CALL LINE(TIME, DELR, LOOP, 1, 0, 75)
CALL PLOT(16., -15., -3)
CALL PLOT(0., 1., 5., -3)
CALL AXIS(0., 0., 10H TIME - SEC, -10, 5., 0., TIME(L), TIME(M))
CALL AXIS(0., 0., 23H NORMAL ACCELERATION - G, 23, 2., 90., NZ(L), NZ(M))
CALL LINE(TIME, NZ, LOOP, 1, 0, 75)
CALL PLOT(0., 3.5, 1., -2)
CALL AXIS(0., 0., 10H TIME - SEC, -10, 5., 0., TIME(L), TIME(M))
CALL AXIS(0., 0., 13H ALTITUDE - FT, 13, 2., 90., ALT(L), ALT(M))
CALL LINE(TIME, ALT, LOOP, 1, 50, 5)
CALL PLOT(5., -17., -2)
CALL PLOT(STOP)
END

```

```

SUBROUTINE GYRATES(T,Y,YP)
DIMENSION Y(30),YP(30)
COMMON/TIME/CYCLE
COMMON/CHECK/SUMCX,SUMCZ,SUMCM,CN,CNQ,CC,CCQ,CMD,E,CMQ
COMMON/CHFCCK2/CNB,CNR,CNP,CNDR,CNDH,CNDF,CLDF,CLDH,CLP,CLR,
CCLDR,CLB
COMMON/PARAM/ECH(49,5),ECV(49),FCD(49,5),ECC(49,5),ECMO(49,5),
1ECMO(49),ECLB(49,9),ECLNF(49),ECLD(49),ECLP(49),ECLR(49),
2ECH(49,9),ECNDF(49),ECNTR(49),ECNP(49),ECNR(49),FCY(49),
3ECYDF(49),ECYDR(49)
COMMON/GEOF/MASS,C,B,THRUS,CG
COMMON/REST/A1,A2,A3,A4,B1,B2,B3,B4,C1,C2,C3,C4,D1,AV,
1FUOGF,CEPS,SEPS,STHE,CTHE,SFE,CFF,RVR2,POH,G,VP,THE,FE,SIGH,
2ALPHA,BETA,OR,DE,OF,OH,NLEF,NEC,DRC,DFC,DHC
COMMON/BIAS/AC,AA,AB,J1,J3,S7,S8,TH
COMMON/STICK/DET,DAT,ORT,DEF,DAF,DRF,FR1,FR2
COMMON/THRUST/SOSFS(3),TWILT(3,11)
C,TSAVE
      REAL MASS
      PS=2116.37*((1.0-.00000687535*Y(7))*5.2561)
      ROH=.002378*((1.0-.00000688*Y(7))*4.256)
      IF (ABS(Y(1)).LT.1.E-20) GOT052
      AL=ATAN2(Y(3),Y(1))
      GO TO 54
 53  AL=SIGN(FUNGE,Y(3))
 54  CONTINUE
      VR=SDPT(Y(1)**2+Y(2)**2+Y(3)**2)
      RVR2=FOH*(VR**2)
      VCVR=Y(2)/VR
      BE=ASIN(VCVR)
      ALPHA=AL+AV
      PETA=BE+AV
      IF (T.LT.0.) GOT052
      EP=1.-(Y(6)*Y(9)+Y(0)*Y(9)+Y(10)*Y(10)+Y(13)*Y(13))
      C11=Y(8)*Y(8)+Y(9)*Y(9)-Y(10)*Y(10)-Y(13)*Y(13)

```

```

C12=2.* (Y(9)*Y(10)+Y(8)*Y(13))
C13=2.* (Y(9)*Y(13)-Y(8)*Y(10))
C23=2.* (Y(10)*Y(13)+Y(8)*Y(9))
C33=Y(8)*Y(8)+Y(13)*Y(13)-Y(9)*Y(9)-Y(10)*Y(10)
FE= ATAN2(C27,C33)
IF(C13.GT.1.) C13=-1.
IF(C13.LT.-1.) C13=-1.
SIGH= ATAN2(C12,C11)
THE= ASIN(-C13)
TH=THE
GO TO 51
52 FE=Y(10)
SIGH=Y(9)
THE=Y(8)
51 CONTINUE
SFE=SIN(FE)
CFE=COS(FE)
STHE=SIN(THE)
CTHE=COS(THE)
SPSI=SIN(SIGH)
CPSI=COS(SIGH)
IF(T.GE.15.5) GO TO 99
IF(T.GE.1F.) Y(5)=+20./AV
99 IF(ABS(CTHE).LT..001) CTHE=.001
PT =Y(4)*AV
QT =Y(5)*AV
RT =Y(6)*AV
AXT =((YP(1)-Y(2)*Y(6)+Y(3)*Y(5))/32.2)*STHE
AYT =((YP(2)-Y(3)*Y(4)+Y(1)*Y(6))/32.2)-CTHE*SFE
AZT =((YP(3)-Y(1)*Y(5)+Y(2)*Y(4))/32.2)-CTHE*CFE

```

***** YF-16 STABILITY AUGMENTATION SYSTEM *****

```

WRITE GEO
Q=RVR2/2.
OP=0/PS
IF(T.LT.0.)GOT056

```

C *** LONGITUDINAL AUGMENTATION ***

```

DEC=0.
DEF1=A9S(DEF)
IF(DEF1.GT.1.75.AND.DEF1.LT.7.25)DEC=(.88/5.5)*(DEF1-1.75)
IF(DEF1.GE.7.25)DEC=(7.12/23.75)*(DEF1-7.25)+.88
IF(DEF.LT.0.)DEC=-DEC
DEC=DEC+DET
C *** ELEVATOR "G" LIMITERS & PILOT WASHOUT REMOVED FROM FCS
GO TO 993
REMOVE
REMOVE
IF(DEC.GT.8.)DEC=8.
DEC1=-1.
IF(0.GT.34.)DEC1=-3.* (Q-34.)/150.-1.
IF(DEC1.LT.-4.)DFC1=-4.
IF(DEC.LT.DEC1)DFC=DEC1
DEC=.5*DEC
C *** YP(26)=8.3*(DEC-Y(26)), NEW MODIFICATION
YP(26)=4.*(DEC-Y(26))
PO=211E.2 $ PSOP0=PS/PO
F11=2.
IF(PSOP0.GT..1.AND.PSOP0.LT..3)F11=-7.8*(PSOP0-.1)+2.
IF(PSOP0.GE..3.AND.PSOP0.LT..6)F11=-1.5*(PSOP0-.3)+.44
IF(PSOP0.GE..4.AND.PSOP0.LT..7)F11=-.7*(PSOP0-.4)+.29
IF(PSOP0.GE..7.AND.PSOP0.LT.1.)F11=(-.08/.3)*(PSOP0-.7)+.08
IF(FSOP0.GE.1.)F11=0.
GLF1=0.
IF(PSOP0.GT..145.AND.PSOP0.LT..3)GLF1=(PSOP0-.145)/.155
IF(PSOP0.GE..3)GLF1=1.
GLF2J=00P-F11

```

```

GLF2N=0.
IF(GLF2I.GT..33.AND.GLF2I.LT..46)GLF2N=.315*(GLF2I-.33)/.13
IF(GLF2I.GE..46.AND.GLF2I.LT..6)GLF2N=.315
IF(GLF2I.GE..6.AND.GLF2I.LT..2.7)GLF2N=-.315*(GLF2I-.6)/2.1+.315
IF(GLF2I.GE..2.7)GLF2N=].
DEC1=Y(26)+GLF1*GLF2N
DEC=DEC1-Y(26)
CONTINUE$NEC=-0.5*DEC
REMOVE
F0=ALPHA
IF(ALPHA.LE.-5.)F0=-5.
IF(ALPHA.GE.30.)F0=70.
YP(14)=10.* (F0-Y(14))
YP(15)=(YP(5)*AV)-Y(15)
YP(16)=15.* (-A7T-1.-Y(16))
S1=.5*Y(16)+.2*Y(15)
DS1=.5*YP(16)+.2*YP(15)
IF(0.LE.-150.)Q1=.7*Y(15)
IF(0.LE.-150.)D1=.7*YP(15)
IF(0.GE.-7000.)Q1=.0952*Y(15)
IF(0.GE.-3000.)D1=.0952*YP(15)
IF(0.GT.150..AND.0.LE.-800.)Q1=Y(15)*(0.7+(150.-Q)*(0.448/650.))
IF(0.GT.150..AND.0.LE.-800.)D1=Y(15)*(0.7+(150.-Q)*(0.448/650.))
IF(0.GT.-800..AND.0.LT.-3000.)Q1=Y(15)*(0.252+(800.-Q)*(0.1568/2200.))
IF(0.GT.-800..AND.0.LT.-3000.)D01=Y(15)*(0.252+(800.-Q)*(0.1568
1/2200.))

C *** CHANGE S2 FOR 1ST LFVEL ALPHA COMPARATOR
S2=Q1+Y(14)-15.
DS2=Q1+YP(14)
IF(S2.LE.0.)S3=S1
IF(S2.LE.0.)DS7=DS1
IF(S2.GT.0.)S3=S1+.161*DS2
IF(S2.GT.0.)DS7=Q1+.161*DS2
C *** CHANGE S4 FOR 2ND LEVEL ALPHA COMPARATOR
S4=Y(14)+Q1-20.4

```

```

YP(17)=3.*QS3+15.*((S3-Y(17))
IF(S4.GT.0.)S5=Y(17)+.5*S4+DEC
IF(S4.LE.0.)S5=Y(17)+DEC
IF(Q.LE.15.)Q3=2.*5*SS
IF(0.GE.?)Q0.=0.3=.34*SS
IF(0.GT.150..AND.0.LE.800.)Q3=(2.5+(150.-Q)*(1.6/650.))*SS
IF(0.GT.800..AND.0.LT.3000.)Q3=(.3+(800.-Q)*(.56/2200.))*SS
IF(0OP.LF.*53)F2=.5*Y(14)
IF(0OP.GF.*1.79)F2=-Y(14)
IF(0OP.GT.*53.AND.0OP.LT.1.79)F2=Y(14)*(.5+(.53-QOP)*(1.5/1.26))
S9=F2+03
S8=S9+Y(19)
IF(APS(S8).LE.25.)05=0.
IF(S3.GT.25.)05=(S8-25.)*5.
IF(S8.LT.-25.)05=(S8+25.)*5.
S6=Q3-05
IF(A2S(Y(18)).LE.25.)S7=SS
IF(Y(18).GT.25.)S7=S6-10000.*((Y(18)-25.))
IF(Y(18).LT.-25.)S7=S6-10000.*((Y(18)+25.))
YP(18)=5.*S7
IF(YP(18).GT.100000.)YP(18)=100000.
IF(YP(18).LT.-100000.)YP(18)=-100000.
S10=S9+Y(18)

```

C *** LATERAL-DIRECTIONAL AUGMENTATION ***

DRC=0.

```

C *** RUDDER PEDAL FORCE
DTR=AQS(DRF)
C *** RUDDER BREAKOUT FORCE UPDATED FROM 20 LB. TO 15 LB.
IF(INTP.LE.15.)DRF3=0.
IF(DRF.GT.15.)DRF3=(DRF-15.)*(30./95.)
IF(DRF.LT.-15.)DRF7=(DRF+15.)*(30./95.)

```

DRC=DRF3-DRT
DAC=0.

C *** AILERON STICK FORCE

DAF1=0.
ADAF=ABS(DAF)
IF (ADAF.LT.0.001) ADAF=.001
IF (ADAF.LE.1.) DAF1=0.
IF (ADAF.LT.6.1) DAF1=((ADAF-1)/5.1*35.)*DAF/ADAF
IF (ADAF.GE.5.1) DAF1=(35.*((ADAF-6.1)/5.1*70.))*DAF/ADAF
IF (ADAF.GE.11.2) DAF1=(105.*((ADAF-11.2)/5.1*175.))*DAF/ADAF
IF (ADAF.GE.16.3) DAF1=200.*DAF/ADAF
Y29=Y29=0.
IF (Y(28).GT.0.) Y28=Y(28)
IF (Y(29).LT.0.) Y29=Y(29)
T21=DAF1-Y28-Y29
YP(27)=10.*T21-10.*Y(27)
TU=TL=0.
IF (Y(27).LT.0.) TL=YP(27)
IF (Y(27).GT.0.) TU=YP(27)
YP(28)=6.*TU-20.*Y(28)
YP(29)=6.*TL-20.*Y(29)
Y(27)=DAF1
DAD=Y(27)+DAT*1.67
P1=.12*(AV*Y(4)-DAC)
IF (P1.GT.20.) P1=20.
IF (P1.LT.-20.) P1=-20.
P4=0.
IF (Y(14).GT.0..AND.Y(14).LE.10.) P4=.65-.065*Y(14)
IF (Y(14).LE.0..AND.Y(14).GE.-10.) P4=.65+.065*Y(14)
P5=0.
IF (DOP.GE.1.129.AND.DOP.LE.1.709) P5=P4
IF (DOP.GT..187.AND.DOP.LT.1.129) P5=(1./.942)*(DOP-.187)*P4
IF (DOP.GT.1.709.AND.QOP.LT.3.23) P5=(1./1.521)*(3.23-QOP)*P4
S11=.0375*Y(14)-P5

REMOVE

```

P2=P1*S11
S17=2.*P1
S18=S10+-125*S17
S19=S10+125*S17
P3=Y(14)*AV*Y(4)/57.3
CP3=(YP(14)*AV*v(4)/57.3)+(Y(14)*AV*YP(4)/57.3)
S12=AV*Y(F)-P3
DS12=AV*YP(5)-D3
YP(19)=1.*P1*S12-Y(19)
YP(20)=3.*YP(19)+15.*((Y(19)-Y(20)))
S13=Y(20)+19.32*AYT
S14=P2+S13
IF(0.0P.LE.-2.04) S14=P2+5*S13
IF(0.0P.GT.-2.04.AND.0.0P.LT.-3.23) S14=P2+S13+ (.5+(.5/1.19)*(0.0P-2.04))
1)

C *** ACTUATOR DYNAMICS AND CONTROL SURFACE POSITIONS
YP(21)=20.* (S19-Y(21))
YP(22)=20.* (S18-Y(22))
YP(23)=20.* (P1-Y(23))
YP(24)=20.* (-P1-Y(24))
YP(25)=20.* (S14-DPC-Y(25))
IF(YP(21).GT.6.0.)YP(21)=60.
IF(YP(22).GT.6.0.)YP(22)=60.
IF(YP(23).GT.5.6.)YP(23)=56.
IF(YP(24).GT.5.6.)YP(24)=56.
IF(YP(25).GT.120.)YP(25)=120.
IF(YP(21).LT.-60.)YP(21)=-60.
IF(YP(22).LT.-56.)YP(22)=-56.
IF(YP(23).LT.-56.)YP(23)=-56.
IF(YP(24).LT.-56.)YP(24)=-56.
IF(YP(25).LT.-56.)YP(25)=-56.
IF(Y(21).GT.25.)Y(21)=25.
IF(Y(22).GT.25.)Y(22)=25.
IF(Y(23).GT.20.)Y(23)=20.

```

```

IF(Y(24).GT.20.)Y(24)=20.
IF(Y(25).GT.30.)Y(25)=30.
IF(Y(21).LT.-25.)Y(21)=-25.
IF(Y(22).LT.-25.)Y(22)=-25.
IF(Y(23).LT.-20.)Y(23)=-20.
IF(Y(24).LT.-20.)Y(24)=-20.
IF(Y(25).LT.-30.)Y(25)=-30.
DE=.5*(Y(21)+Y(22))
DH=-.5*(Y(21)-Y(22))
DF=Y(23)
DR=Y(25)

C *** DLEF SCHEMULING
DLEFT=2.1*(.5*Y(15)+Y(14)-2.)
DLEFT=DLEFT*1.6/2.1
IF(DLEFT.GT.25.0)DLEFT=25.0
IF(DLEFT.LT.0.)DLEFT=0.
IF(YP(30)=5.* (DLEFT-Y(30))
IF(YP(30).GT.30.)YP(30)=30.
IF(YP(30).LT.-30.)YP(30)=-30.
IF(Y(30).GT.25.)Y(30)=25.
IF(Y(30).LT.0.)Y(30)=0.
DLEFT=Y(30)
AA=F1 & AR=F2
CONTINUE
RIALTF=Y(7)/5000.+1.
IALTF=IALTF
PERIALF=PERIALF-IALTF
SOS=(SOS*(IALTF+1)-SOS=S*(IALTF))*PERIALF+SOS*(IALTF)
AMACH=VR/SOS
RIAMACH=AMACH/.1+.1.

IAMACH=RIAMACH
PERIAM=RIAMACH-IAMACH
TMILT1=(TMILT(IAMACH+1,IAMACH,IALTF))*PERIAM
+TMILT(IAMACH,IALTF)
TMILT2=(TMILT(IAMACH+1,IAMACH,IALTF+1))-TMILT(IAMACH,IALTF+1))

```

```

2 *PERIAM+TMILT*(IAMACH,IAITF+1)
TMIL=(TMILT2-TMILT1)*PERIALF+TMILT1
THRUS=TMIL

THRUT=TMIL
IF(TMIL.LT.1.) THRUT=1.
IF(ITLE.*.05) THRUT=THRUT
THRUS=THRUT/THRUT*TSAVE
*6 CONTINUE

TOM=THRUS/MASS
***** AIRCRAFT STATE EQUATIONS AND EULER RELATIONS *****
C *** INTERPOLATION ON ALPHA
DELH=DE
RIA=25.*ALPHA/5.
IF ((ABS(ALPHA)).GT.120.) STOP "ALPHA"
IA=RIA
PERA=RIA-IA

C *** INTERPOLATION ON BETA
RIB=1.*ABS(BETA)/5.
IF (ABS(BETA).GT.40.) RI B=9.
IB=PI3

PER9=PIB-IA
C *** INTERPOLATION ON DLFF
PERD=OLEF/25.
C *** INTERPOLATION ON DELH
RIH1=Z.*DFLH/10.
IH1=PIH1
IF(DELH.GT.10.) IH1=4
IF(DELH.EN.25.) IH1=5
IF(DELH.LT.-10.) IH1=1
PERH1=RIH1-IH1
IF(DELH.GT.10.) PERH1=(DELH-10.)/15.
IF(DELH.EN.25.) PERH1=0.
IF(DFLH.LT.-10.) PERH1=(DE-H+25.)/15.

C *** DETERMINATION OF AERO PARAMETERS
CM01=(ECMO(IA+1,IH1)-ECMO(IA,IH1))*PERA+ECMO(IA,IH1)

```

```

CM02=(ECMO((IA+1, IH1+1))-ECMO((IA, IH1+1))*PERA+ECMO((IA, IH1+1))
CM0=(CM02-CM01)*PEPH1+CM01
CMQ=(ECM0((IA+1))-ECM0((IA)))*PERA+ECM0((IA))
CNQ=(ECN0((IA+1))-ECN0((IA)))*PERA+ECN0((IA))
CCQ=(ECC0((IA+1))-ECC0((IA)))*PERA+ECC0((IA))
CY3=(ECY3((IA+1))-ECY3((IA)))*PERA+ECYB((IA))
CLD2=(ECLDR((IA+1))-ECLDR((IA)))*PERA+ECLDR((IA))
CYDR=(ECYDR((IA+1))-ECYDP((IA)))*PERA+ECYDR((IA))
CHDR=(ECNDR((IA+1))-ECNDP((IA)))*PERA+ECNDR((IA))
CNP=(ECNP((IA+1))-ECNP((IA)))*PERA+ECNP((IA))
CNP=(ECNR((IA+1))-ECNP((IA)))*PERA+ECNR((IA))
CLP=(ECLP((IA+1))-ECLP((IA)))*PERA+ECLP((IA))
CLR=(ECLP((IA+1))-ECLP((IA)))*PERA+ECLP((IA))
CHDF=(ECNDF((IA+1))-ECNDF((IA)))*PERA+ECNDF((IA))
CLDF=(ECLDF((IA+1))-ECLDF((IA)))*PERA+ECLDF((IA))
CYDF=(ECYDF((IA+1))-ECYDF((IA)))*PERA+ECYDF((IA))
CHR1=(ECNR((IA+1, IR))-ECN((IA, IR)))*PERA+ECNR((IA, IR))
CLB1=(ECLB((IA+1, IR))-ECLB((IA, IR)))*PERA+ECLB((IA, IR))
CNB2=(ECN((IA+1, IR+1))-ECV3((IA, IR+1)))*PERA+ECNB((IA, IR+1))
CLB2=(ECLB((IA+1, IR+1))-ECLB((IA, IR+1)))*PERA+ECLB((IA, IR+1))
CHB=(CNB2-CM01)*PERP+CH91
CLB=(CLB2-CLB1)*PERP+CLB1
CH1=(ECN((IA+1, IH1))-ECN((IA, IH1)))*PERA+ECN((IA, IH1))
CN2=(ECN((IA+1, IH1+1))-ECN((IA, IH1+1)))*PERA+ECN((IA, IH1+1))
CH=(CN2-CM1)*PEPH1+CM1
CC1=(ECC((IA+1, IH1))-ECC((IA, IH1)))*PERA+ECC((IA, IH1))
CC2=(ECC((IA+1, IH1+1))-ECC((IA, IH1+1)))*PERA+ECC((IA, IH1+1))
CC=(CC2-CC1)*PEPH1+CC1
C * * * TOTAL AERODYNAMIC COEFFICIENTS
IF (BETA.LT.0.) CL9=-CL9
IF (BETA.LT.0.) CHB=-CHB
SUMCY=CYA*BETA+CYD*ND+CYDF*DF
SUMCX=CC-(P4/VP)*CC0*Y(5)
SUMCN=CN3+CNDP*NR*CNDF*DF+(C4/VR)*(CNF*Y(4)+CNR*Y(6))

```

```

SUMCL=CL9+CLDR*CLDF*DF+(A4/VR)*(CLP*Y(4)+CLR*Y(6))
SUMCM=CM0+(PL/VR)*CM0*Y(5)
SUMCN=SUMCM-(CG-.35)*SUMCZ
SUMCY=SUMCN*(CG-.35)*C*SUMCY/B
YP(1)=-G*ST-E+Y(2)*Y(6)-Y(3)*Y(5)+2*VR2*D1*SUMCX+TOM*CEPS
YP(2)=G*CTHE*SFE+Y(3)*Y(4)-Y(1)*Y(6)+RVR2*D1*SUMCY
YP(3)=G*CTHE*CFF+Y(1)*Y(5)-Y(2)*Y(4)+QVR2*D1*SUMC7+TOM*SEPS
YP(4)=(A1*Y(5)*Y(6)+A2*(Y(4)*Y(5)*(1.+C1)-C2*Y(5)*Y(6)+C3*QVR2*
1*SUMCN)+A3*QVR2*SUMCL)/(1.-A2*C2)
YP(5)=B1*Y(4)*Y(6)+P2*(Y(6)*2-Y(4)*2)+RVR2*B3*SUMCM
YD(6)=C1*Y(4)*Y(5)+C2*(YP(4)-Y(5)*Y(6))+RVR2*C3*SUMCN
YP(7)=Y(1)*STHE-Y(2)*CTHE*SFE-Y(3)*CTHE*CFF
IF(T.LT.0.)GOT049
YP(8)=.5*(-Y(9)*Y(4)-Y(12)*Y(5)-Y(13)*Y(6))+2.*EP*Y(8)
YP(9)=.5*(Y(8)*Y(4)+Y(10)*Y(6)-Y(13)*Y(5))+2.*EP*Y(9)
YP(10)=.5*(Y(8)*Y(5)-Y(9)*Y(6)+Y(13)*Y(4))+2.*EP*Y(10)
GO TO 50
L9 YP(8)=Y(5)*CFE-Y(6)*SFE
YD(9)=(Y(E)*SFE+Y(6)*CFE)/CTHE
YP(10)=Y(4)+YP(?)*STHE
F0 CONTINUE
YP(11)=Y(1)*CTHE*CPSI+Y(2)*(SFE*STHE*CPSI-CFE*SPSI)+Y(3)*(CFE*STHE
1*CPSI+SFE*SPSI)
YP(12)=Y(1)*CTHE*SPSI+Y(2)*(SFE*STHE*SPSI+CFE*CPSI)+Y(3)*(CFE*STHE
1*SPSI-SFE*CPSI)
YP(13)=.5*(Y(8)*Y(6)+Y(9)*Y(5)-Y(10)*Y(4))+2.*EP*Y(13)
RETURN
END

```

```

SUBROUTINE CONTROL(T)
COMMON/STICK/DET,DAT,ORT,DEF,DAF,DRF,FB1,FB2
COMMON/STICKF/ DRAFT(93),DRFT(93),DEFT(93),
COMMON/REST/A1,A2,A3,A4,B1,B2,B3,B4,C1,C2,C3,C4,D1,AV,
1FUDGE,CEPS,SEPS,STHF,CTHE,SFE,CFF,RVR2,ROH,G,VR,THE,FE,SIGH,
ZALPHA,BETA,DR,DF,DH,DLEF,DC,NRC,DFC,NHC
COMMON/TRTM/RED,GAMAD,AL,EN, SUMCY,RLIFT,XCY,TCONST,GCONST
C,THEO,SIGH0,FF0
COMMON/FLY/BEND
BT=T
RIC=9T*2.+1.
IC=PIC
PERPIC=PIG-IC
IF (T.GE.15.) DAF=SDAF
IF (T.GE.15.) GO TO 1
IF(FE.LT.FEO) DAF=((FEO-FE)*AV+1)*2.
IF(FE.GT.FEO) DAF=((FEO-FE)*AV-1)*2.
SDAF=DAF
IF(FE.EQ.FEO) DAF=SDAF
DEF=DRF=0.
      RETURN
      END

```

```

SUBROUTINE PKGXYZ(X,Y,P3,N,DX,EMAX,F)
DIMENSION Y(30),Y0(30),YT(30),YP(30),P0(30),P1(30),P2(30),P3(30)

X0=X
X=X+DX
H=H+H
H=0.5*(X-X0)
IF (ABS(X-X0)-ABS(H))1,3,3
DO 4 I=1,N
YC(I)=Y(I)
HT=H
XT=XJ
DO 5 I=1,N
YT(I)=Y0(I)
ASSIGN 6 TO K
GO TO 20
DO 7 I=1,N
YP(I)=Y(I)
HT=0.5*H
ASSIGN 9 TO K
GO TO 20
DO 10 I=1,N
YT(I)=Y(I)
XT=X2+HT
ASSIGN 11 TO K
CALL F(XT,YT,P0)
DO 21 I=1,N
Y(I)=YT(I)+C*.5*HT*P0(I)
CALL F(XT+0.5*HT,Y,P1)
DO 22 I=1,N
Y(I)=YT(I)+HT*(.207106781*P0(I)+.292893219*P1(I))
CALL F(XT+0.5*HT,Y,P2)
DO 23 I=1,N
Y(I)=YT(I)+HT*(.777106781*(P2(I)-P1(I))+P2(I))
CALL F(XT+HT,Y,P3)
DO 24 I=1,N

```

```

24      YT(I)=YT(I)+HT*(P0(I)+.585795438*P1(I)+3.41421356*P2(I)+P3(I))/5.0
      GO TO K,(6,9,11)
11      RMAX=0
      DO 12 I=1,N
      R=ANS((0.03*(Y(I)-YP(I)))/Y(I))
      IF(ABS(Y(I))-LT.EMAX).LT.EMAX)R=ANS((0.03*(Y(I)-YP(I)))/EMAX)
      RMAX=AMAX1(R,RMAX)
      Y(I)=Y(I)+(Y(I)-YP(I))/15.0
      IF(RMAX-EMAX)>13,13,17
13      X0=X0+H
      IF(X0-X)>15,14,15
      RETURN
14      IF(RMAX-0.03*EMAX)>30,30,2
15      H=HT
      XT=X0
      DO 19 I=1,N
16      YP(I)=YT(I)
17      YT(I)=YD(I)
      GO TO 6
      END
18
19

```

```

SUBROUTINE TURNTRM(Y,YP,YC)
DIMENSION Y(30),YP(30),Y(7)
COMMON/GEOM/MASS,C,B,THRUS,CG
COMMON/REST/A1,A2,A3,A4,91,B2,B3,B4,C1,C2,C3,C4,O1,AV,
1FUDGE,CEPS,SEPS,STHE,CTHE,SFE,CFE,RVR2,ROH,G,V,THE,FE,SIGH,
2ALPHA,BETA,DR,DF,DF,DH,DLEF,DEC,DRC,DFC,DHC
COMMON/CHECK/SUMCX,SUMC7,SUMCM,CN,CNQ,CC,CCQ,CMO,CMDE,CMQ
COMMON/OTHER/IX,IY,I7,IX7,S
COMMON/CHFCCK2/CN3,CNR,CNP,CNDR,CNDH,CNDF,CLDF,CLDH,CLR,CLR,
CCLNR,CLB
COMMON/TRTM/BED,GAMAD,AL,EN, SUMCY,RLIFT,XCY,TCONST,GCONST
C,THEO,SI,IO,FE0
EXTERNAL CYRATFS
REAL IX,IY,I7,IX7,IR,MASS
GAMMA=0.
VR=100.
GAMAD=0.
BCONST=0.
ALFA=AL*AV
ALPHA=ALFA
DLEF=25.* (ALPHA-2.)/15.5
IF (DLEF.GT.25.) DLEF=25.
IF (DLEF.LT.0.) DLEF=0.
GCONST=1.
TCOMST=1.
BET =RE*AV
T=J.
T=-1.
Y(2)=0.
RE=BED/AV
BET=BET*AV$BETA=RET
EMG=MASS*G
CF=0H=0.
DA=DE=DR=0.
CNTR=TT=0.

```

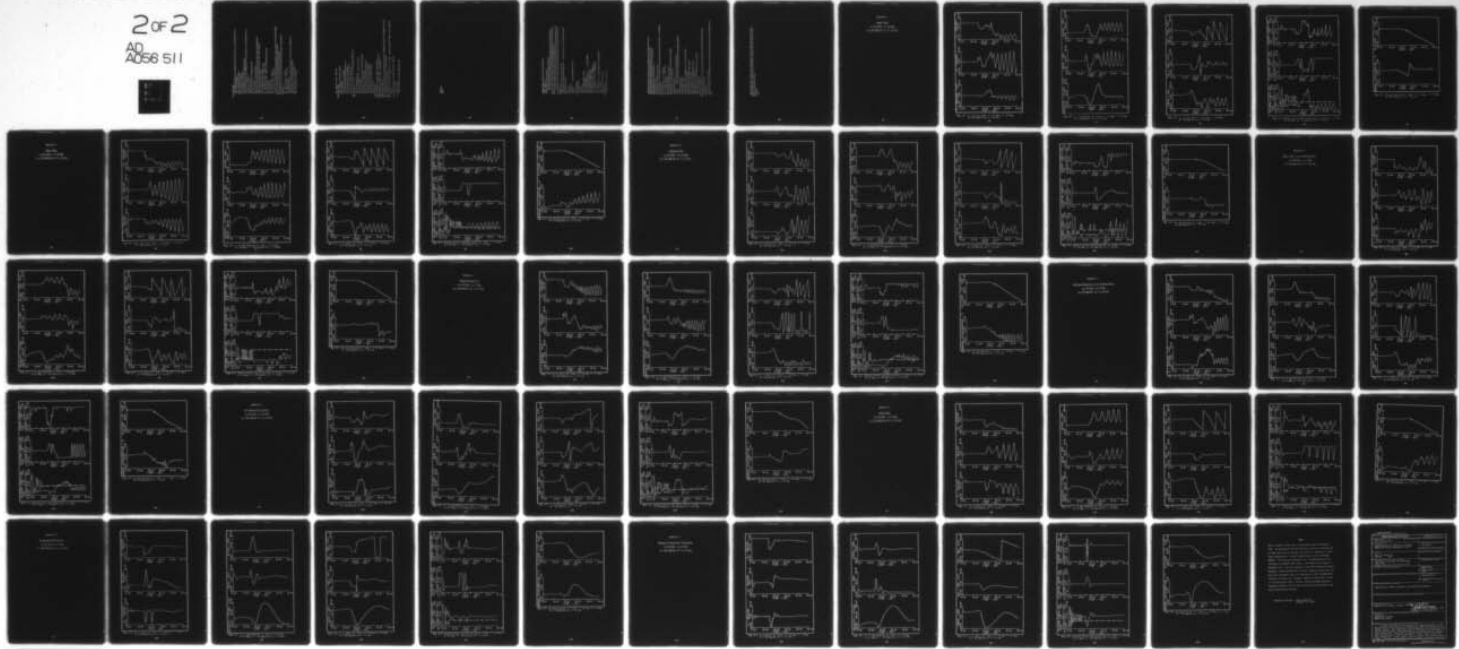
AD-A056 511 AIR FORCE INST OF TECH WRIGHT-PATTERSON AFB OHIO SCH--ETC F/G 1/3
INVESTIGATION OF THE YF-16 IN HIGH ANGLE OF ATTACK ASYMMETRIC F--ETC(U)
MAR 78 E B HOUSE

UNCLASSIFIED

AFIT/GAE/AA/78M-6

NL

2 of 2
AD
A056 511



END
DATE
FILED
9-78
DDC

```

E0 CONTINUE
Y(2)=VR*SIN(BE)*Y(1)=SQRT((VR**2-Y(2)**2)/(1.+TAN(AL)**2))
Y(3)=Y(1)*TAN(AL)
CALL GYRATES(T,Y,YP)
FZZ=COS(AL)*EMG*EN
FXX=-SIN(AL)*EMG*EN
VR=SQRT(AQS*(2.*FZZ/ROH/S/SJYC2))
Y(2)=VR*SIN(BE)*Y(1)=SQRT((VR**2-Y(2)**2)/(1.+TAN(AL)**2))
Y(3)=Y(1)*TAN(AL)
RVR2=ROH*VR*VR
THRUS=-FXX-PVR2*D1*SUMCX*4ASS
DO 150 I=1,3
  CALL ANGLE(Y,YP,XB,YB,ZB)
  DSUMCM=-(R1*Y(4)+Y(6)+R2*(Y(6)**2-Y(4)**2))/RVR2/83
  TSUM=DSUMCM-CM0-R4/VR*CM1*Y(5)+(CG-.35)*SUMC?
  CMDE=.0025*ALPHA-.125
  IF (ALPHA.LT.10.) CMDE=-.10
  IF (ALPHA.GT.20.) CMDE=-.075
  IF (ALPHA.GT.25.) CMDE=-.0025*ALPHA-.0125
  CMDE=.1*CMDE
  DE=TSUM/CMDE
  IF (DE.GT.25.) DE=25.
  IF (DE.LT.-25.) DE=-25.
  DA=(-A1*Y(5)*Y(6)-A2*(Y(4)*Y(5)*(1.+C1)-C2*Y(5)*Y(6)+C3*RVR2
  C*(CG-.35)*C*SUMCY/R+CNR+CNDR*DR+C4/VR*(CNP*
  CY(4)+CNF*Y(6)))-A3*RVR2*(CLR+CLDR*DR+
  CA4/VR*(CLP*Y(4)+CLR*Y(6)))/(C3*2V22*(CNDF)+A3*RVR2*(CCLDF))
  IF (DA.GT.20.) DA=20.
  IF (DA.LT.-20.) DA=-20.
  DF=DA/4.
  DSUMCN=(-C1*Y(4)*Y(5)-C2*(YP(4)-Y(5)*Y(6))/RVR2/C3
  CP=(DSUMCN-CNR-CNDF*DF-C4/VR*(CNP*
  CNP*Y(4)+CNF*Y(6)))/CNDR
  IF (DR.GT.30.) DR=30.

```

```

IF (DR.LT.-30.) DR=-30.

150 CONTINUE
CALL ANGLF(Y,YP,XR,YR,ZR)
CNTR=CNTR+1.

IF(CNTR.GT. 5.) GOTOTO20
TSTG=XCY/MASS+G*SQRT(EN**2-1.)
OUT1=ABS(CLIFT-FM)/MASS
IF(ABS(TSTG).GT.*2) GO TO 50
IF(OUT1.GT.*05) GO TO 50
20 Y1=Y(8)*57.38Y2=Y(1C)*57.38Y3=Y(9)*57.3
F4 CONTINUE
GAMMA=GAMMA+57.3
P1=Y(4)*AV$01=Y(5)*AV$R1=Y(5)*AV
WRITE(6,8H0) VR
WRITE(6,7E3) EN, RCONST, TCONST, GCONST
WRITE(6,1I5) DA, DE, DR
WRITE(6,9I6) OUT1, TSTG, ALFA, RET
WRITE(6,1I2) GAMMA, Y1, Y2, Y3
WRITE(6,8C8) (YP(I),I=1,12)
WRITE(6,1C1) P1, C1, R1, THRUS
WRITE(6,1C9)

21 CONTINUE
1C1 FORMAT(* P,O,R,THRUS *,4F10.3)
1C2 FCRMAT(* GAMMA THETA PHI PSI*,4F7.2)
1C5 FCRMAT(12H DA,DF,DR = ,3F10.2)
1C9 FORMAT(1X//)
7E3 FCRMAT(* EN=*,FF.2,* BCONST=*,F5.2,* TCONST=*,F5.2)
8C8 FCRMAT(12H YP(1-12) = ,2(5E12.5/))
8C0 FCRMAT(* VP= *,F7.*1)
9C6 FCRMAT(* XS LFT *,E12.4,* XS SIDF *,E12.4,* ALFA BETA *,F5.2,2X,,F
CE.2)
9C7 FFORMAT(22HVP AROVE 800 TRY AGAIN)
DO 22 K=1,7
22 Y0(K)=Y(K)
THE0=Y(8)$FEO=Y(10)$SIGHO=Y(9)

```

**RETURN
END**

```
SUBROUTINE ANGLE(Y,YP,XB,YB,ZB)
REAL MASS,IY
```

```
DI MENSION Y(30),YP(30)
```

```
COMMON/GEOM/MASS,C,B,THRUS,CG
```

```
COMMON/RFST/A1,A2,A3,A4,A1,B2,B3,B4,C1,C2,C3,C4,D1,AV,
```

```
IJUDGE,CEPS,SEPS,STHE,CTHE,SFE,RVR2,ROH,G,VR,THE,FE,SIGH,
```

```
ZALPHA,BETA,DR,DF,DF,DF,OLEF,DEC,DRC,DFC,DHC
```

```
COMMON/CHECK/SUMCX,SUMCZ,SUMCM,CN,CND,CNO,CCO,CMO,CMDE,CMQ
```

```
COMMON/CHECK2/C19,CNR,CNP,CNDH,CNDF,CLOH,CLP,CLR,
```

```
CCLDP,CL9
```

```
COMMON/OTHER/IX,IY,IZ,IX^,S
```

```
COMMON/TRIM/3ED,GAMAD,AL,EN,
```

```
C,THEO,SIGH0,FE0
```

```
T=-1.
```

```
GAMA=0.
```

```
BE=3ED/AV
```

```
CHEGA= G/VR* SORT(EN**2-1.)
```

```
CR=C
```

```
1 EMG=MASS*G
```

```
GAMMA=5./AV
```

```
TGH=0.
```

```
CR=CR+1.
```

```
CALL GYRATES(T,Y,YP)
```

```
TM=THRUSS/MASS
```

```
XB=(RVR2*D1*(SUMCX
```

```
) + TGM)*MASS
```

```
YB=RVR2*D1*MASS*SUMCY
```

```
ZB=RVR2*D1*MASS*SUMCZ
```

```
IF (TCONST.NE.0.) GAMMA=0.
```

```
IF (GCONST.NE.0.) GAMMA=GAMA
```

```
GETOUT=0.
```

```
IF (TCONST.NE.0..OR.GCONST.NE.0.) GOT06
```

```
DO 4 I=1,2
```

```
GAMMA=GAMMA-5./57.3
```

```
4 CONTINUE
```

```
PSTP=ATAN(Y(2)/Y(1))
```

```

THETP=ATAN(SQRT(SIN(AL)*2/(COS(AL)*2+TAN(BE)*2)))
SGAM=SIN(GAMMA)*SP=SIN(PSIP)*ST=SIN(THETP)
CGAM=COS(GAMMA)*CT=COS(THETP) &CP=COS(PSIP)
AAA=XB*ST*CP-YB*ST*SP-ZB*ST
BBB=XB*SP*YB*CP
CCC=XB*CT*CP-YB*CT*SP+7B*ST
TPHIP=(EBR*(-EMG+SGAM+CCC)/CGAM-AAA*EMG*SQRT(EN*EN-1.))/BBB*B
CBB+AAA*AAA)
IF (TPHIP.GT.-1.) TPHIP=1.
IF (TPHIP.LT.-1.) TPHIP=-1.
PHIP=ASIN(TPHIP)
SF=SIN(PHIP) &CF=COS(PHIP)
TTHET=CP*RT*SGAM-SP*SF*CGAM+CP*ST*CF*CGAM
PTHET=SQRT(1.-TTHET**2)
Y(8)=ACOS(PTHET)
Y(9)=ACOS(TPSI)
Y(10)=ACOS(TPHI)
C7=G/(D1*FVR2)
Y(10)=ATAN((-CYN*RED-CYDF*JF-CYDR*DR)/C7)
Y(4)=-OMEGA*STH(Y(8))
Y(5)=OMEGA*COS(Y(8))*SIN(Y(10))
CALL GYRATES(T,Y,YP)
Y(6)=OMEGA*COS(Y(8))*COS(Y(10))
IF(SETOUT.EQ.1.) GOT07
IF(TCONST.NE.0..OR.GCONST.NE.0.) GOT07
IF(L.EQ.2.) GOT05
TGH=YP(3)/YP(1)
5 GAMMA=GAMMA-5.* (Y(3)/Y(1)-YP(3)/(TGH-YP(3)/YP(1)))/AV
GETOUT=1..GOT06
7 CONTINUE
IF (CR.EQ.1.) GO TO 1
RLIFT=-SIN(Y(R))*XB+SIN(Y(10))*YC-COS(Y(10))*COS(Y(8))*Z

```

```
XY=-COS(Y(8))*SIN(Y(9))+XB+(COS(Y(10))*COS(Y(9))-SIN(Y(10))*  
ISIN(Y(8))*SIN(Y(9)))*YB+(SIN(Y(10))*COS(Y(9))+COS(Y(10))*  
2Y(8))*SIN(Y(9))*ZA  
RETURN  
END
```

Appendix E

Erect Spin

$\alpha = 21 \text{ deg}$, $\beta = 10 \text{ deg}$

$q = 20 \text{ deg/sec}$ at $t = 15 \text{ sec}$

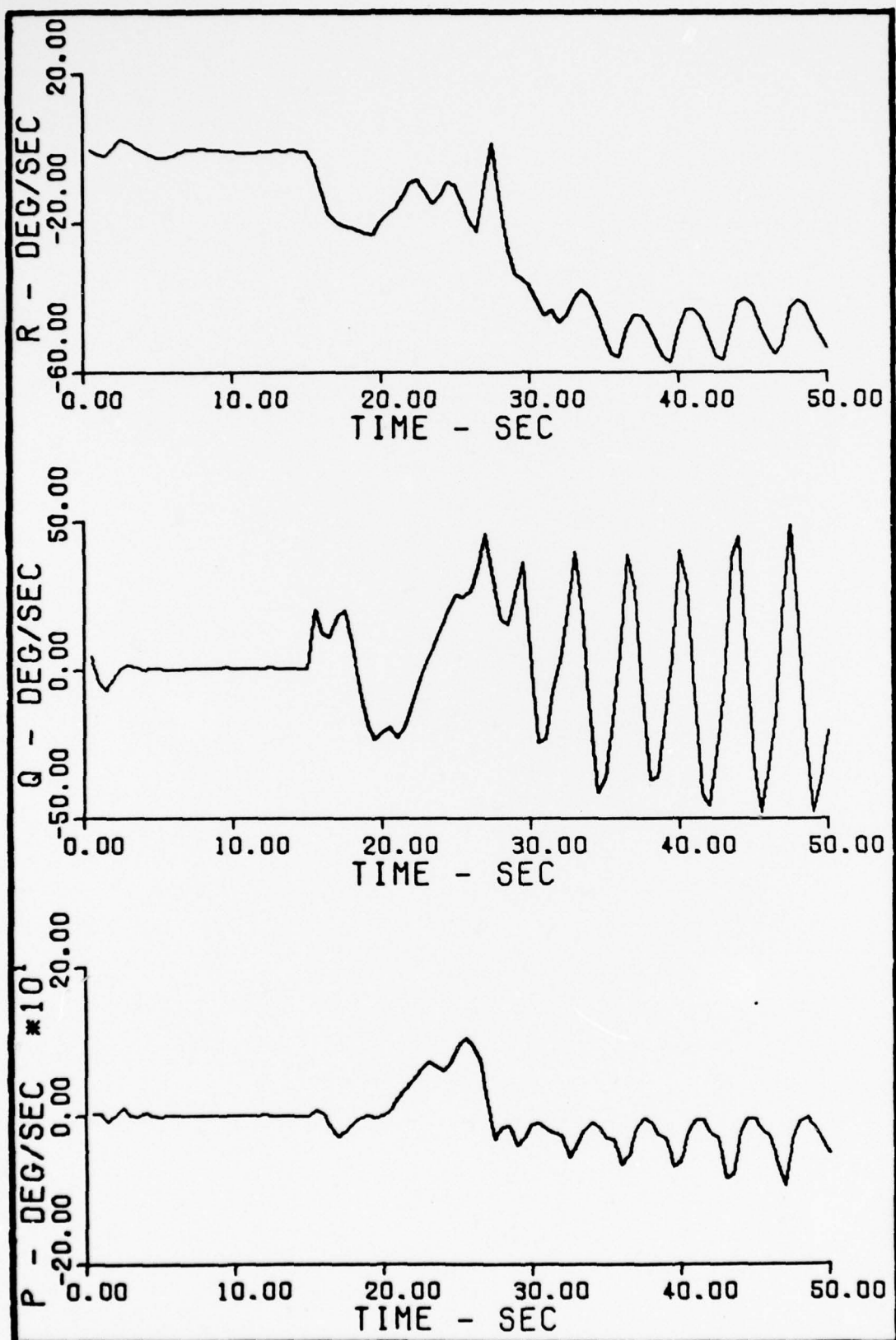


Fig. E-1 p, q, r vs. time, $\alpha = 21$ deg, $\beta = 10$ deg,
 $q = 20$ deg/sec at $t = 15$ sec

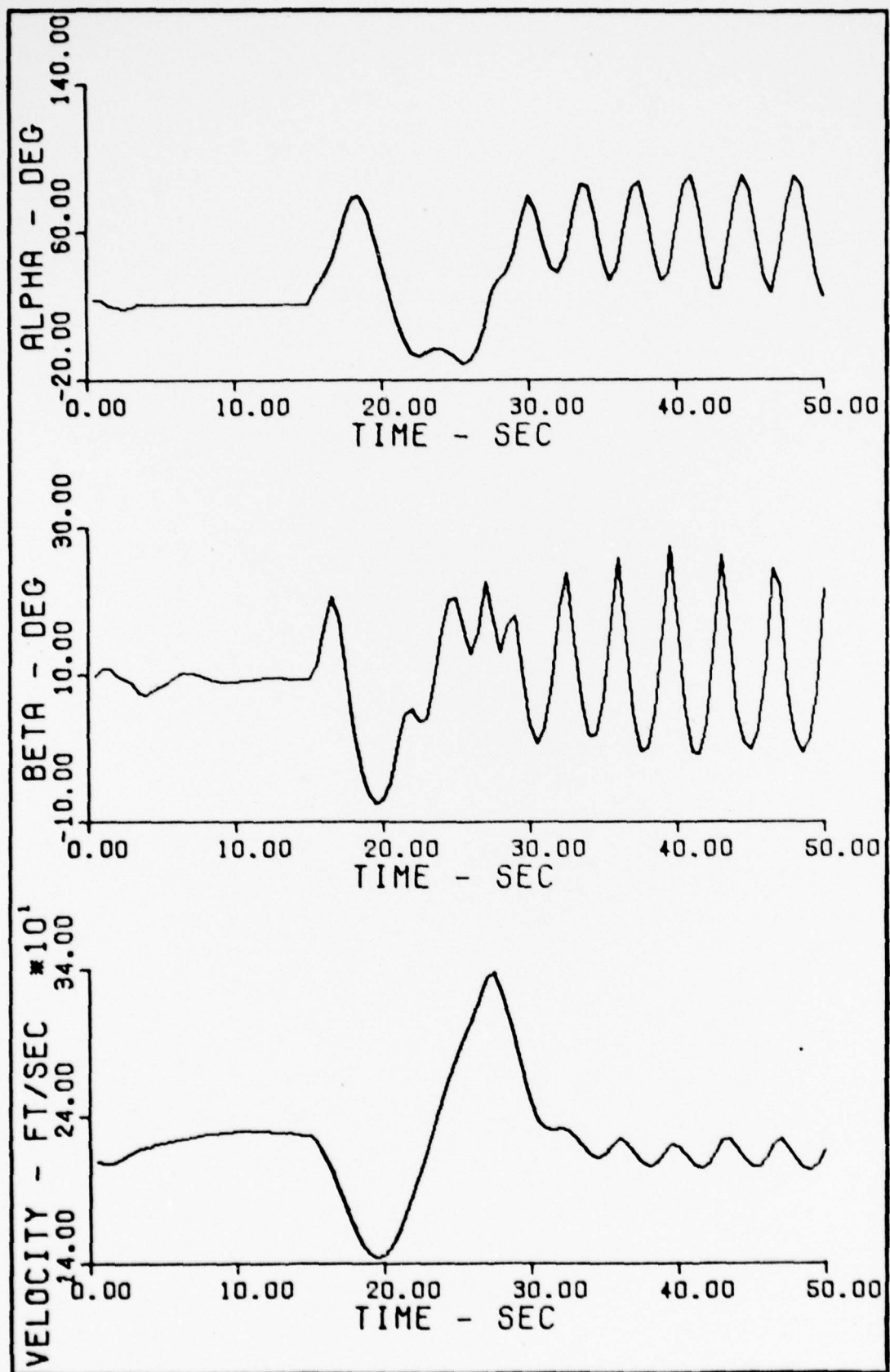


Fig. E-2 α , β , velocity vs. time, $\alpha = 21$ deg, $\beta = 10$ deg
 $q = 20$ deg/sec at $t = 15$ sec

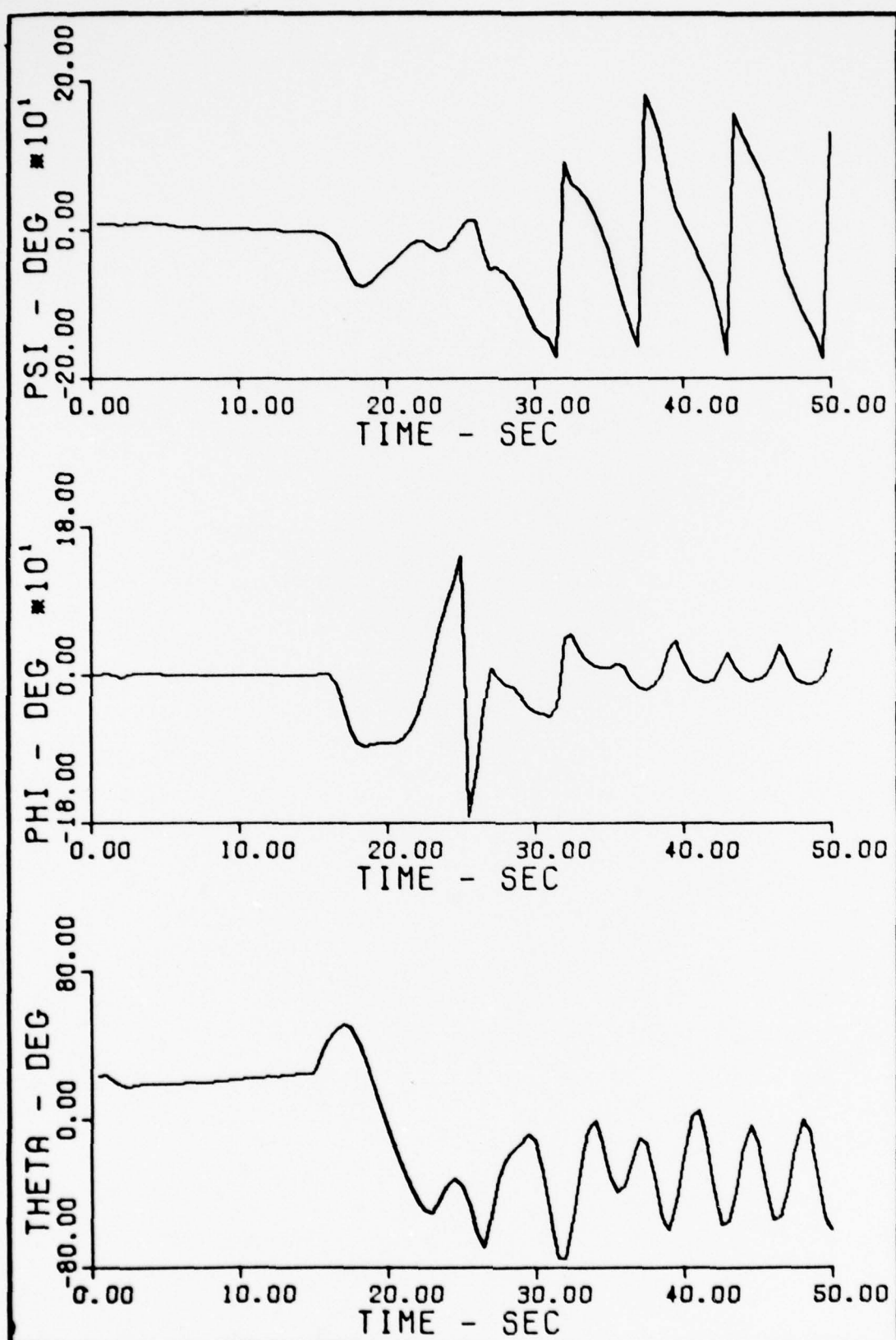


Fig. E-3 θ, ϕ, ψ vs. time, $\alpha = 21$ deg, $\beta = 10$ deg,
 $q = 20$ deg/sec at $t = 15$ sec

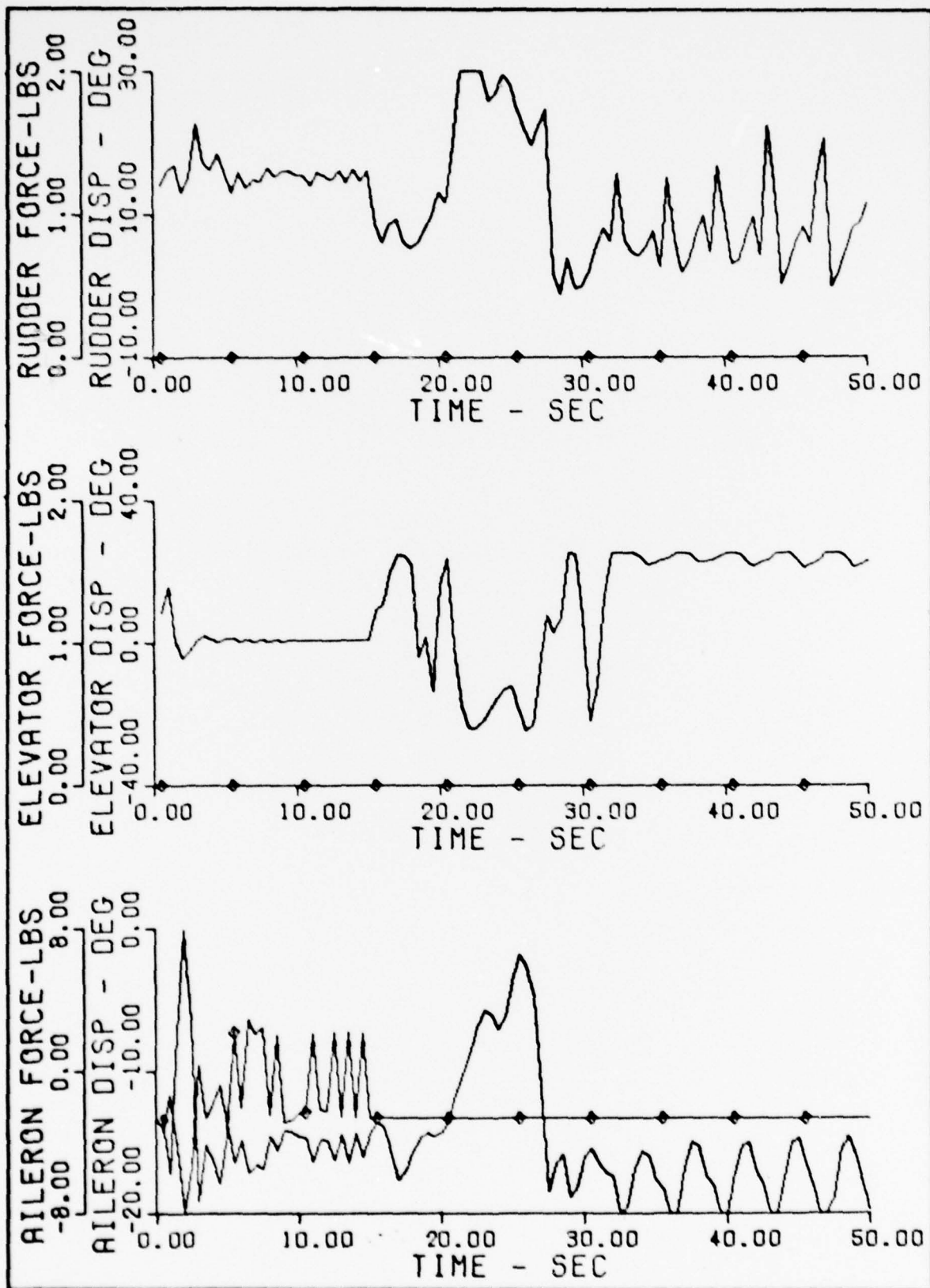


Fig. E-4 Control Forces and Deflections vs. time, $\alpha = 21$ deg
 $s = 10$ deg, $q = 20$ deg/sec at $t = 15$ sec

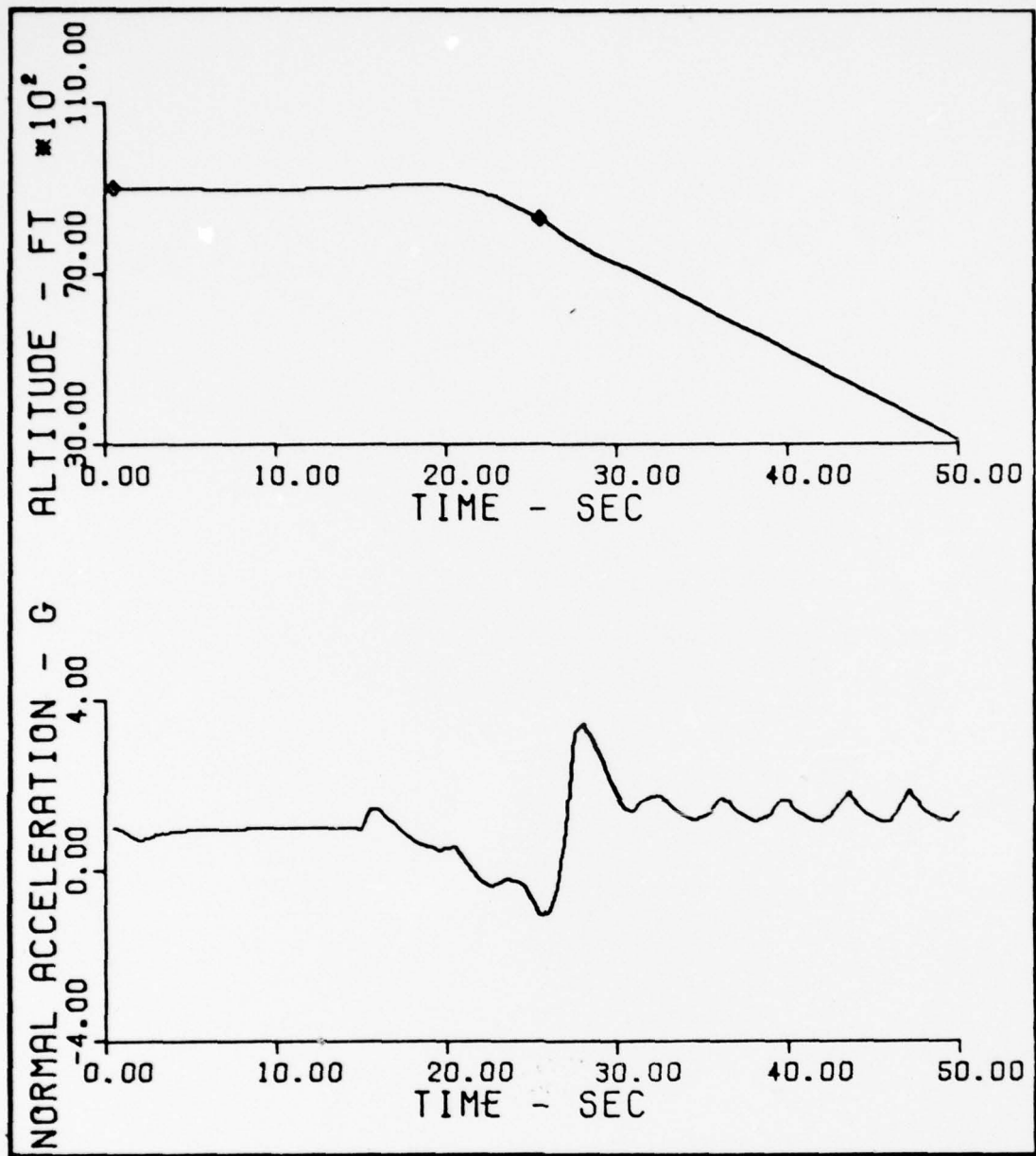


Fig. E-5 N_z and Altitude vs. time, $\alpha = 21$ deg, $\beta = 10$ deg,
 $q_z = 20$ deg/sec at $t = 15$ sec

Appendix F

Erect Spin

$\alpha = 21 \text{ deg}$, $\beta = 10 \text{ deg}$

$r = -20 \text{ deg/sec}$ at $t = 15 \text{ sec}$

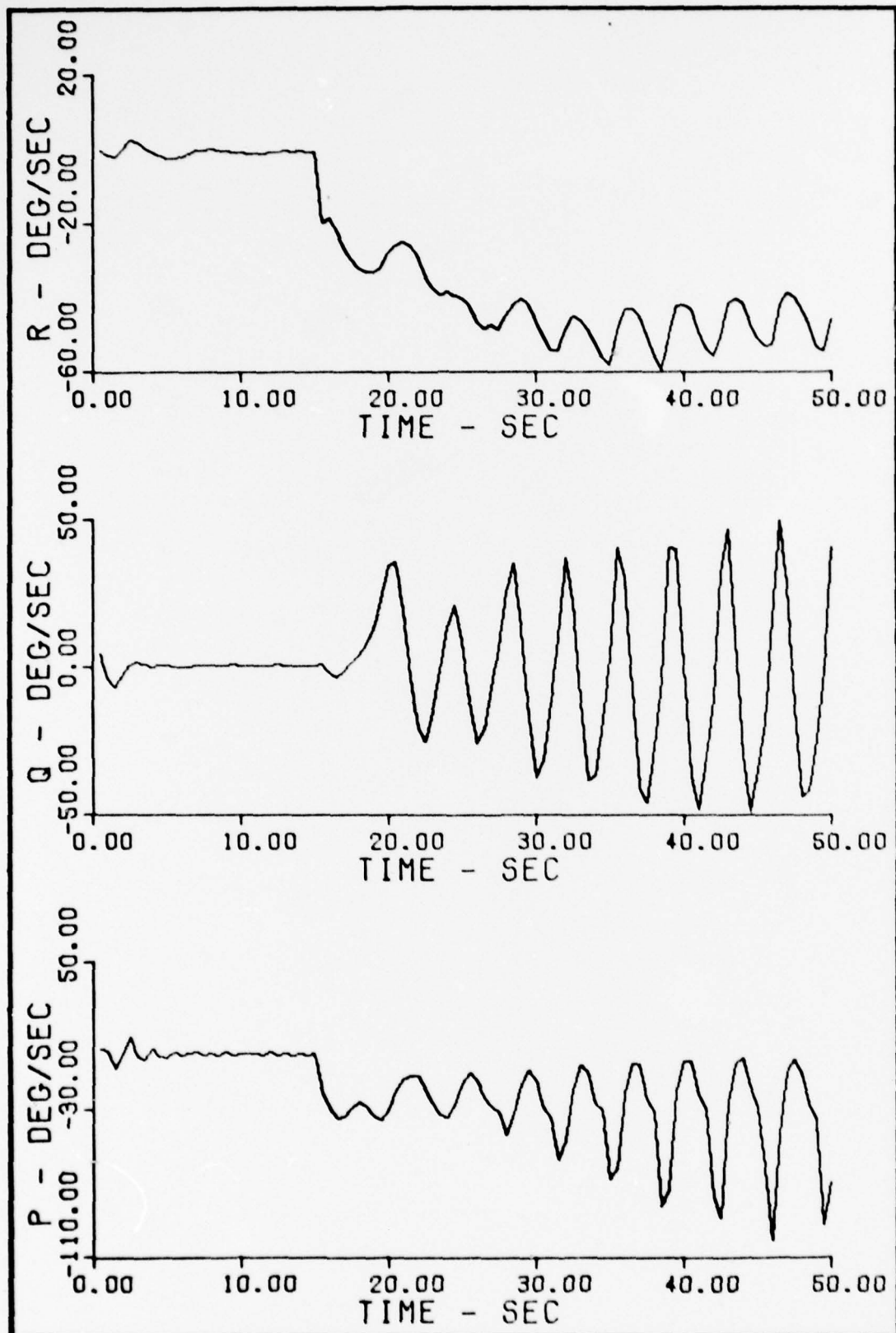


Fig. F-1 p,q, and r vs. time, $\alpha = 21$ deg, $\beta = 10$ deg,
 $r = -20$ deg/sec at $t = 15$ sec

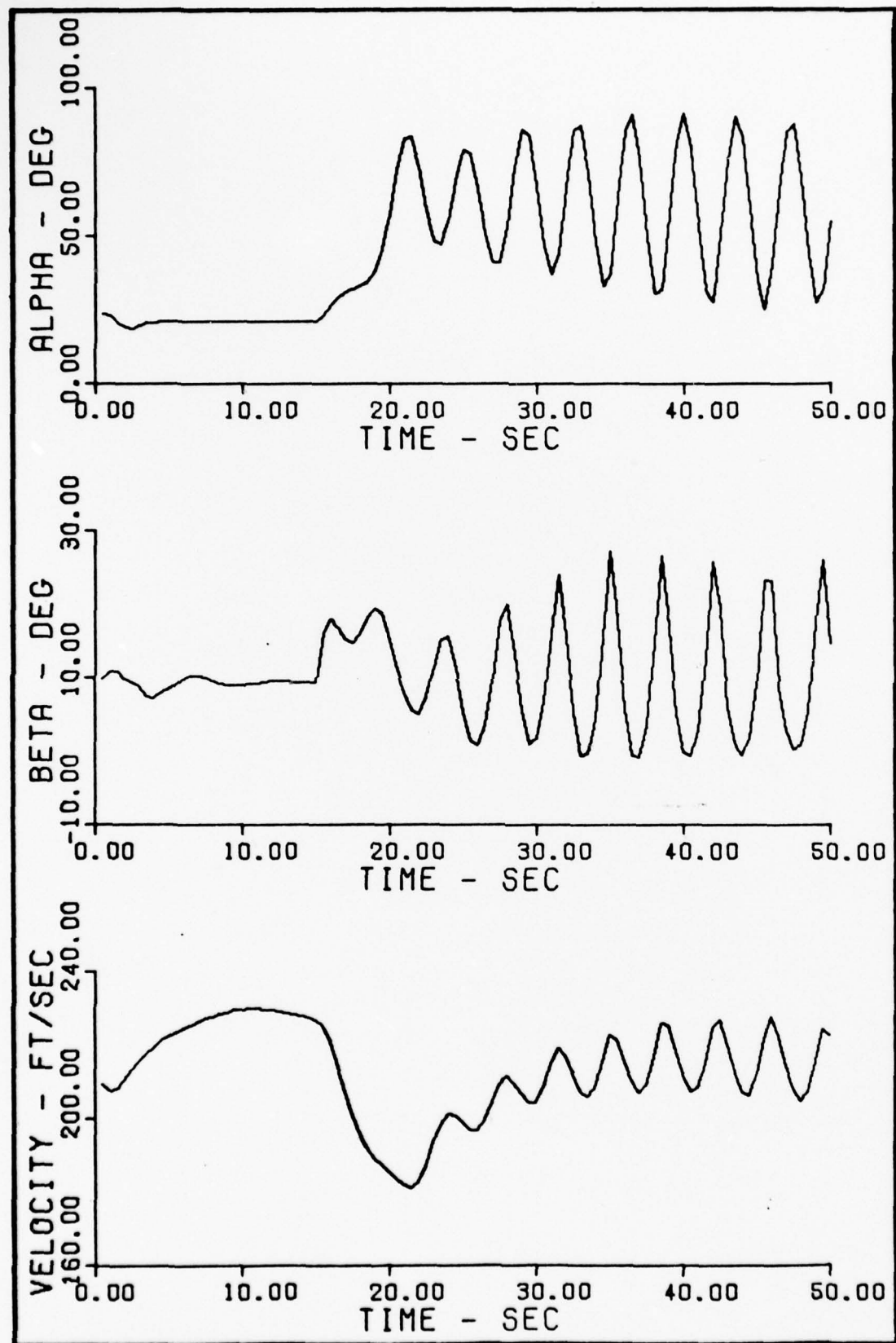


Fig. F-2 α , β , and Velocity vs. time, $\alpha = 21$ deg,
 $\beta = 10$ deg, $r = -20$ deg/sec at $t = 15$ sec

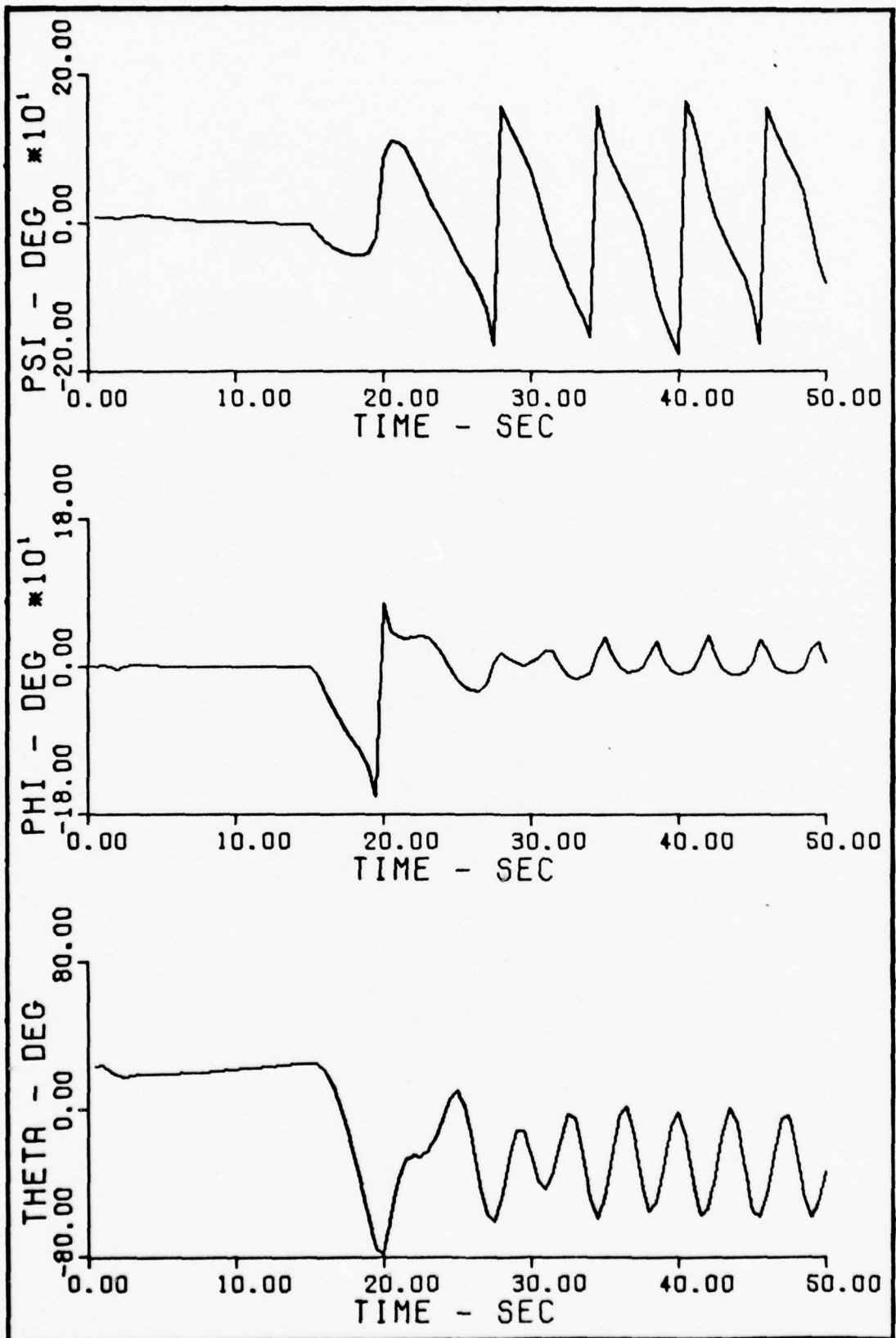


Fig. F-3 θ , ϕ , and ψ vs. time, $\alpha = 21$ deg, $\beta = 10$ deg,
 $r = -20$ deg/sec at $t = 15$ sec

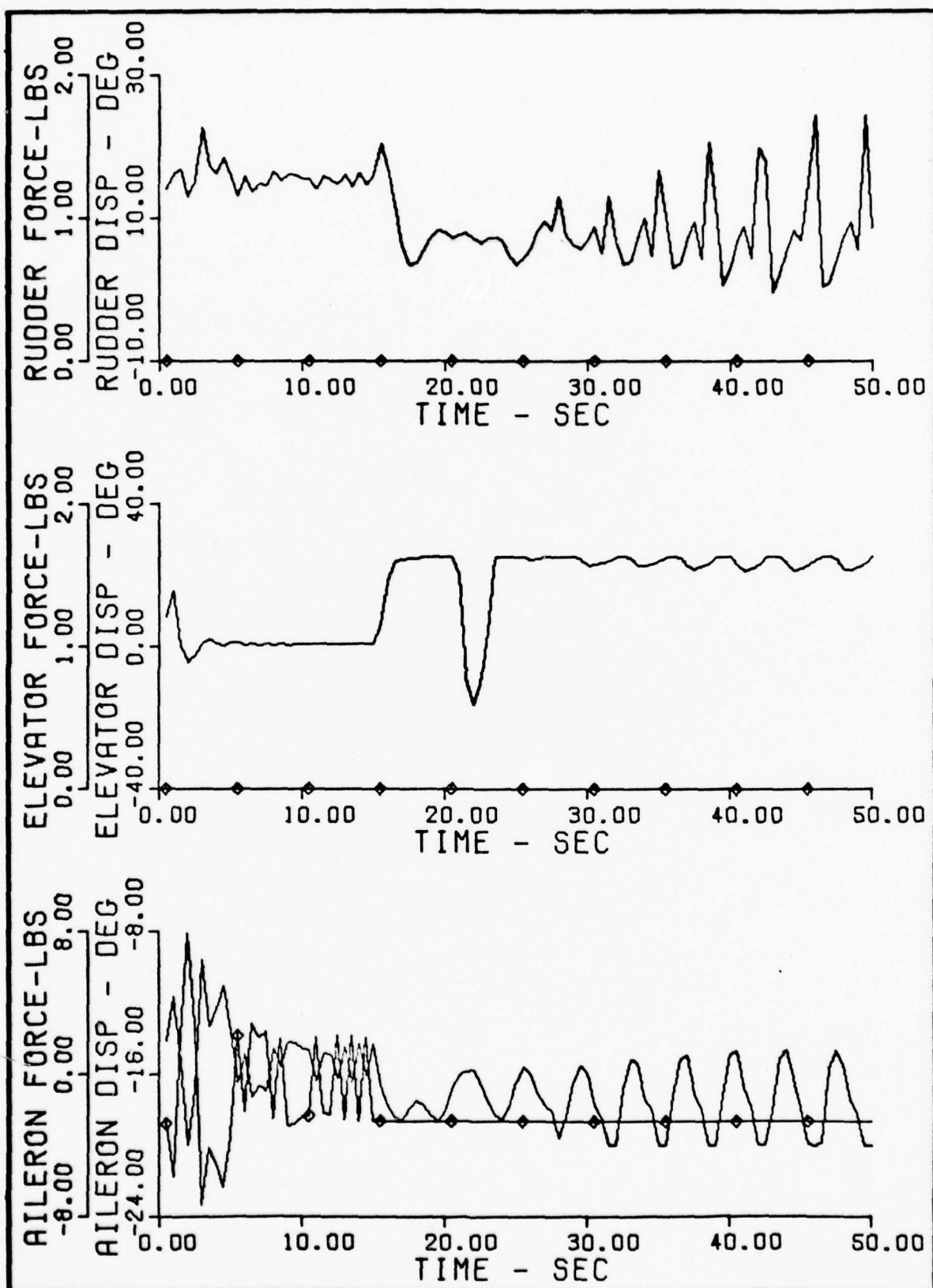


Fig. F-4 Control Forces and Deflections vs. time, $\alpha = 21$ deg,
 $\beta = 10$ deg, $r = -20$ deg/sec at $t = 15$ sec

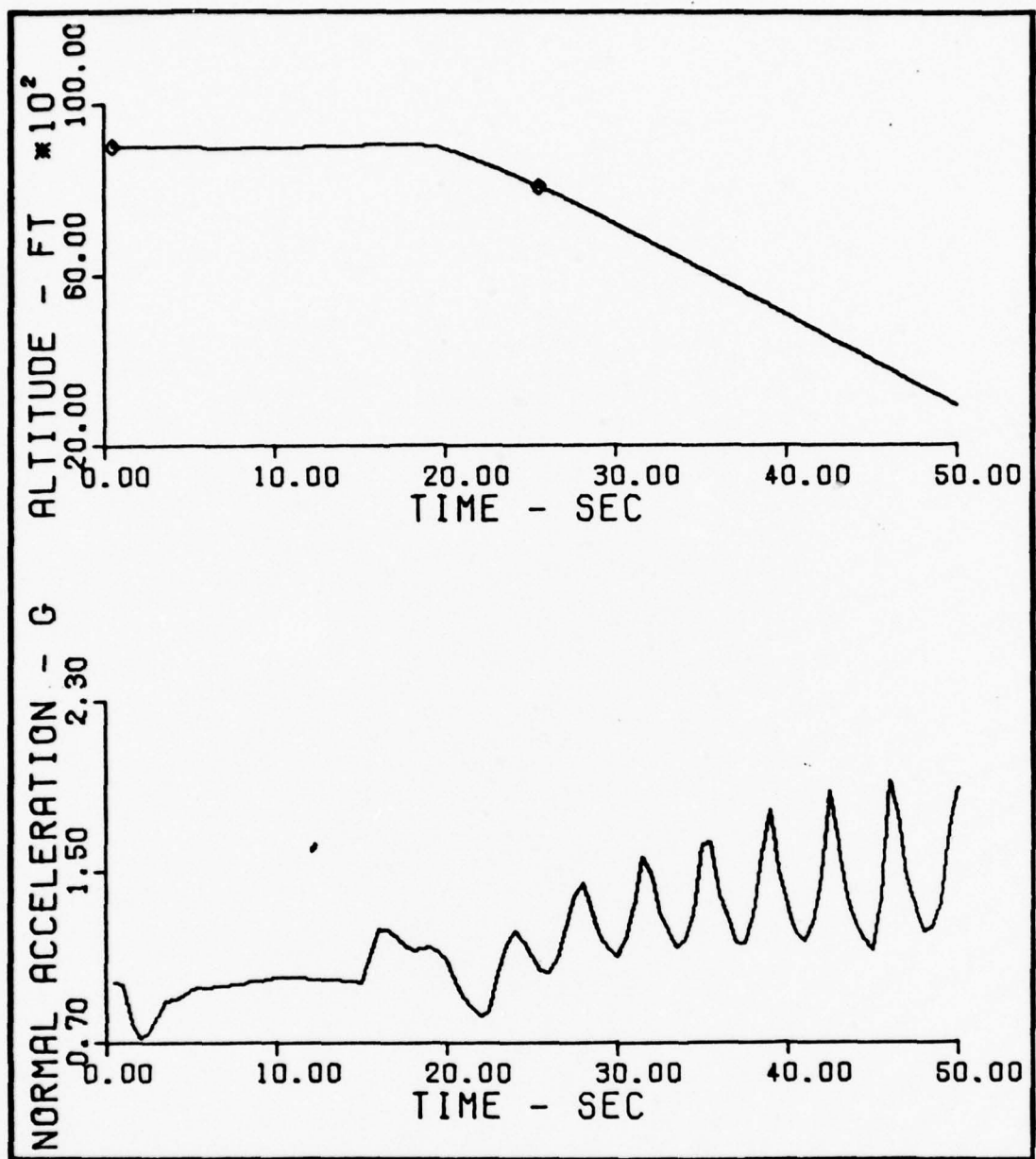


Fig. F-5 N and Altitude vs. time, $\alpha = 21$ deg, $\beta = 10$ deg
 $r^z = -20$ deg/sec at $t = 15$ sec

Appendix G

Inverted Spin

$\alpha = 23 \text{ deg}$, $\beta = 13 \text{ deg}$

$q = 30 \text{ deg/sec}$ at $t = 20 \text{ sec}$

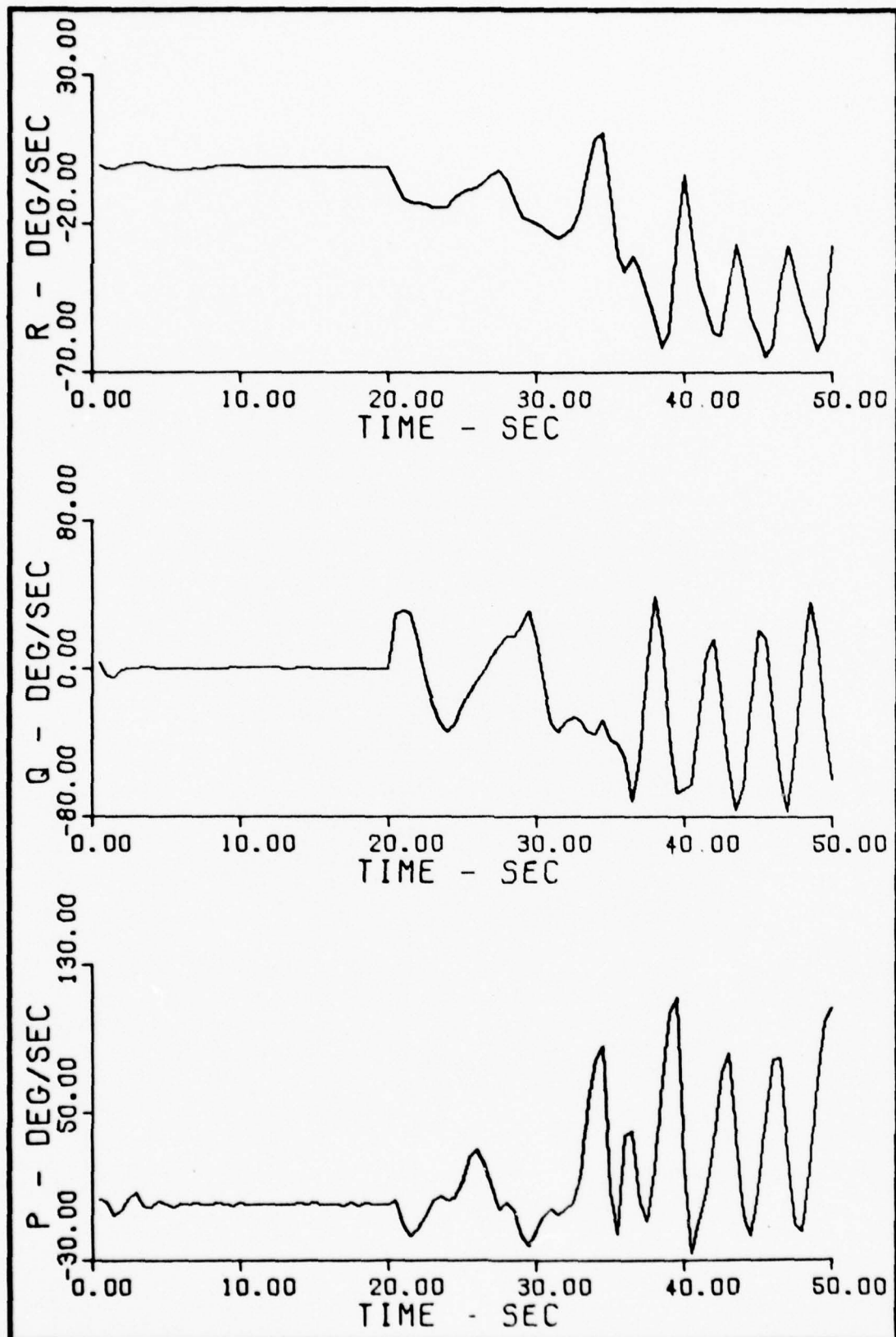


Fig. G-1 p, q, and r vs. time, $\alpha = 23$ deg, $\beta = 13$ deg,
 $q = 30$ deg/sec at $t = 20$ sec

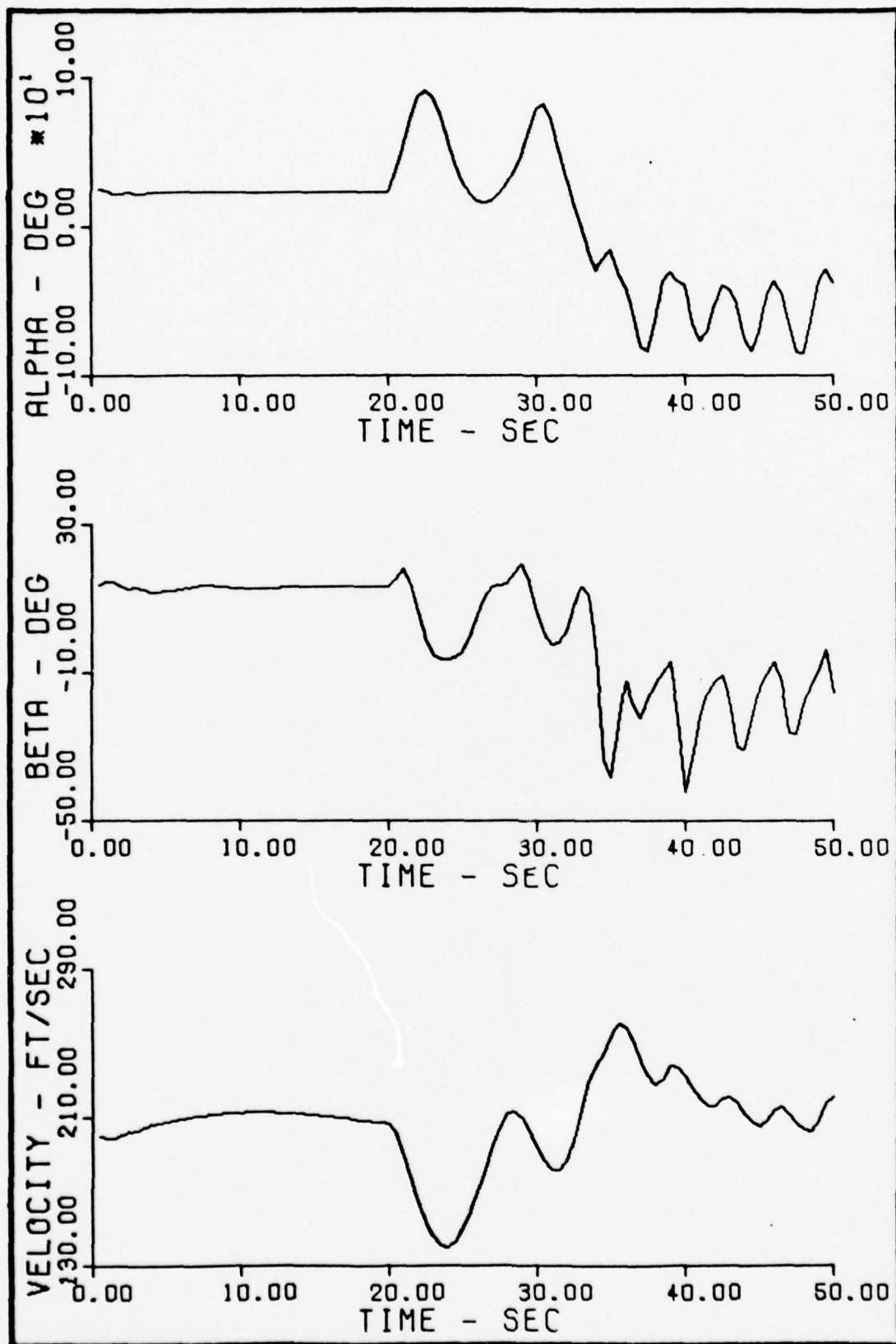


Fig. G-2 α , β , and Velocity vs. time, $\alpha = 23$ deg,
 $\beta = 13$ deg, $q = 30$ deg/sec at $t = 20$ sec

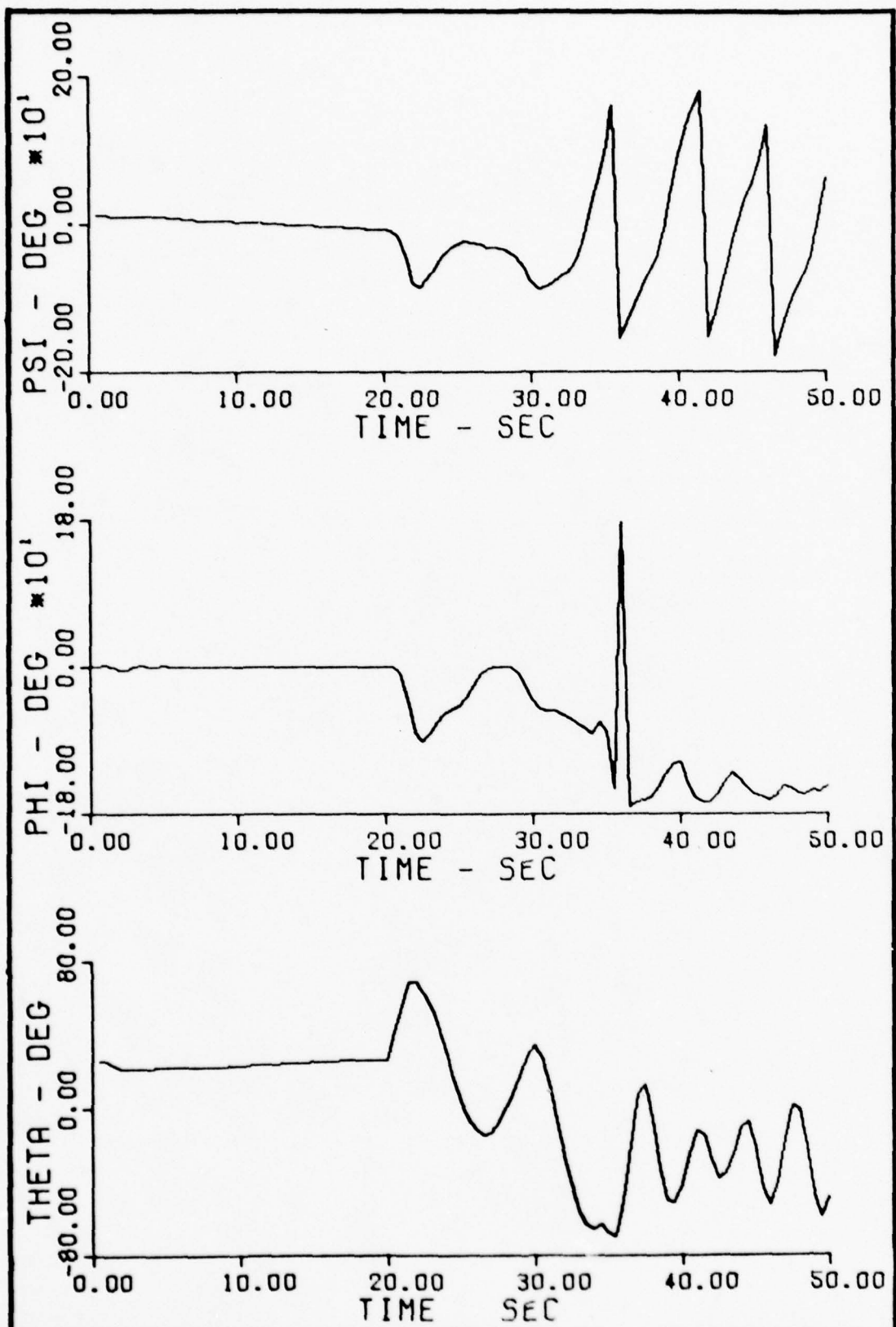


Fig. G-3 θ , ϕ , and ψ vs. time, $\alpha = 23$ deg, $\beta = 13$ deg,
 $q = 30$ deg/sec at $t = 20$ sec

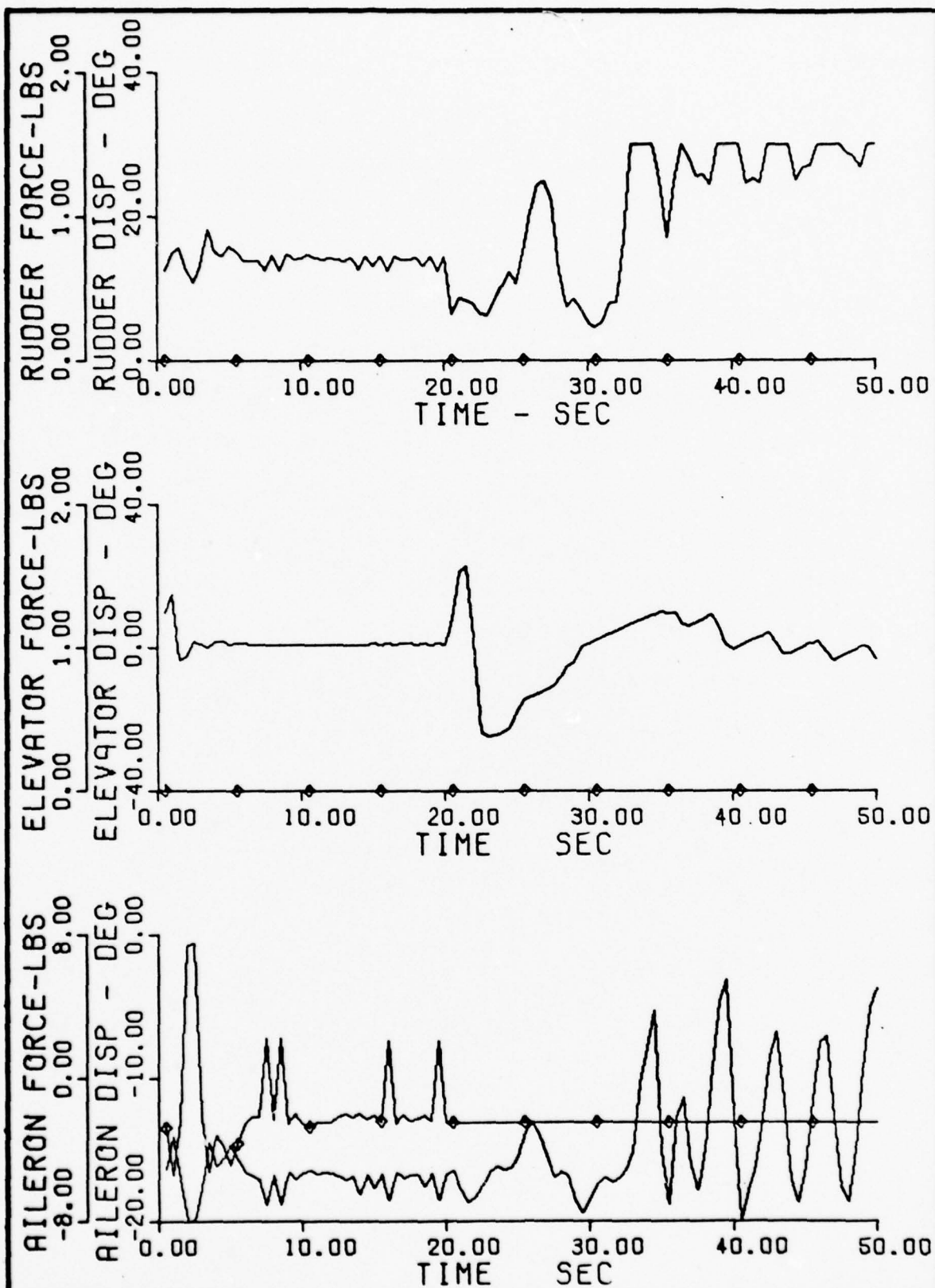


Fig. G-4 Control Forces and Deflections vs. time, $\alpha = 23$ deg,
 $\beta = 13$ deg, $q = 30$ deg/sec at $t = 20$ sec

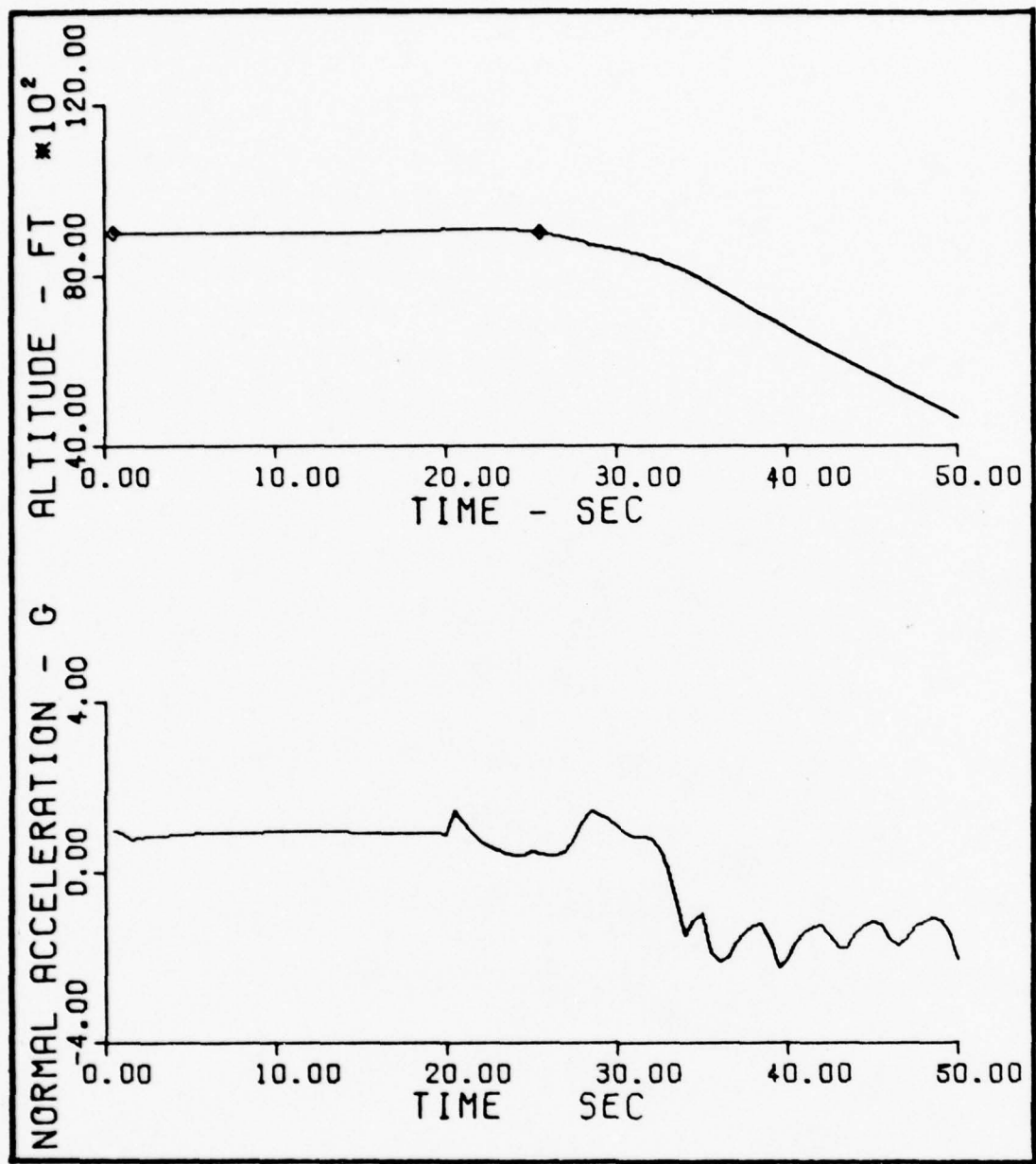


Fig. G-5 N_z and Altitude vs. time, $\alpha = 23$ deg, $\beta = 13$ deg,
 $q = 30$ deg/sec at $t = 20$ sec

Appendix H

Erect Spin to an Inverted Spin

$\alpha = 19 \text{ deg}$, $\beta = 4 \text{ deg}$

$r = -30 \text{ deg/sec}$ at $t = 15 \text{ sec}$

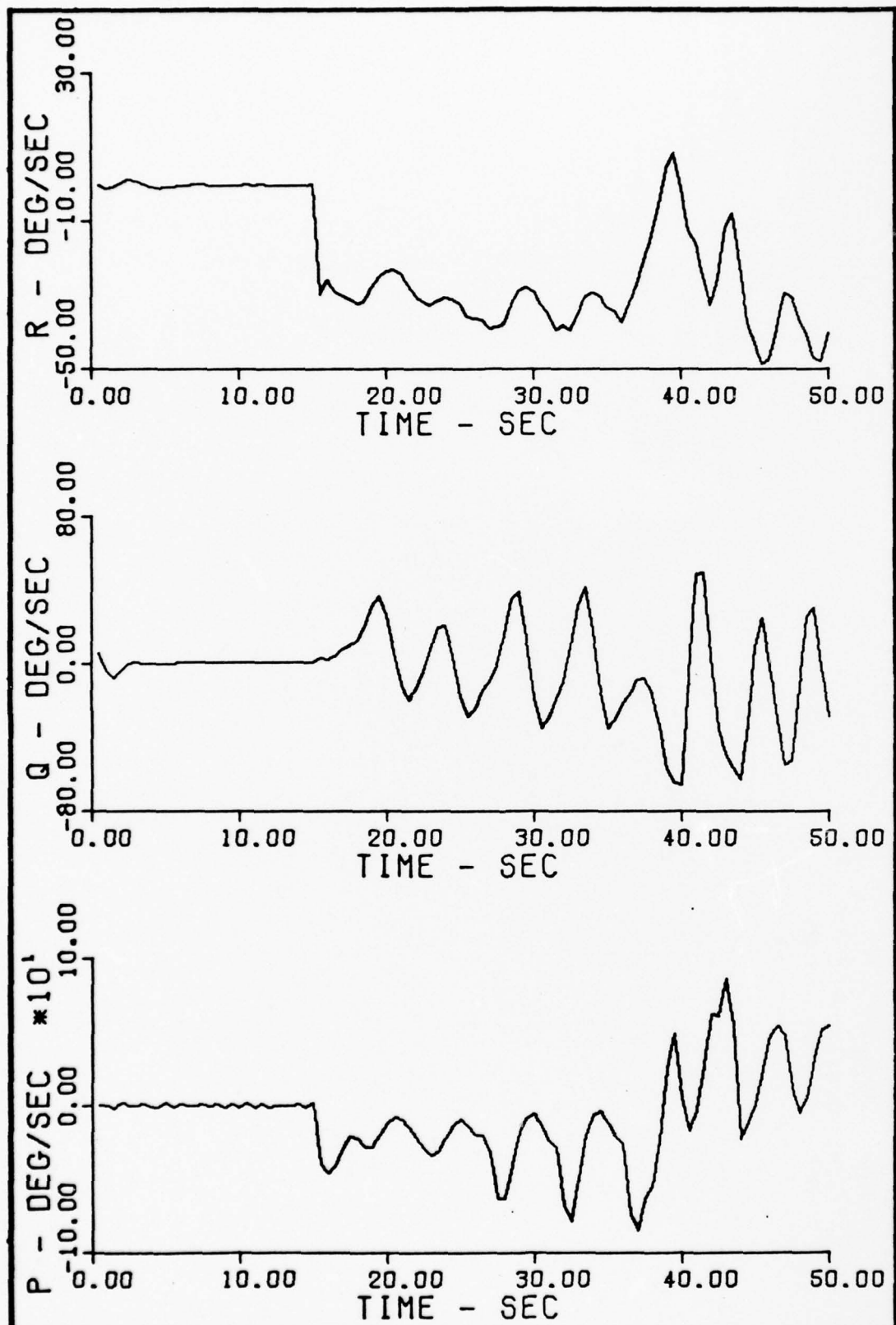


Fig. H-1 p, q, and r vs. time, $\alpha = 19$ deg, $\beta = 4$ deg,
 $r = -30$ deg/sec at $t = 15$ sec

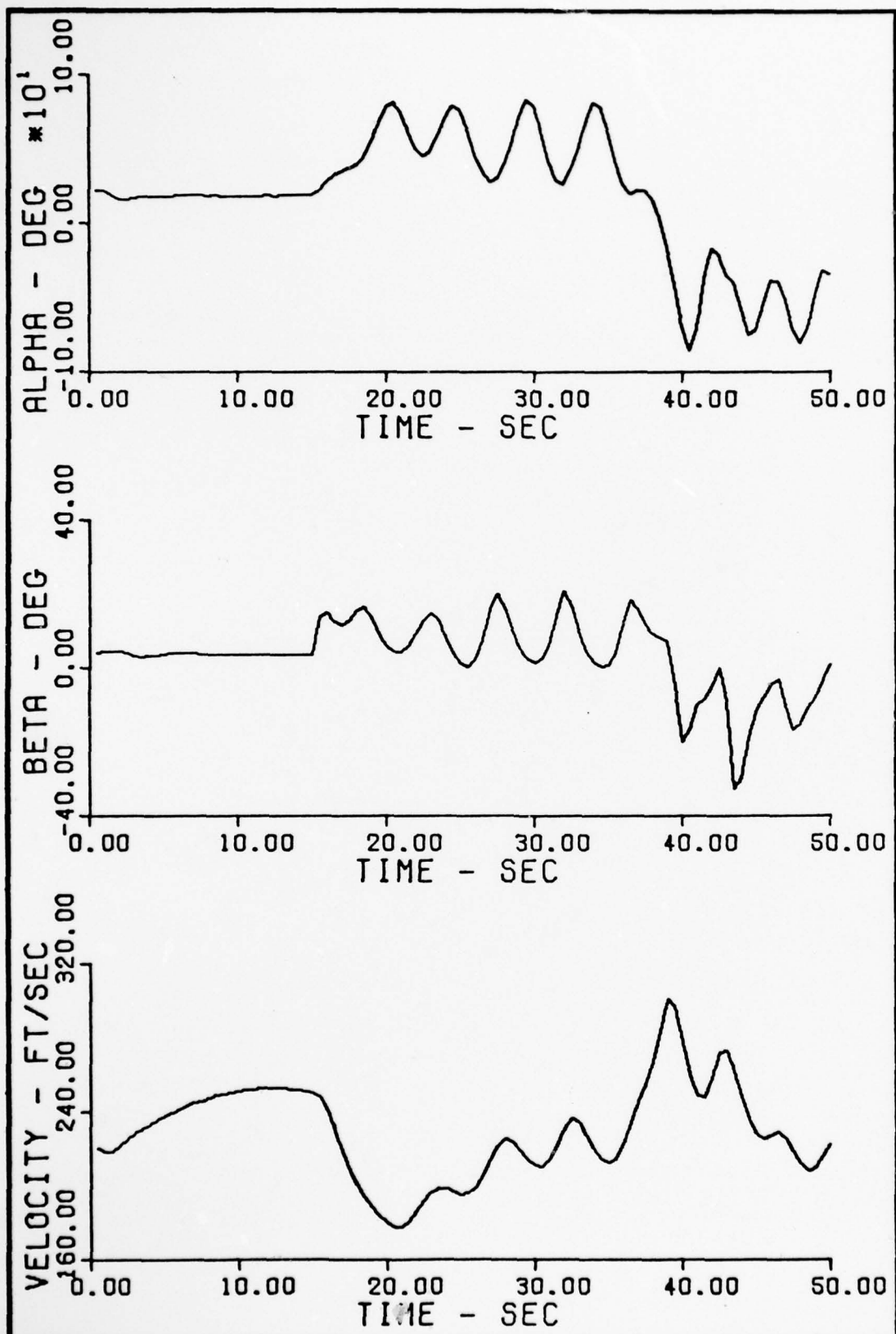


Fig. H-2 α , β , and Velocity vs. time, $\alpha = 19$ deg,
 $\beta = 4$ deg, $r = -30$ deg/sec at $t = 15$ sec

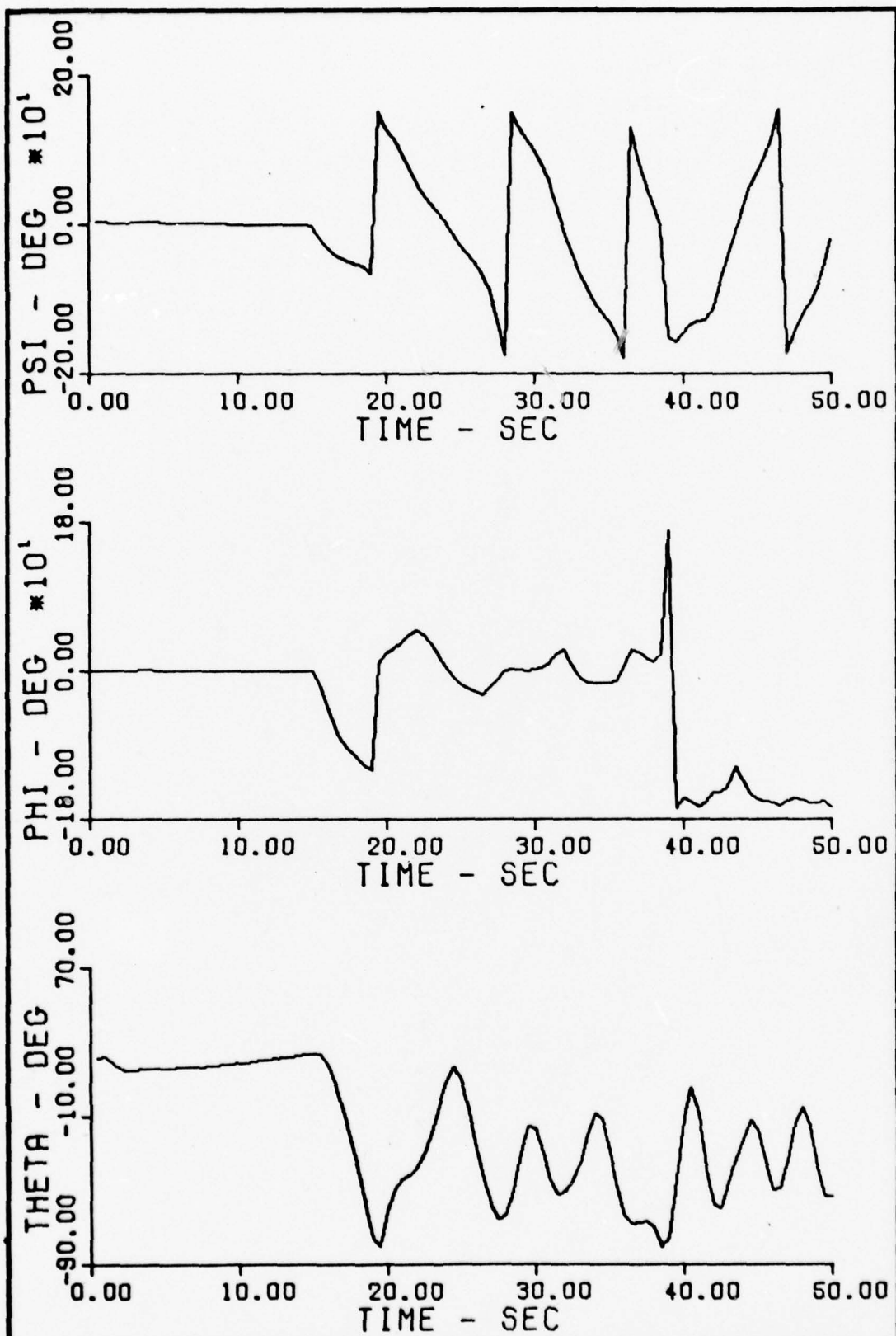


Fig. H-3 θ , ϕ , and ψ vs. time, $\alpha = 19$ deg, $\beta = 4$ deg,
 $r = -30$ deg/sec at $t = 15$ sec

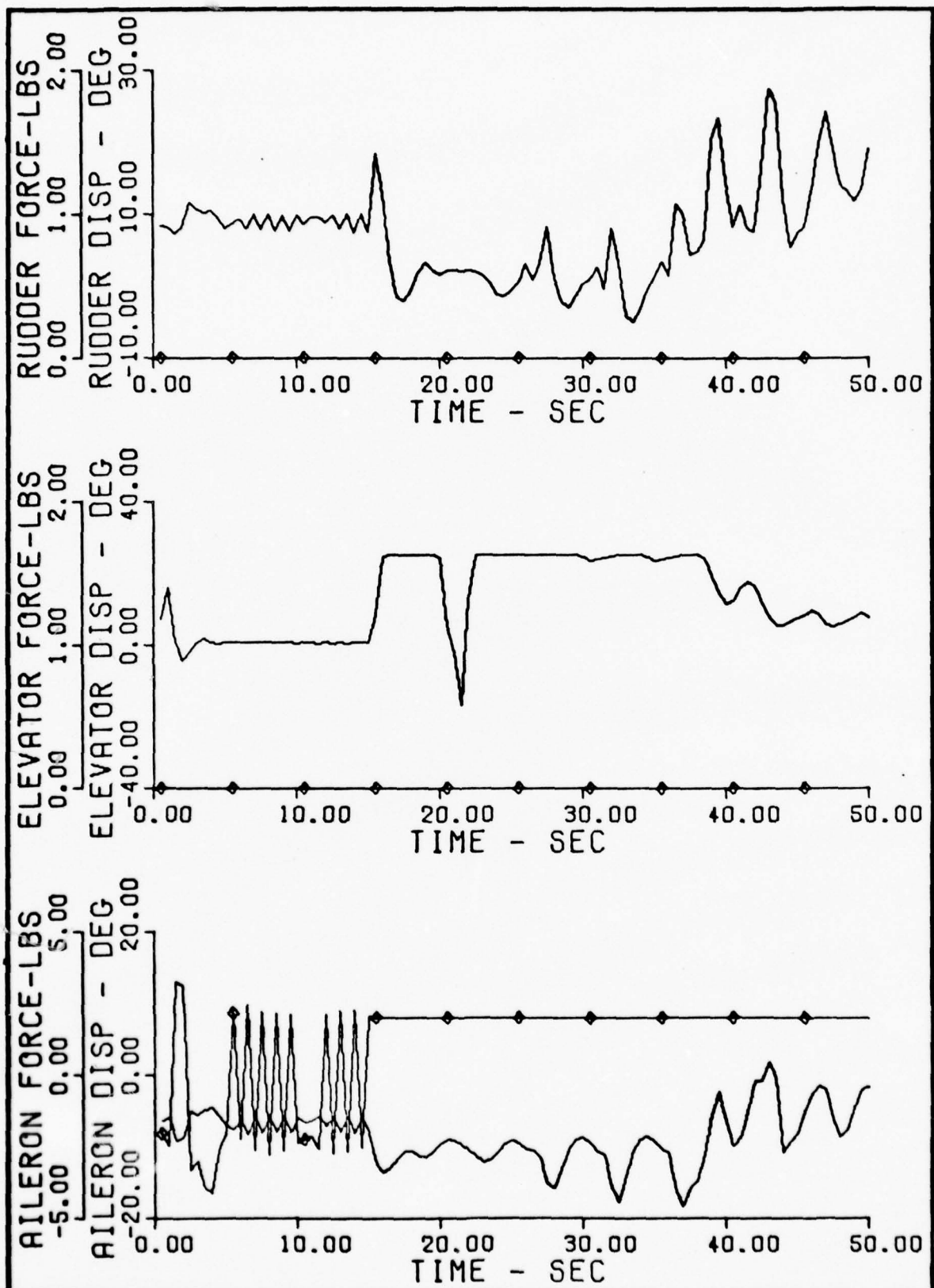


Fig. H-4 Control Forces and Deflections vs. time, $\alpha = 19$ deg,
 $\beta = 4$ deg, $r = -30$ deg/sec at $t = 15$ sec

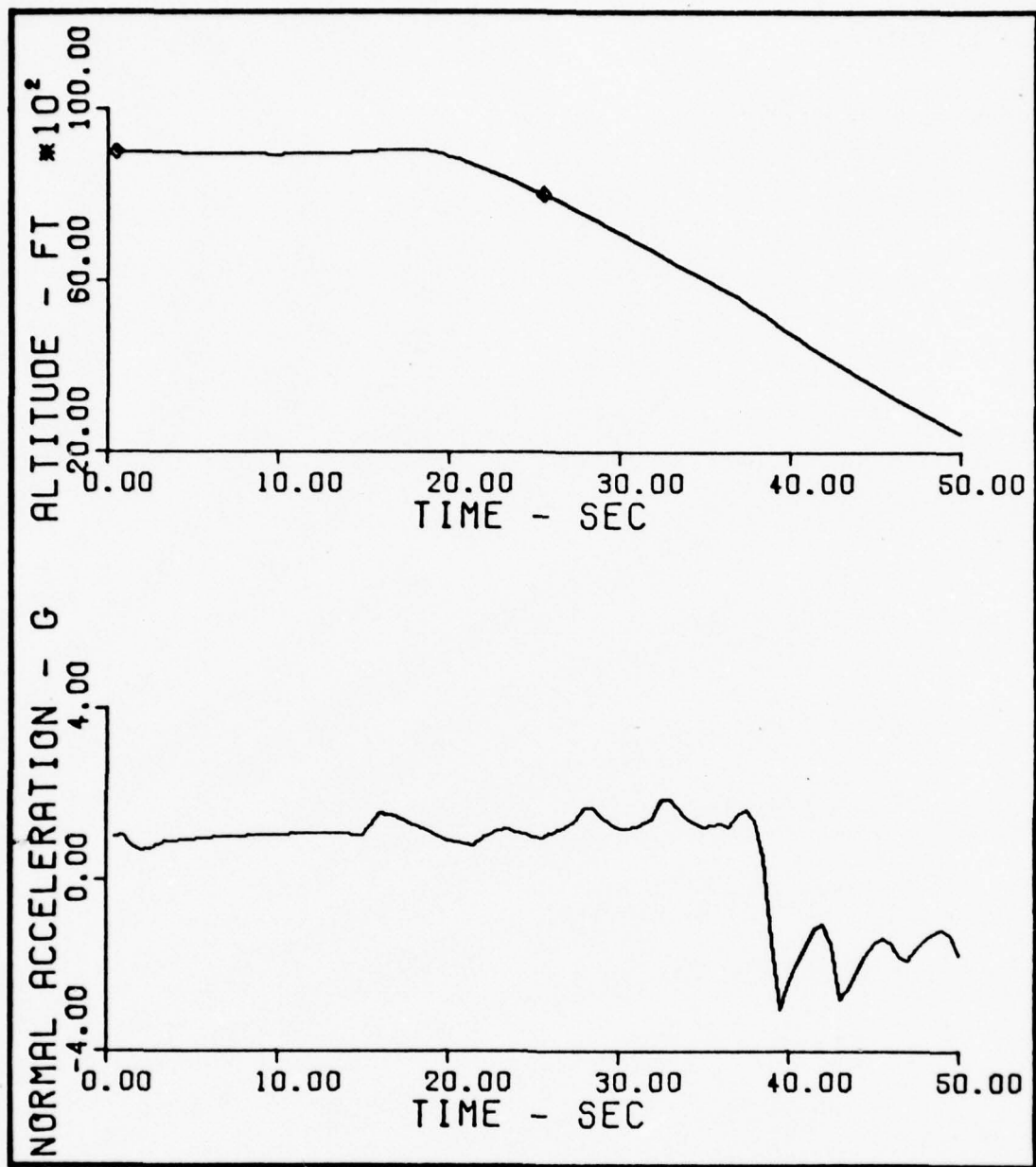


Fig. H-5 N_z and Altitude vs. time, $\alpha = 19$ deg, $\beta = 4$ deg,
 $r_z = -30$ deg/sec at $t = 15$ sec

Appendix I

Rolling Departure

$\alpha = 19 \text{ deg}$, $\beta = 9 \text{ deg}$

$q = 20 \text{ deg/sec}$ at $t = 15 \text{ sec}$

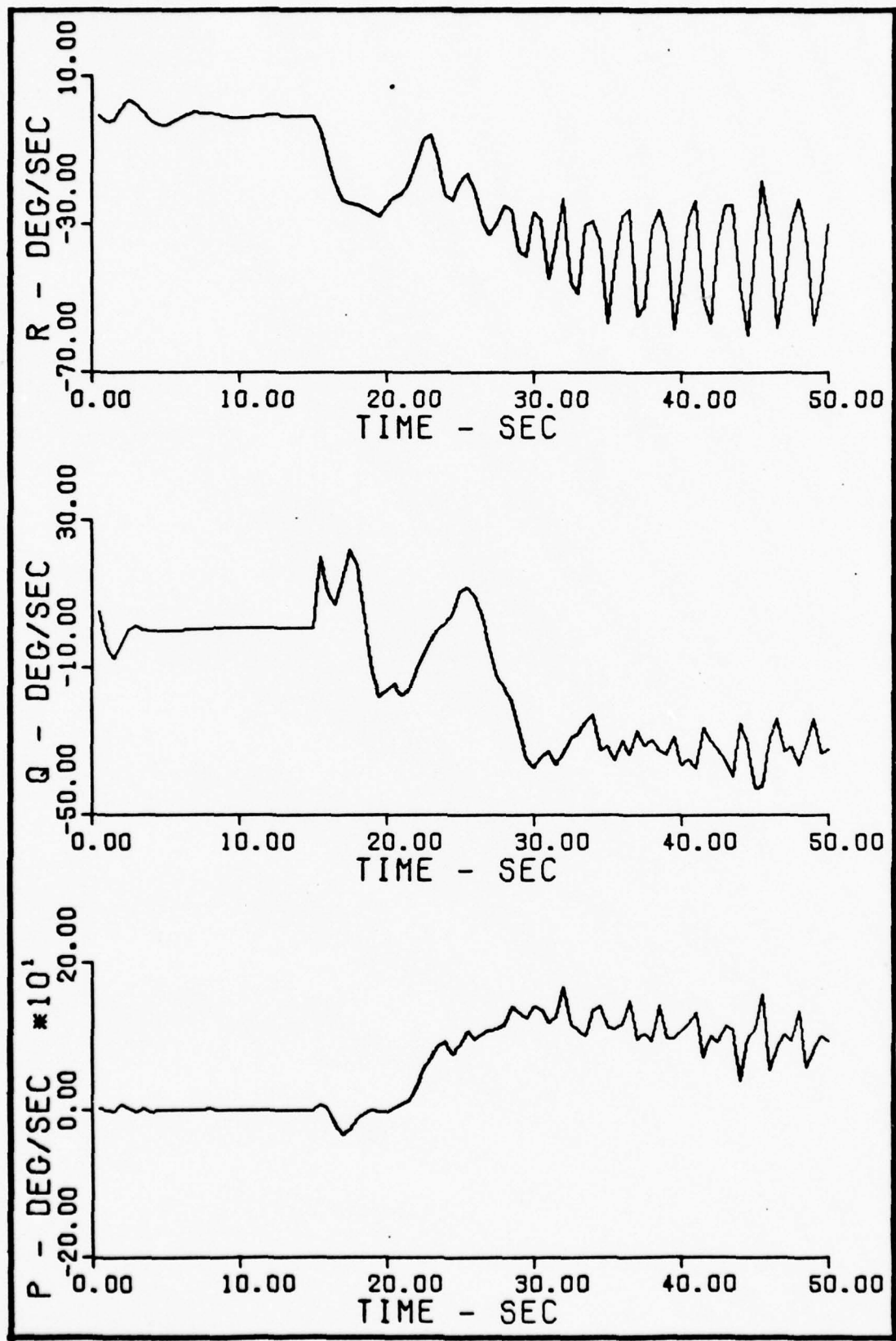


Fig. I-1 p, q, and r vs. time, $\alpha = 19$ deg, $\beta = 9$ deg,
 $q = 20$ deg/sec at $t = 15$ sec

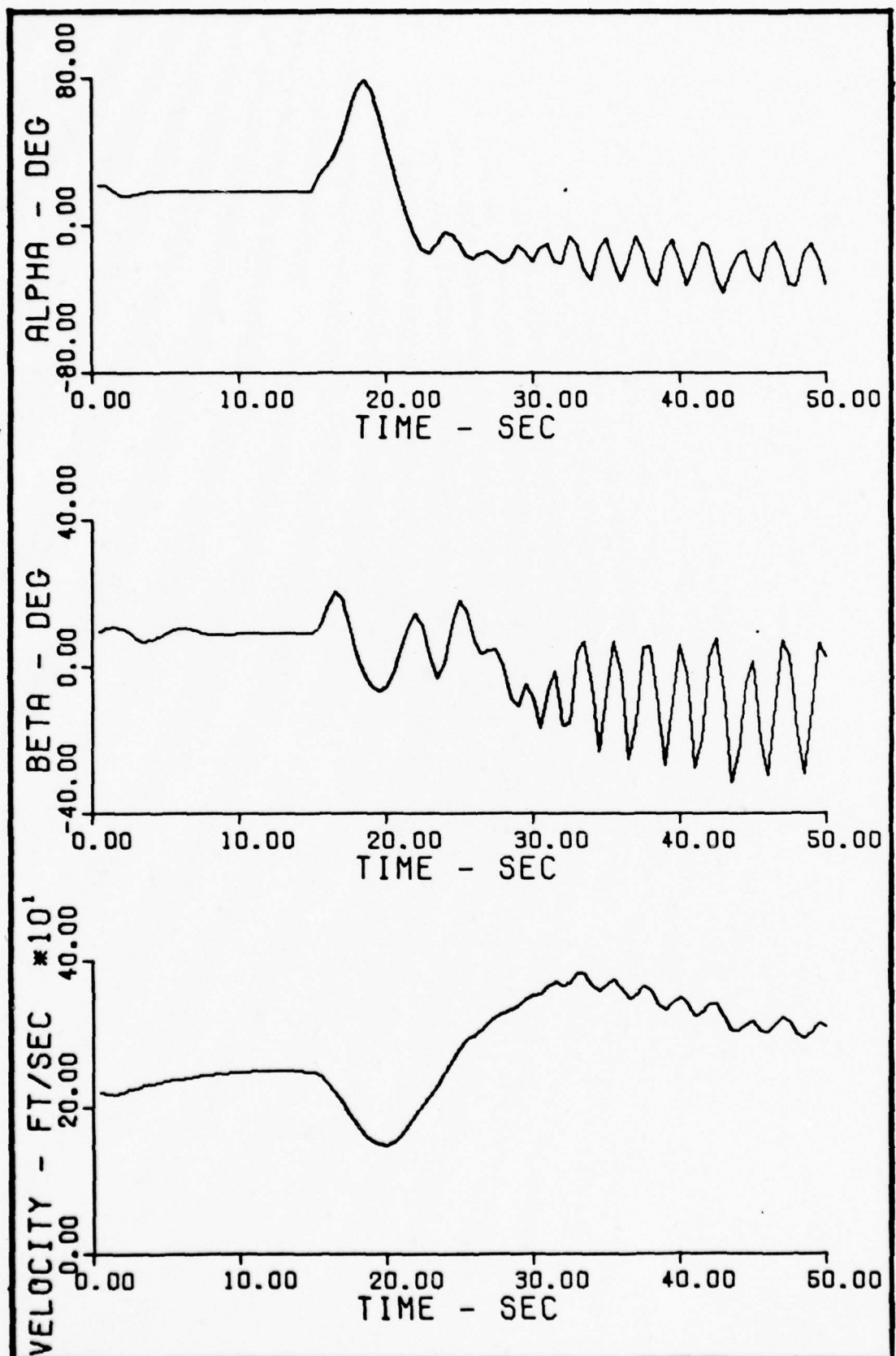


Fig. I-2 α , β , and Velocity vs. time, $\alpha = 19$ deg,
 $\beta = 9$ deg, $q = 20$ deg/sec at $t = 15$ sec

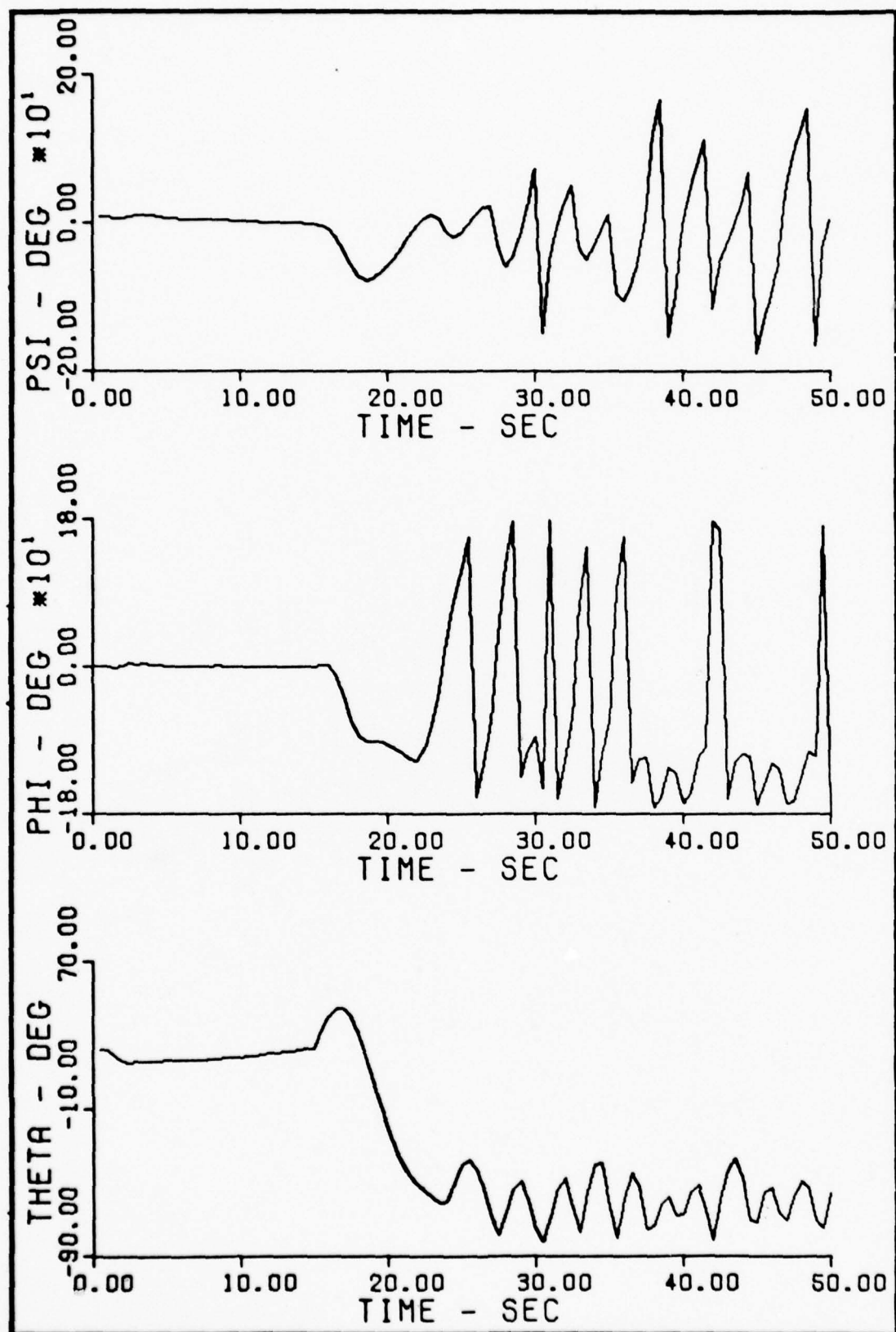


Fig. I-3 θ , ϕ , and ψ vs. time, $\alpha = 19$ deg, $\beta = 9$ deg,
 $q = 20$ deg/sec at $t = 15$ sec

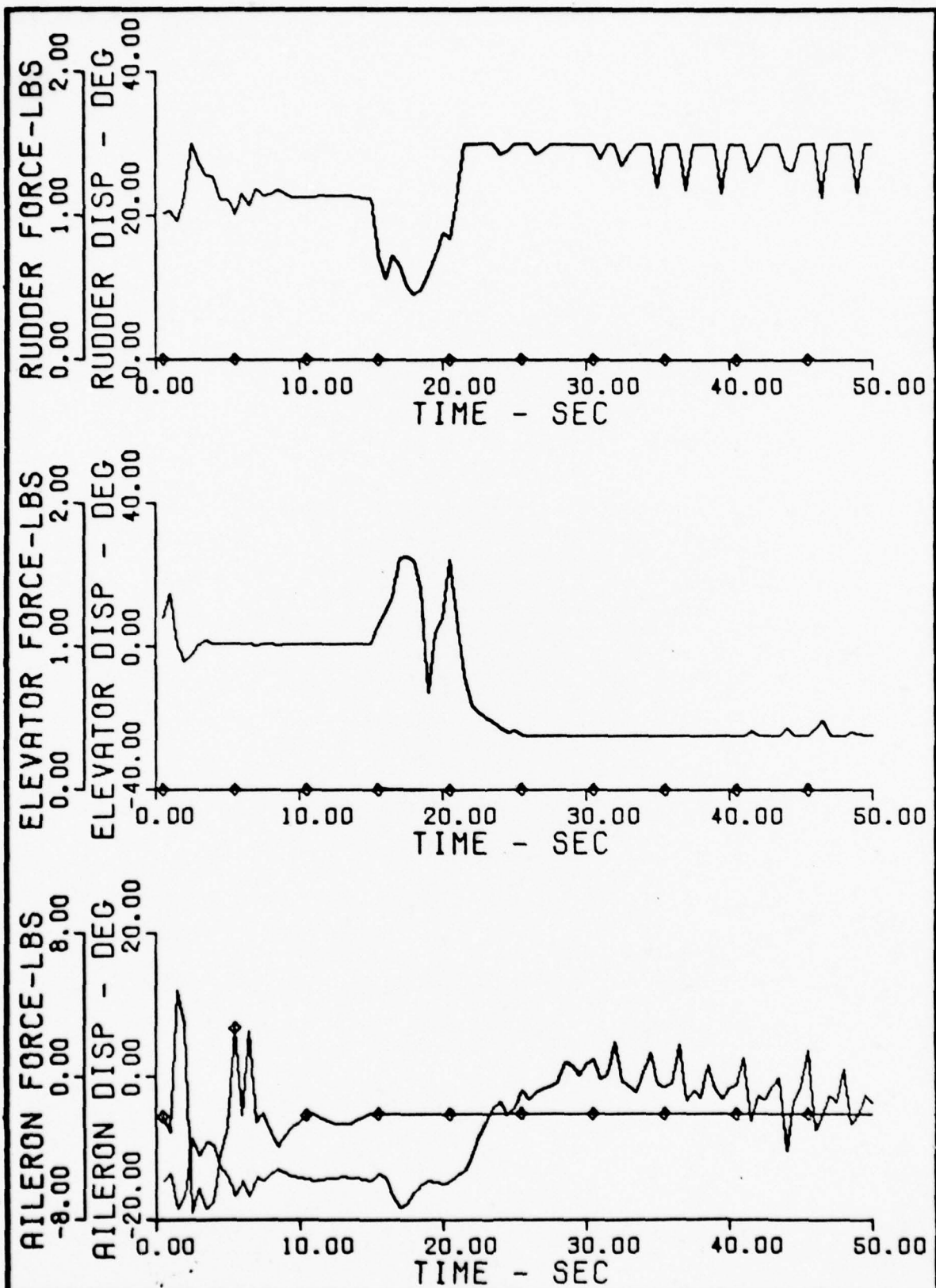


Fig. I-4 Control Forces and Deflections vs. time, $\alpha = 19$ deg,
 $\beta = 9$ deg, $q = 20$ deg/sec at $t = 15$ sec

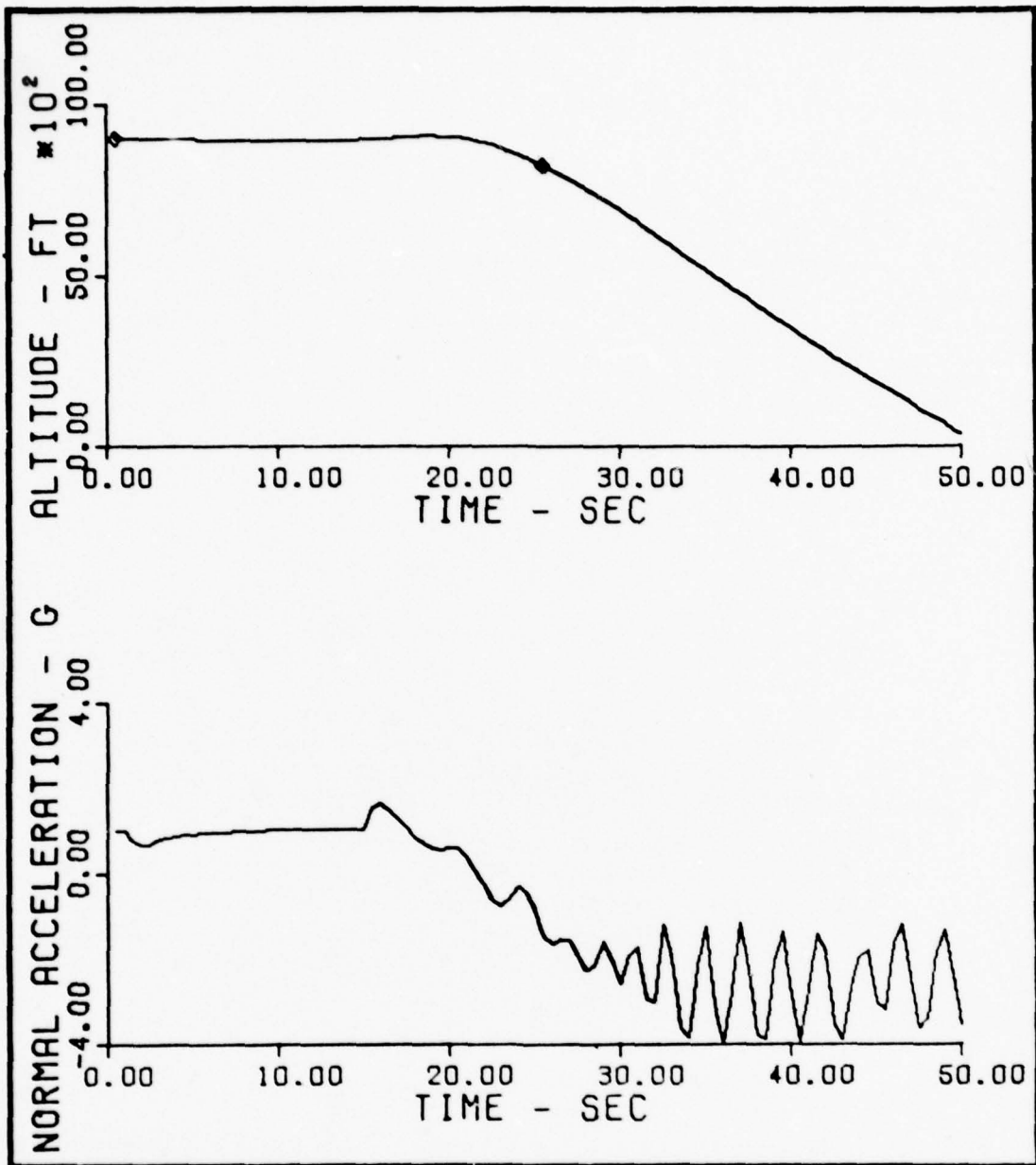


Fig. I-5 N_z and Altitude vs. time, $\alpha = 19$ deg, $\beta = 9$ deg,
 $q_z = 20$ deg/sec at $t = 15$ sec

Appendix J

Rolling Departure to an Inverted Spin

$\alpha = 17 \text{ deg}$, $\beta = 9 \text{ deg}$

$q = 20 \text{ deg/sec}$ at $t = 15 \text{ sec}$

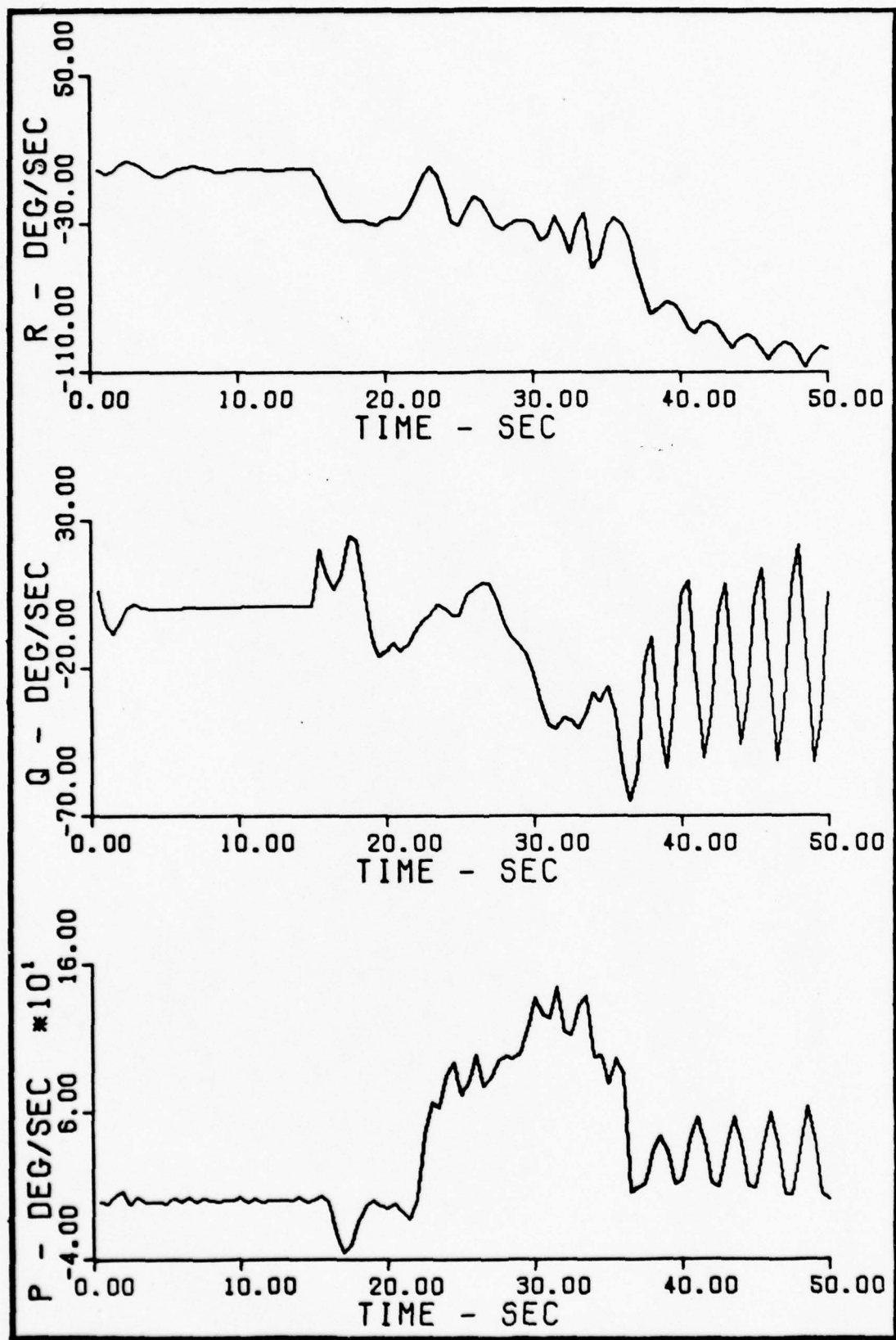


Fig. J-1 p, q, and r vs. time, $\alpha = 17$ deg, $\beta = 9$ deg,
 $q = 20$ deg/sec at $t = 15$ sec

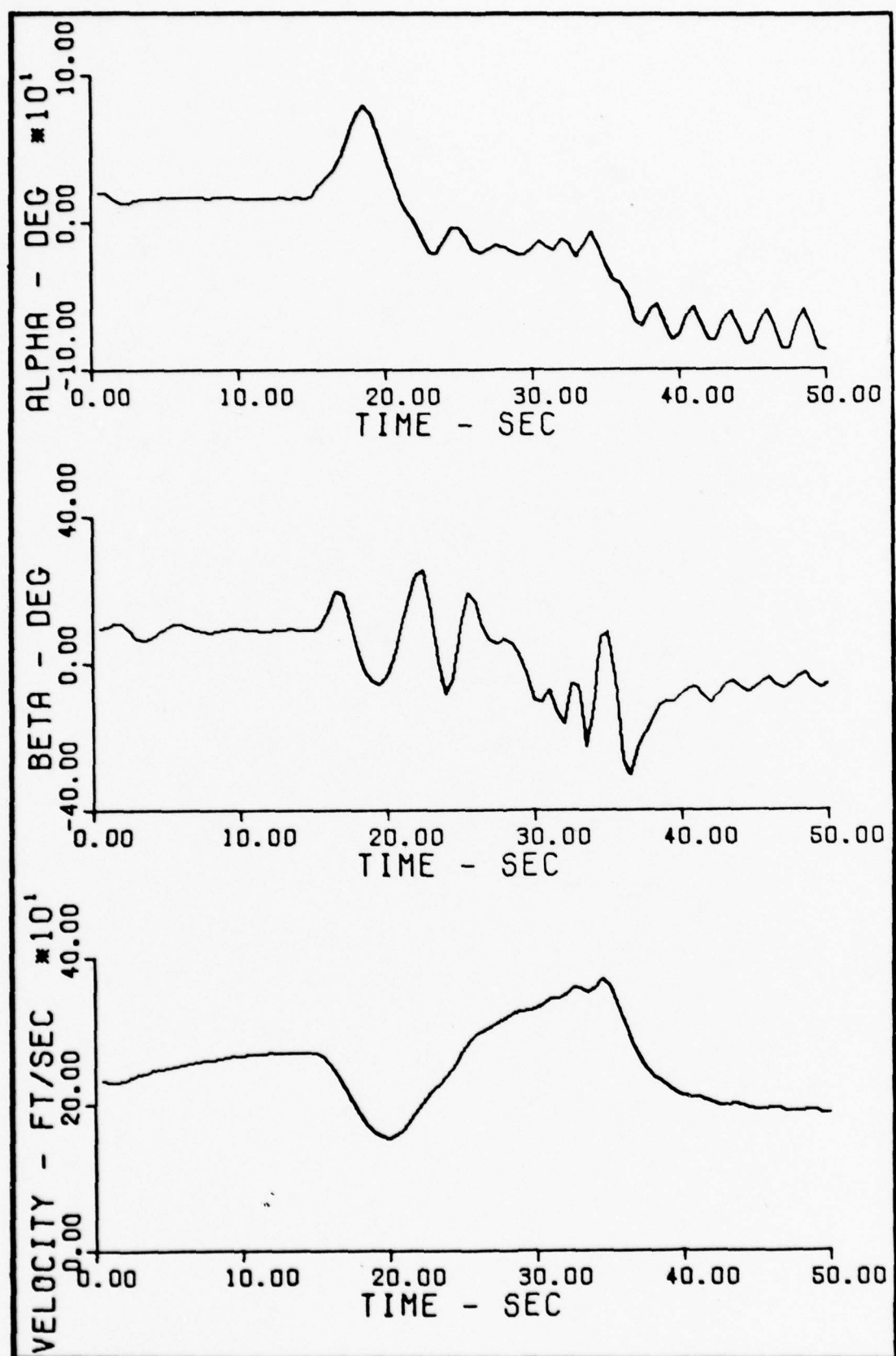


Fig. J-2 α , β , and Velocity vs. time, $\alpha = 17$ deg,
 $\beta = 9$ deg, $q = 20$ deg/sec at $t = 15$ sec

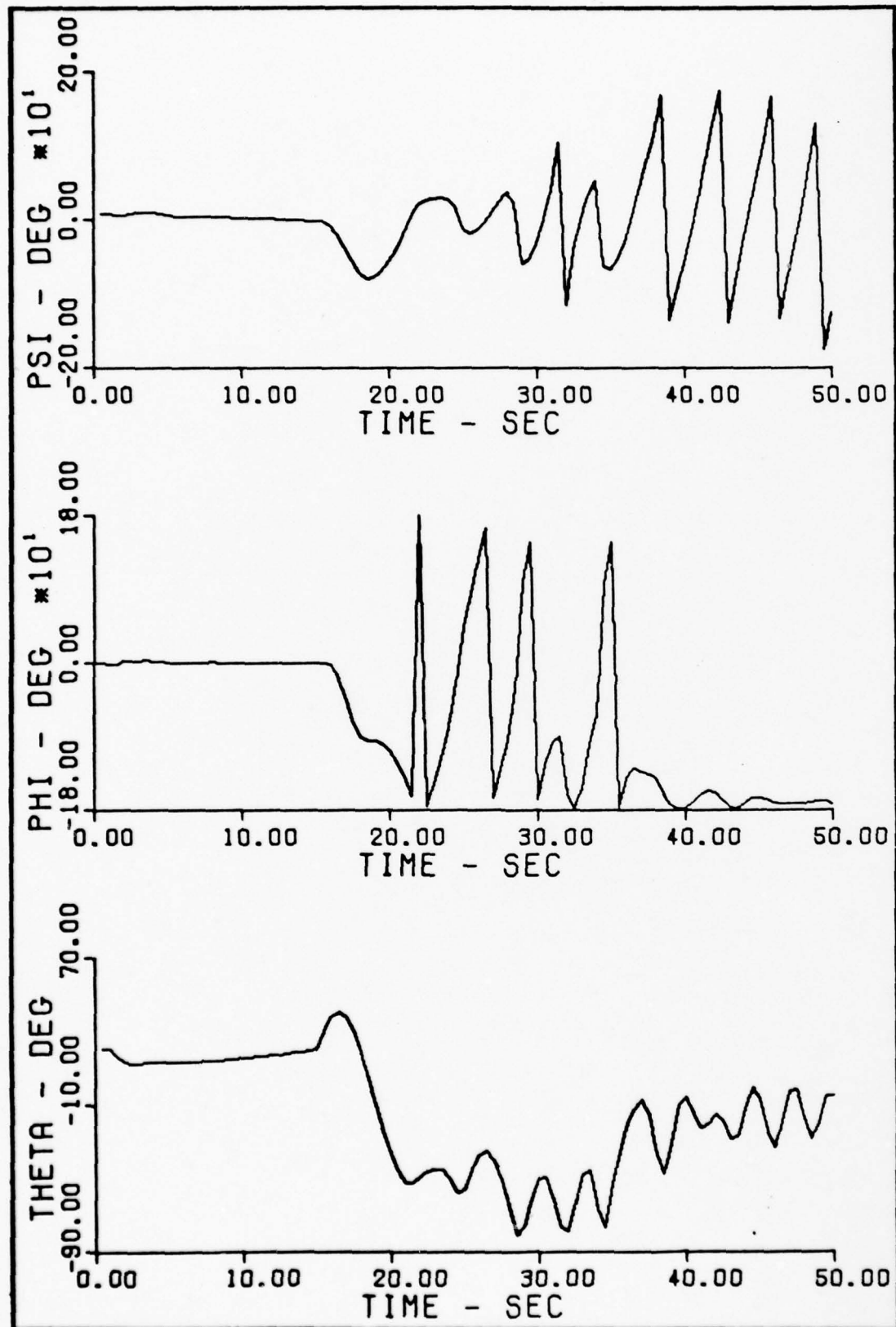


Fig. J-3 θ , ϕ , and ψ vs. time, $\alpha = 17$ deg, $\beta = 9$ deg,
 $q = 20$ deg/sec at $t = 15$ sec

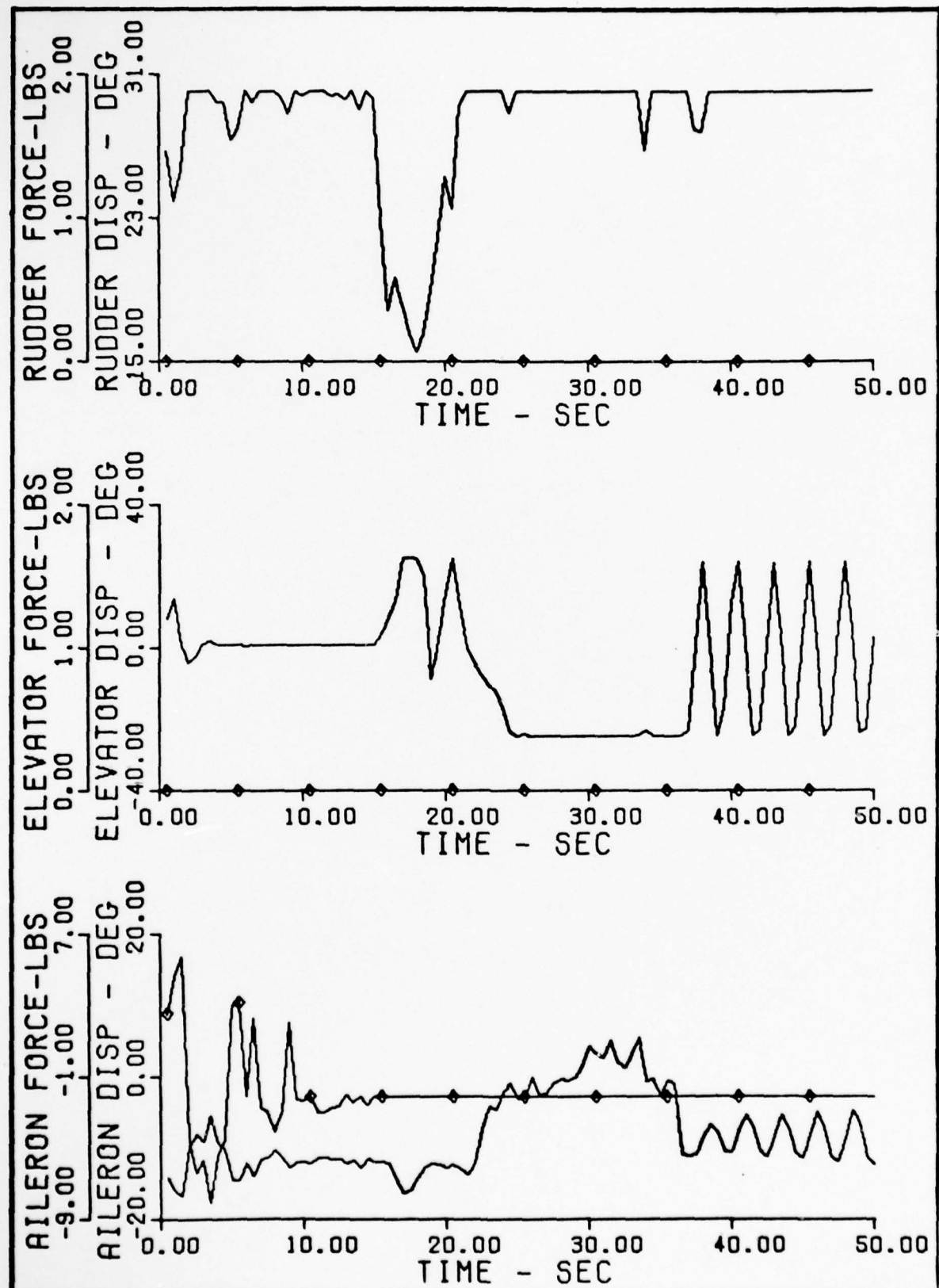


Fig. J-4 Control Forces and Deflections vs. time, $\alpha = 17$ deg,
 $\beta = 9$ deg, $q = 20$ deg/sec at $t = 15$ sec

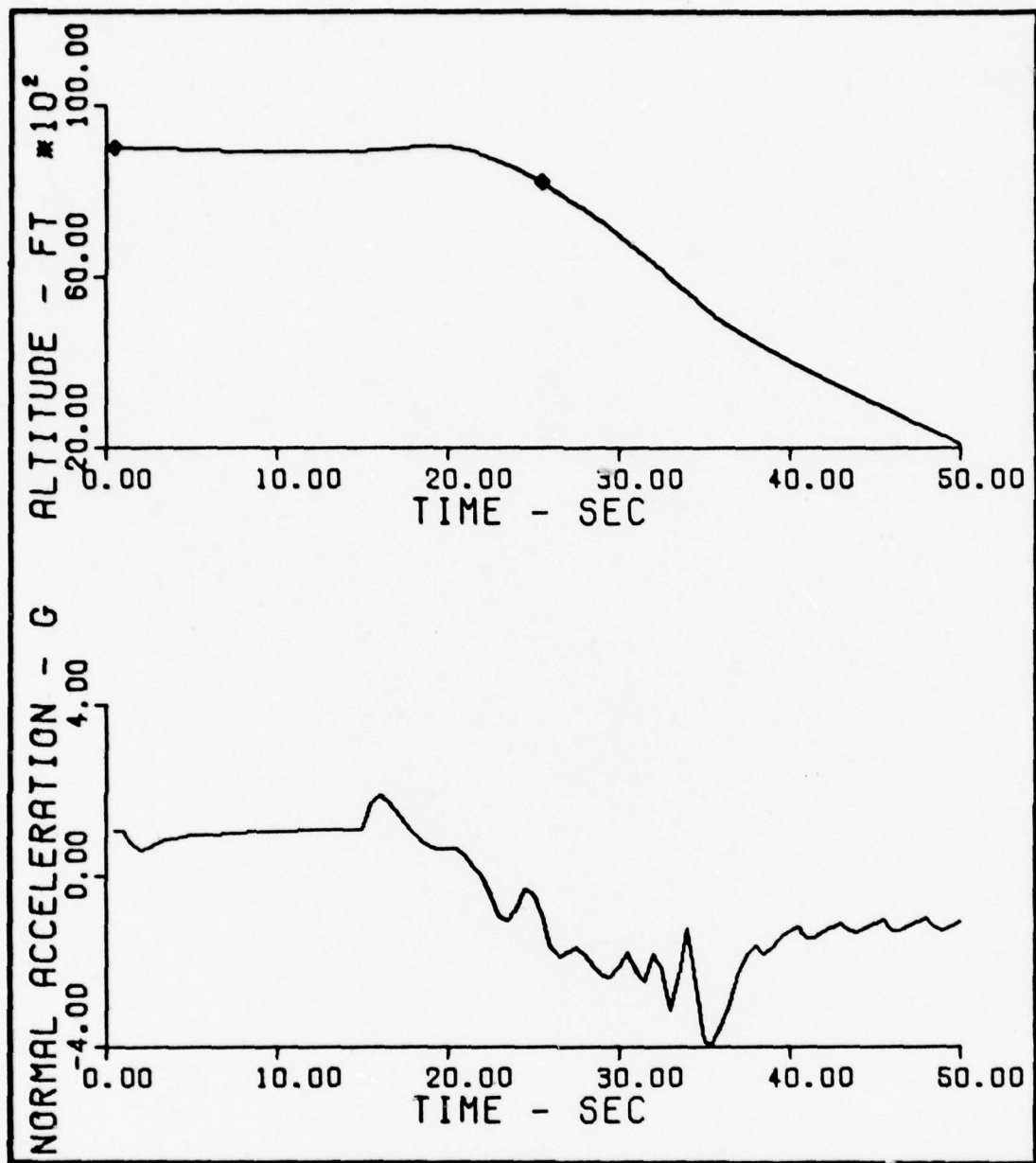


Fig. J-5 N_z and Altitude vs. time, $\alpha = 17$ deg, $\beta = 9$ deg,
 $q = 20$ deg/sec at $t = 15$ sec

Appendix K

No Uncontrolled Motion

$\alpha = 21 \text{ deg}$, $\beta = 10 \text{ deg}$

$q = 20 \text{ deg/sec}$ at $t = 15 \text{ sec}$

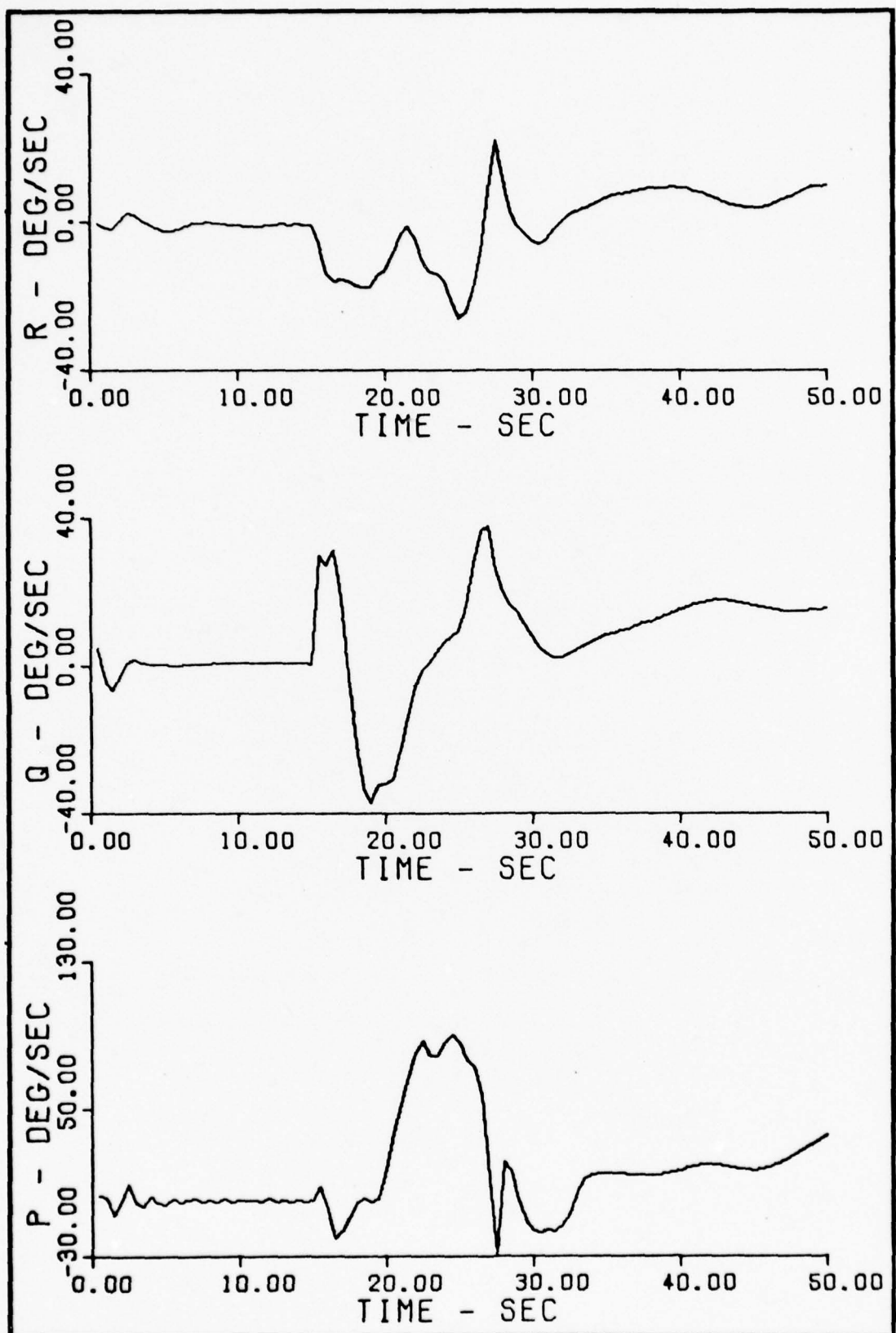


Fig. K-1 p, q, and r vs. time, $\alpha = 21$ deg, $\beta = 10$ deg,
 $q \approx 20$ deg/sec at $t = 15$ sec

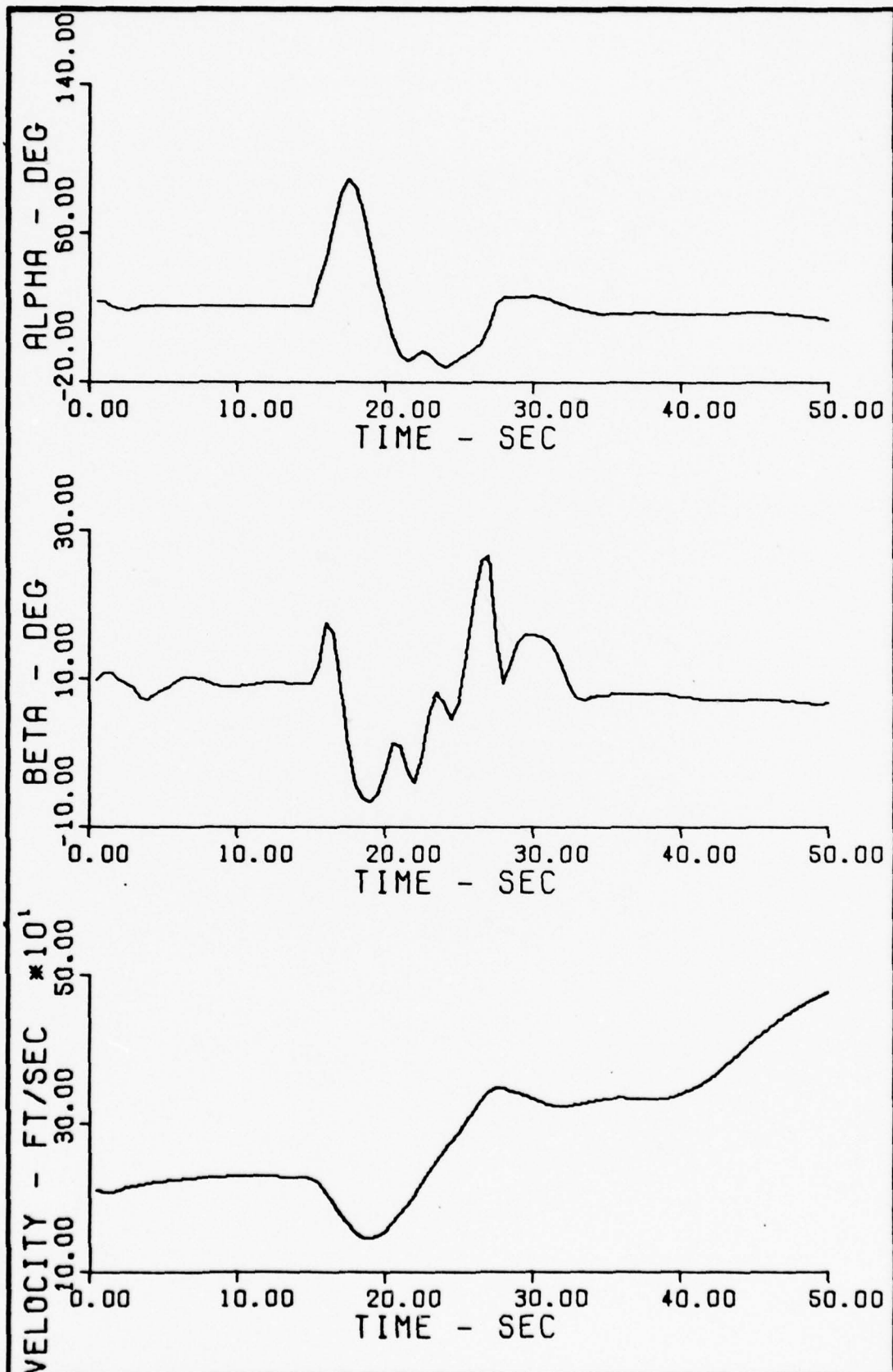


Fig. K-2 α , β , and Velocity vs. time, $\alpha = 21$ deg,
 $\beta = 10$ deg, $q = 20$ deg/sec at $t = 15$ sec

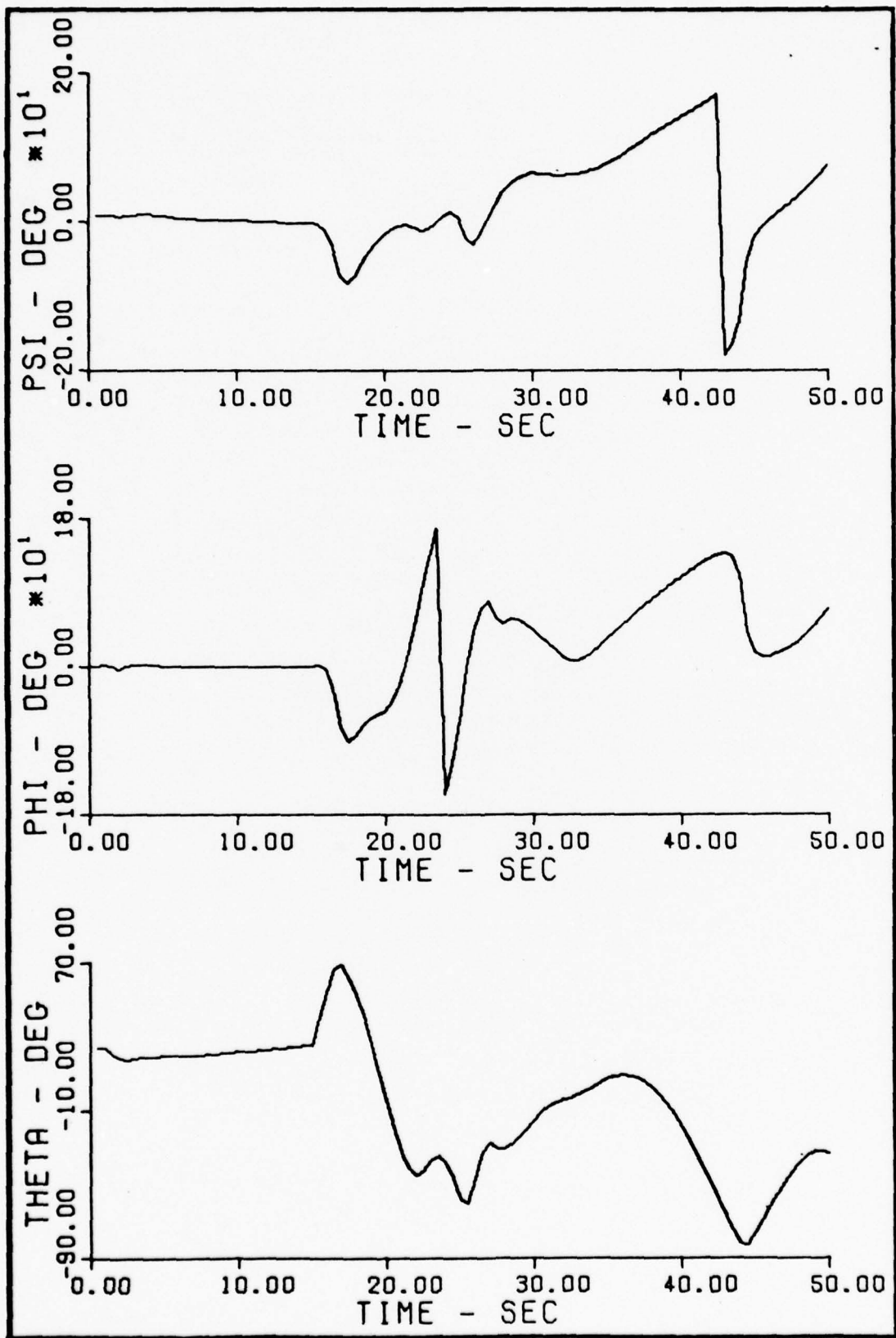


Fig. K-3 θ , ϕ , and ψ vs. time, $\alpha = 21$ deg, $\beta = 10$ deg,
 $q = 20$ deg/sec at $t = 15$ sec

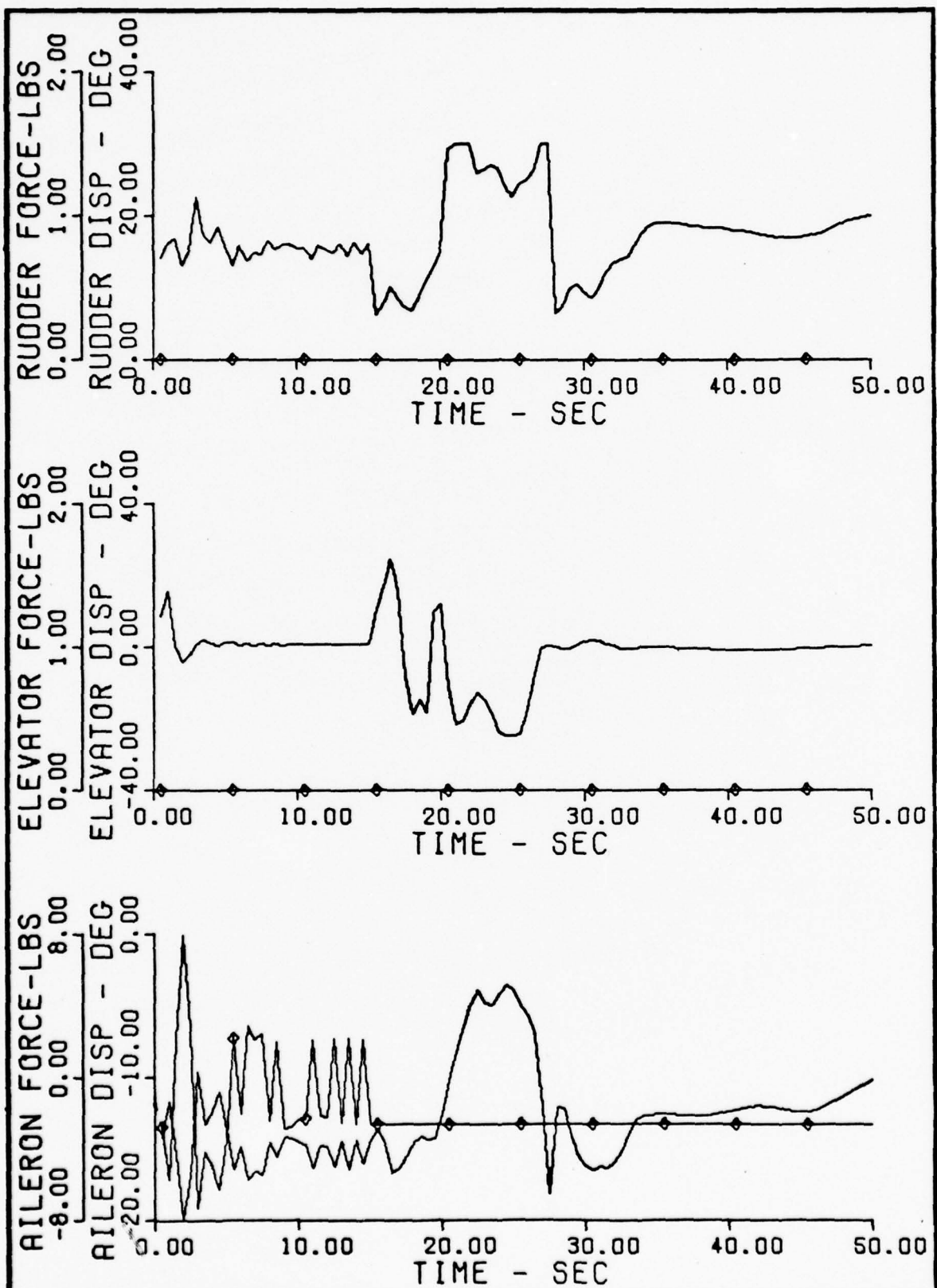


Fig. K-4 Control Forces and Deflections vs. time, $\alpha = 21$ deg,
 $\beta = 10$ deg, $q = 20$ seg/sec at $t = 15$ sec

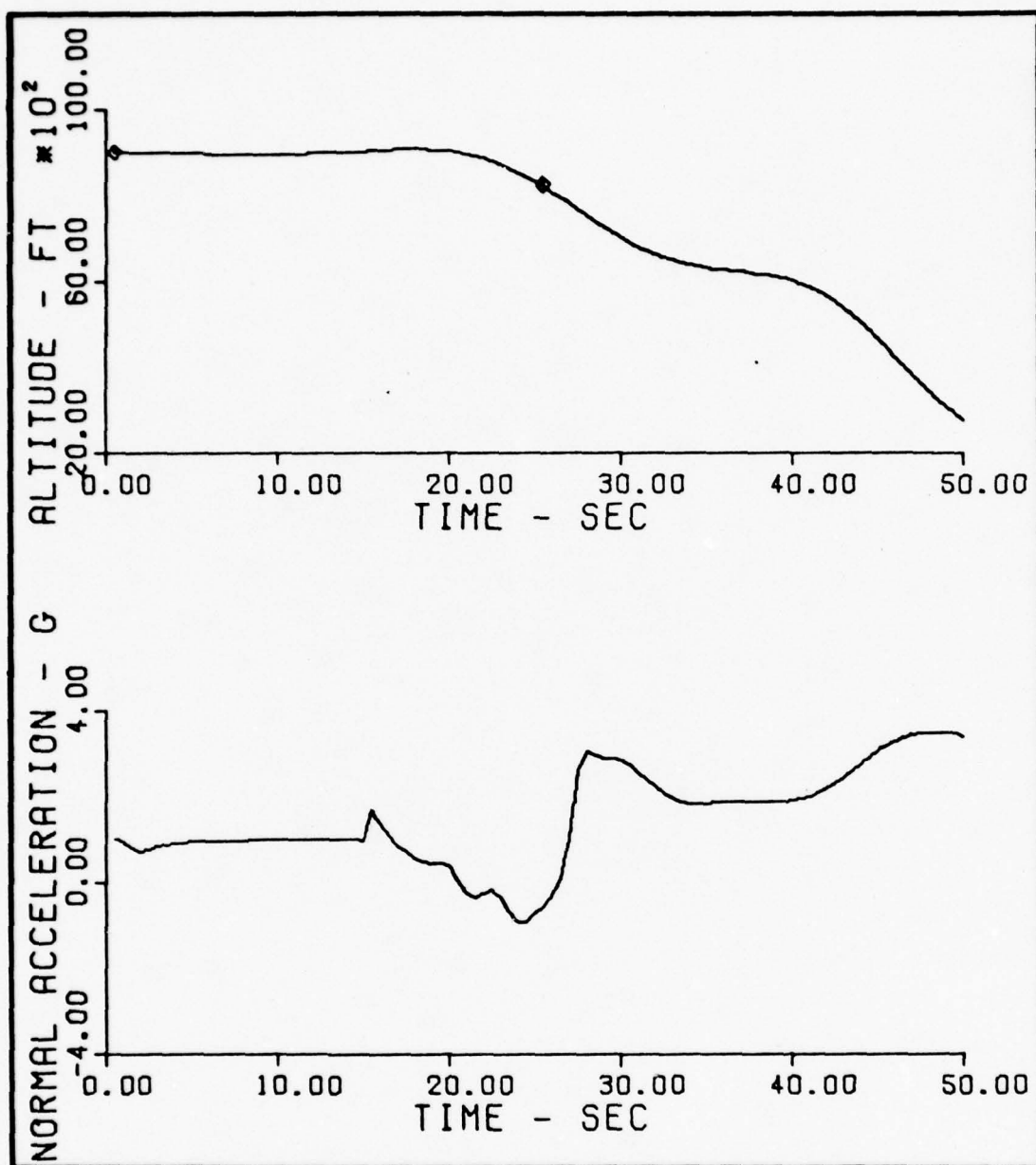


Fig. K-5 N_z and Altitude vs. time, $\alpha = 21$ deg, $\beta = 10$ deg,
 $q = 50$ deg/sec at $t = 15$ sec

Appendix L

Erect Spin

$\alpha = 25 \text{ deg}$, $\beta = 6 \text{ deg}$

$r = -20 \text{ deg/sec}$ at $t = 15 \text{ sec}$

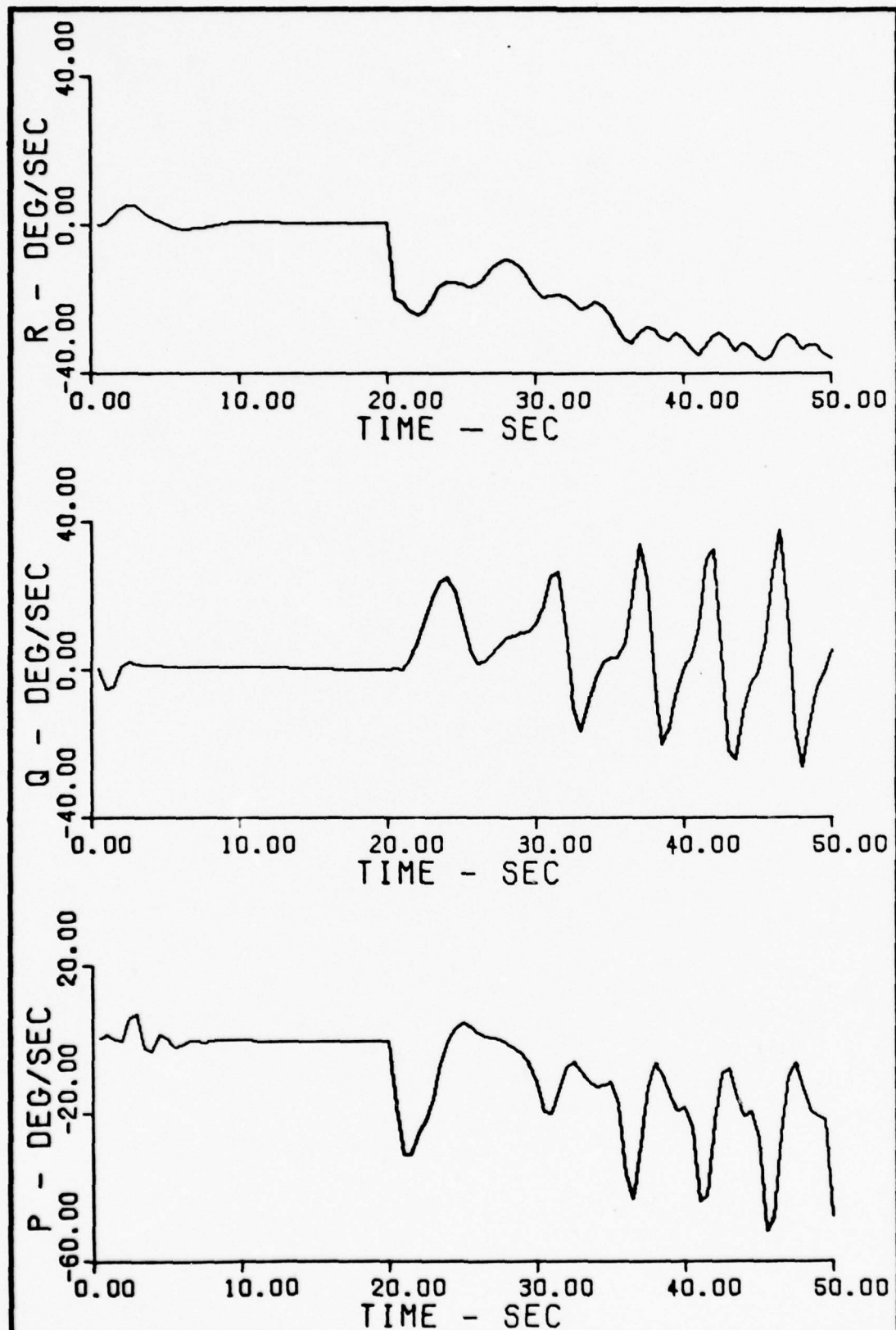


Fig. L-1 p, q, and r vs. time, $\alpha = 25$ deg, $\beta = 6$ deg,
 $r = -20$ deg/sec at $t = 15$ sec

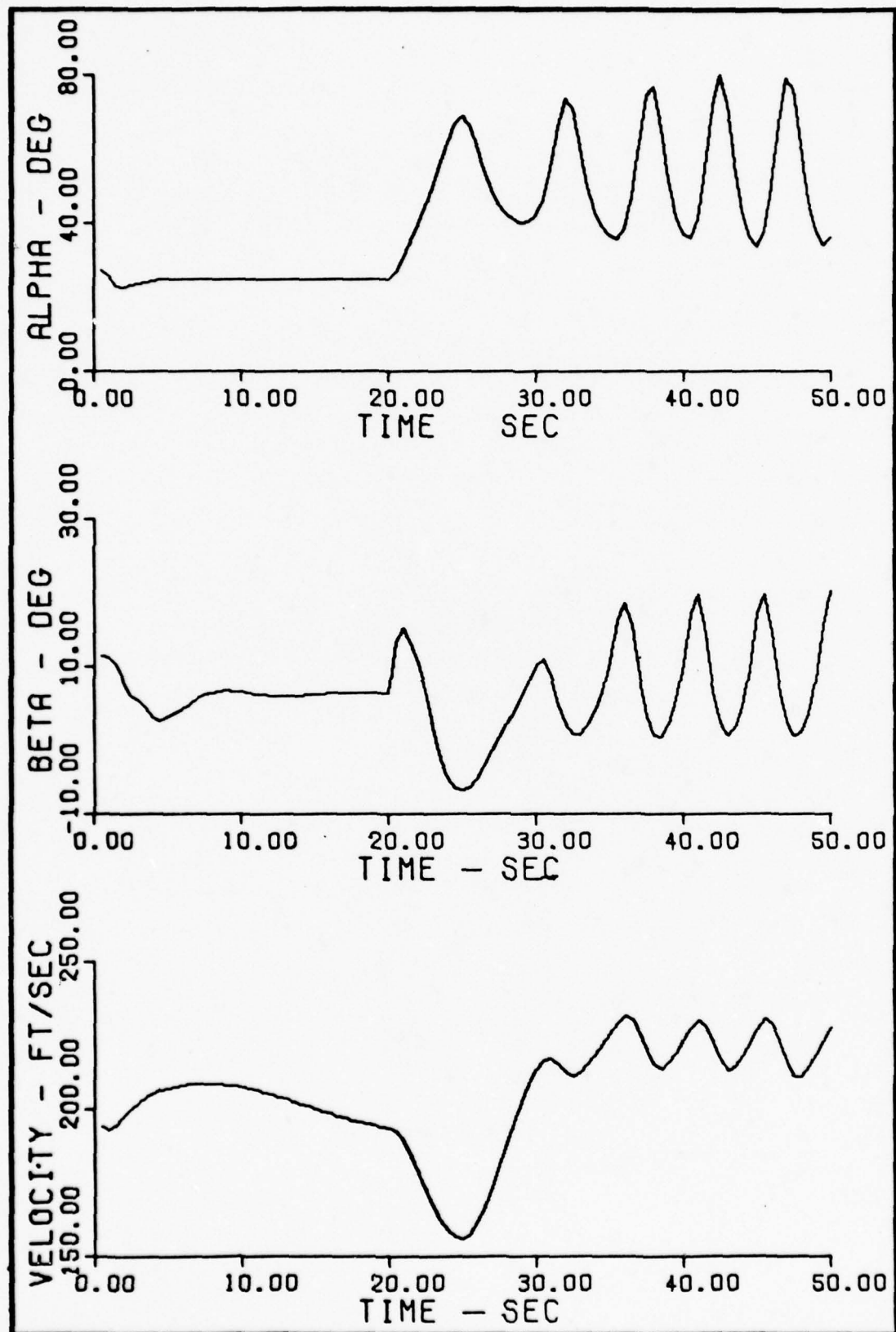


Fig. L-2 α , β , and Velocity vs. time, $\alpha = 25$ deg,
 $\beta = 6$ deg, $r = -20$ deg/sec at $t = 15$ sec

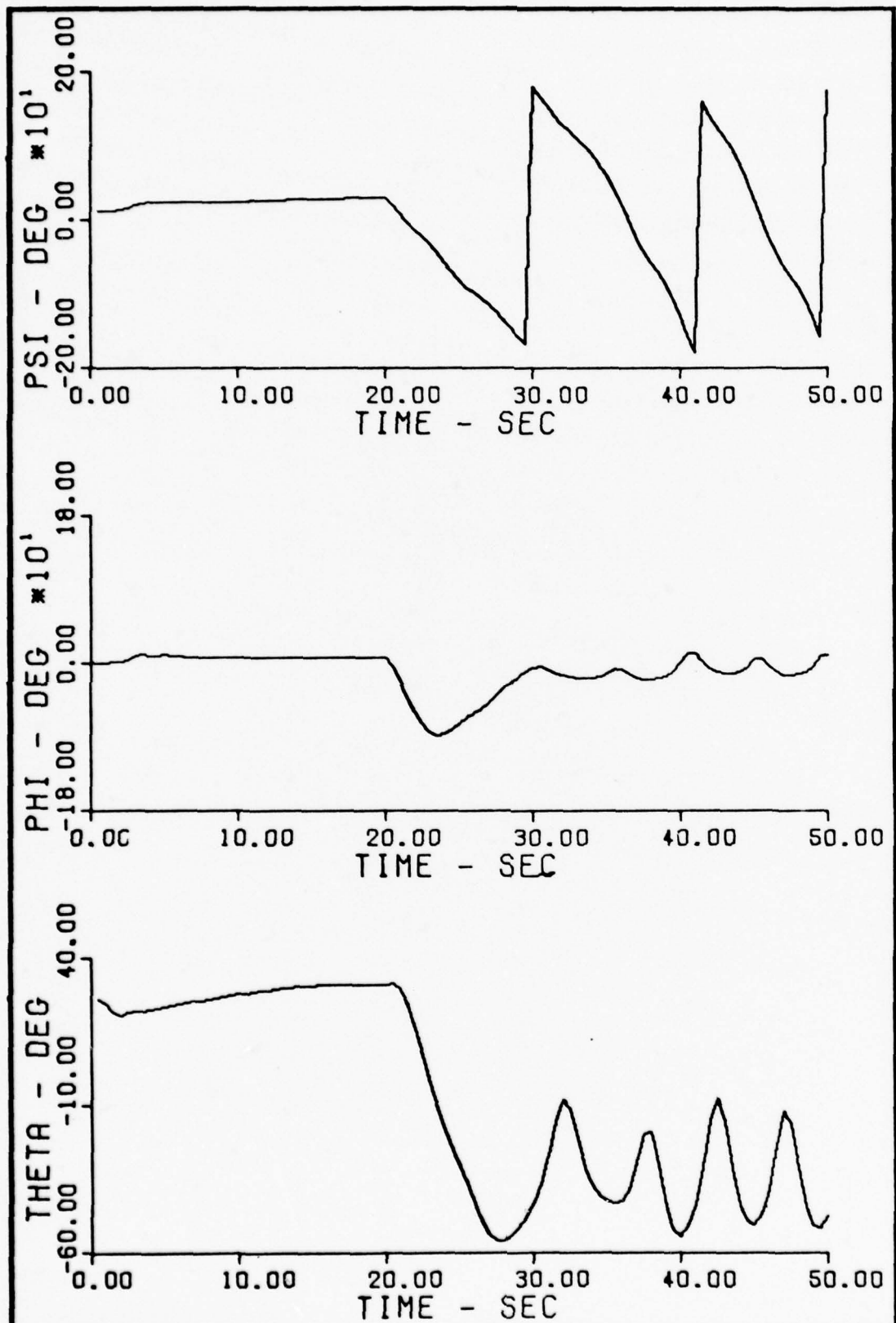


Fig. L-3 θ , ϕ , and ψ vs. time, $\alpha = 25$ deg, $\beta = 6$ deg,
 $r = -20$ deg/sec at $t = 15$ sec

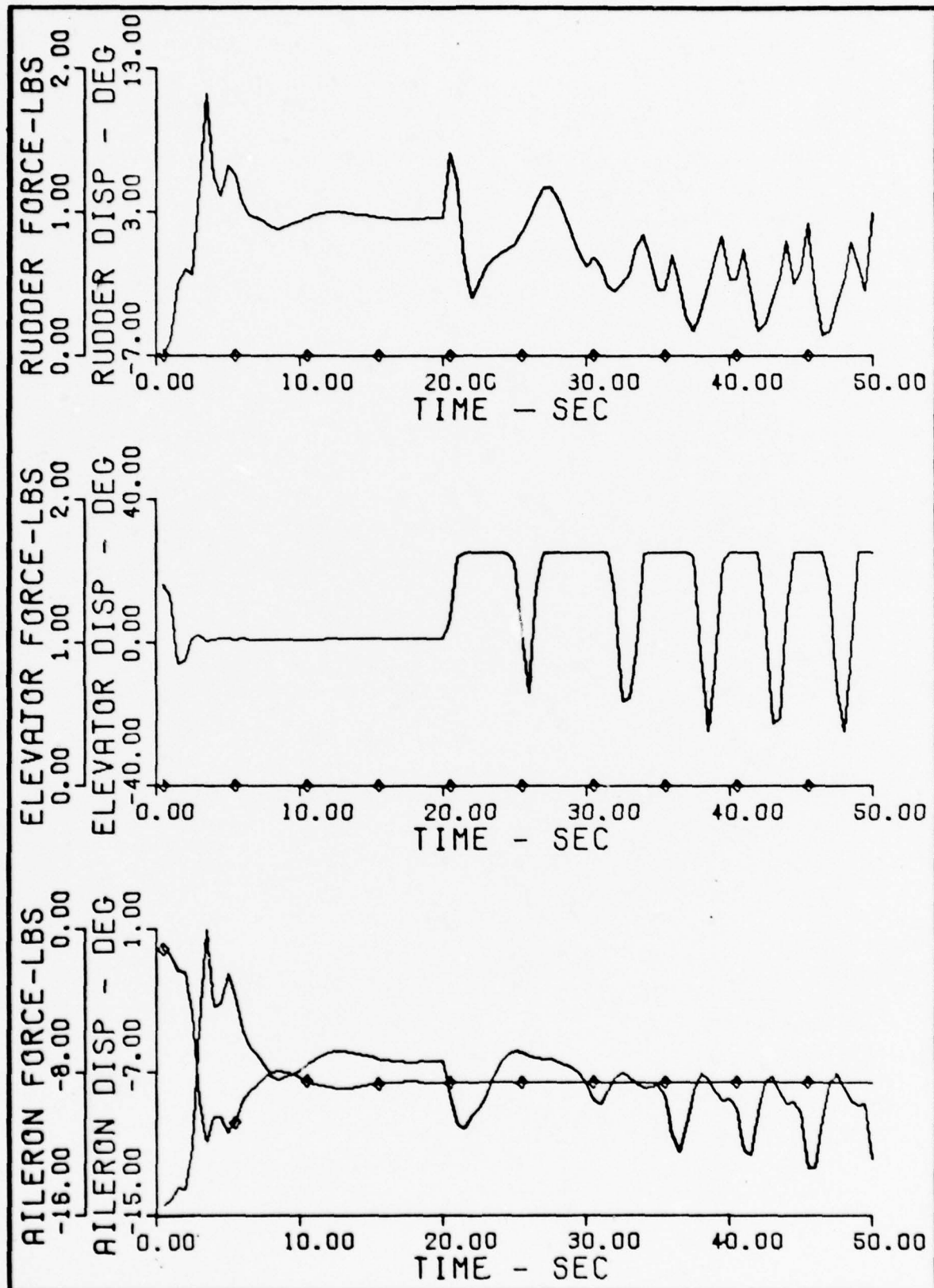


Fig. L-4 Control Forces and Deflections vs. time, $\alpha = 25$ deg,
 $\dot{\alpha} = 6$ deg, $r = -20$ deg/sec at $t = 15$ sec

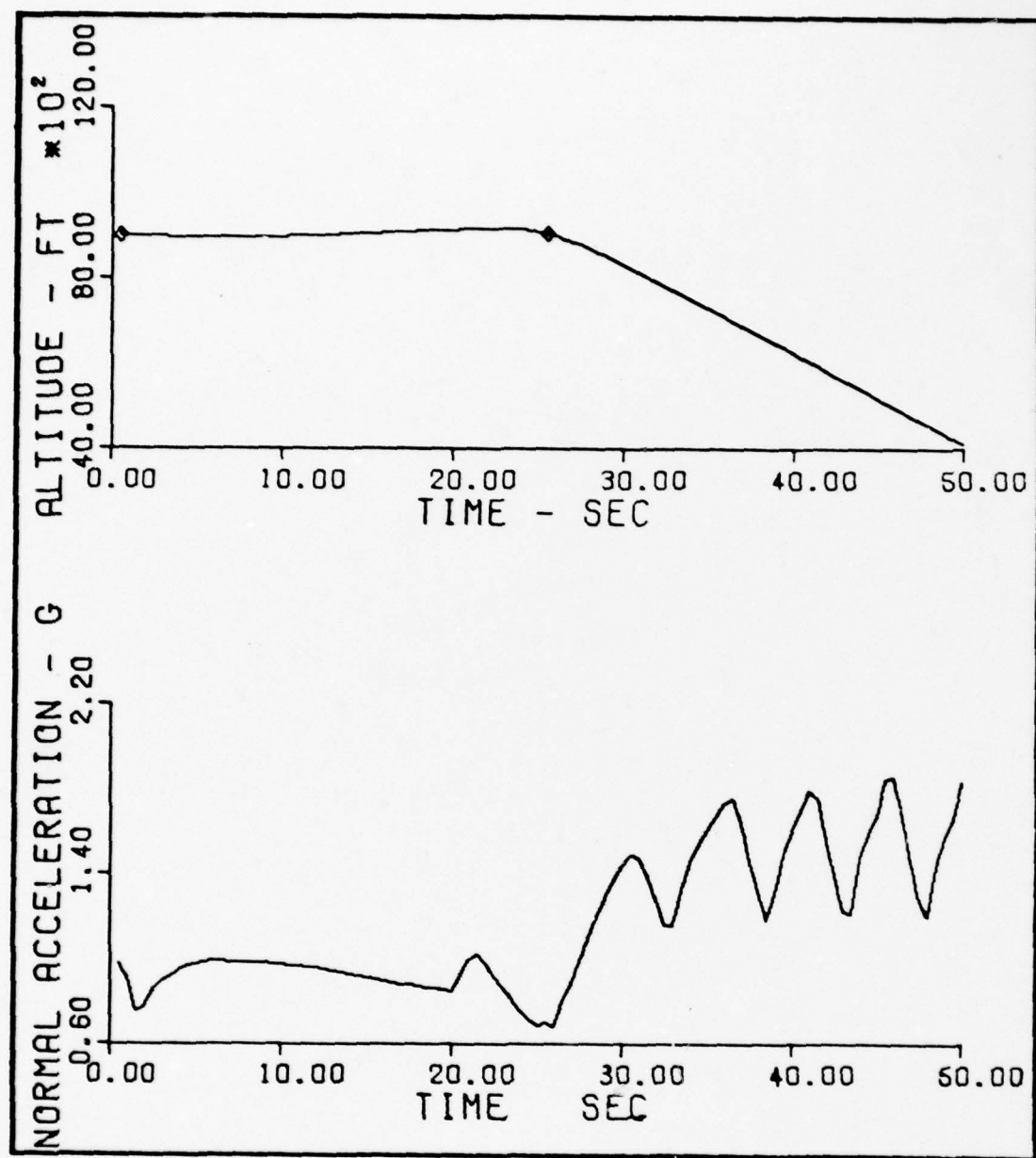


Fig. L-5 N_z and Altitude vs. time, $\alpha = 25$ deg, $\dot{\theta} = 6$ deg,
 $r = -20$ deg/sec at $t = 15$ sec

Appendix M

No Uncontrolled Motion

$\alpha = 25 \text{ deg}$, $\beta = 6 \text{ deg}$

$r = -30 \text{ deg/sec}$ at $t = 15 \text{ sec}$

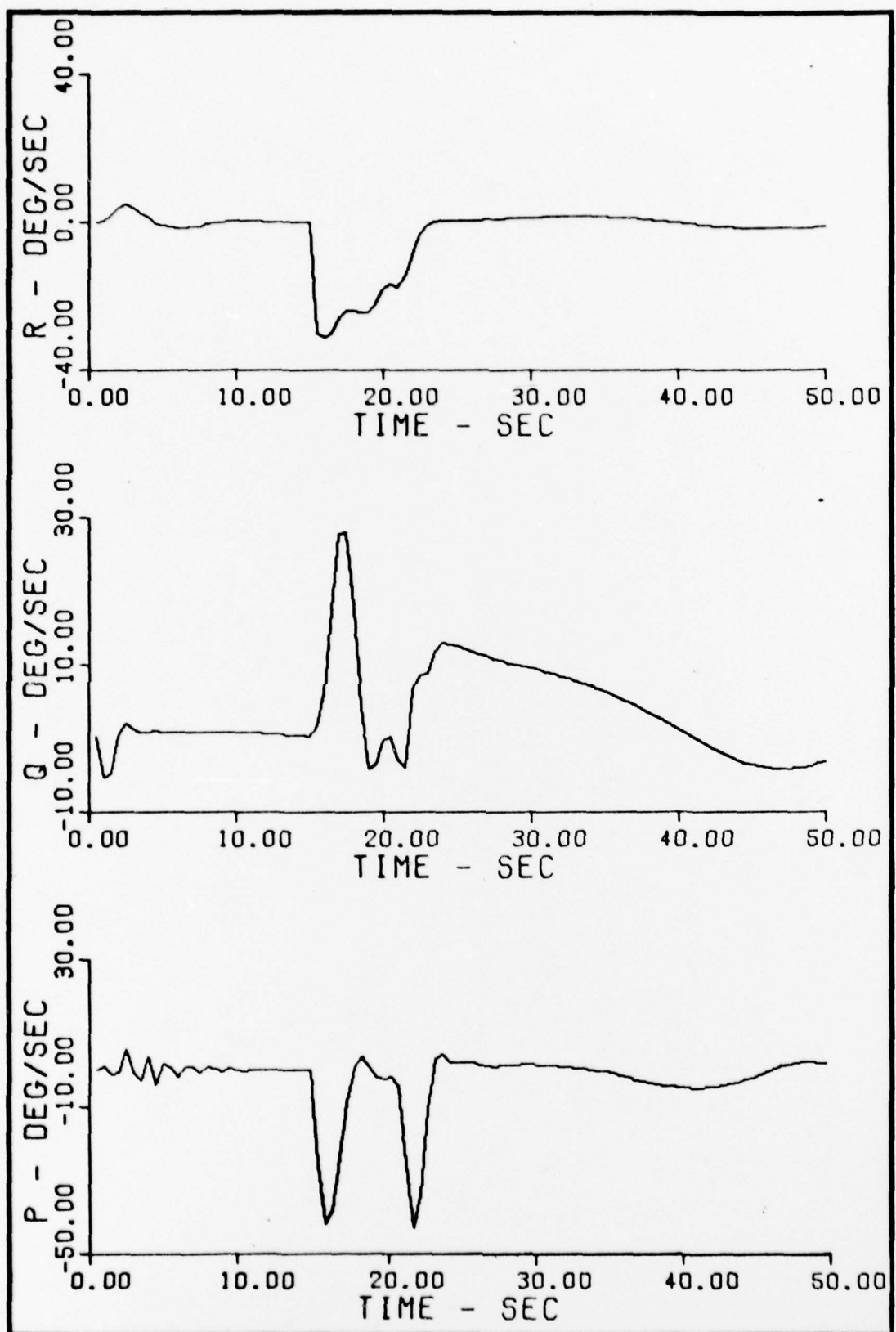


Fig. M-1 p, q, and r vs. time, $\alpha = 25$ deg, $\beta = 6$ deg,
 $r = -30$ deg/sec at $t = 15$ sec

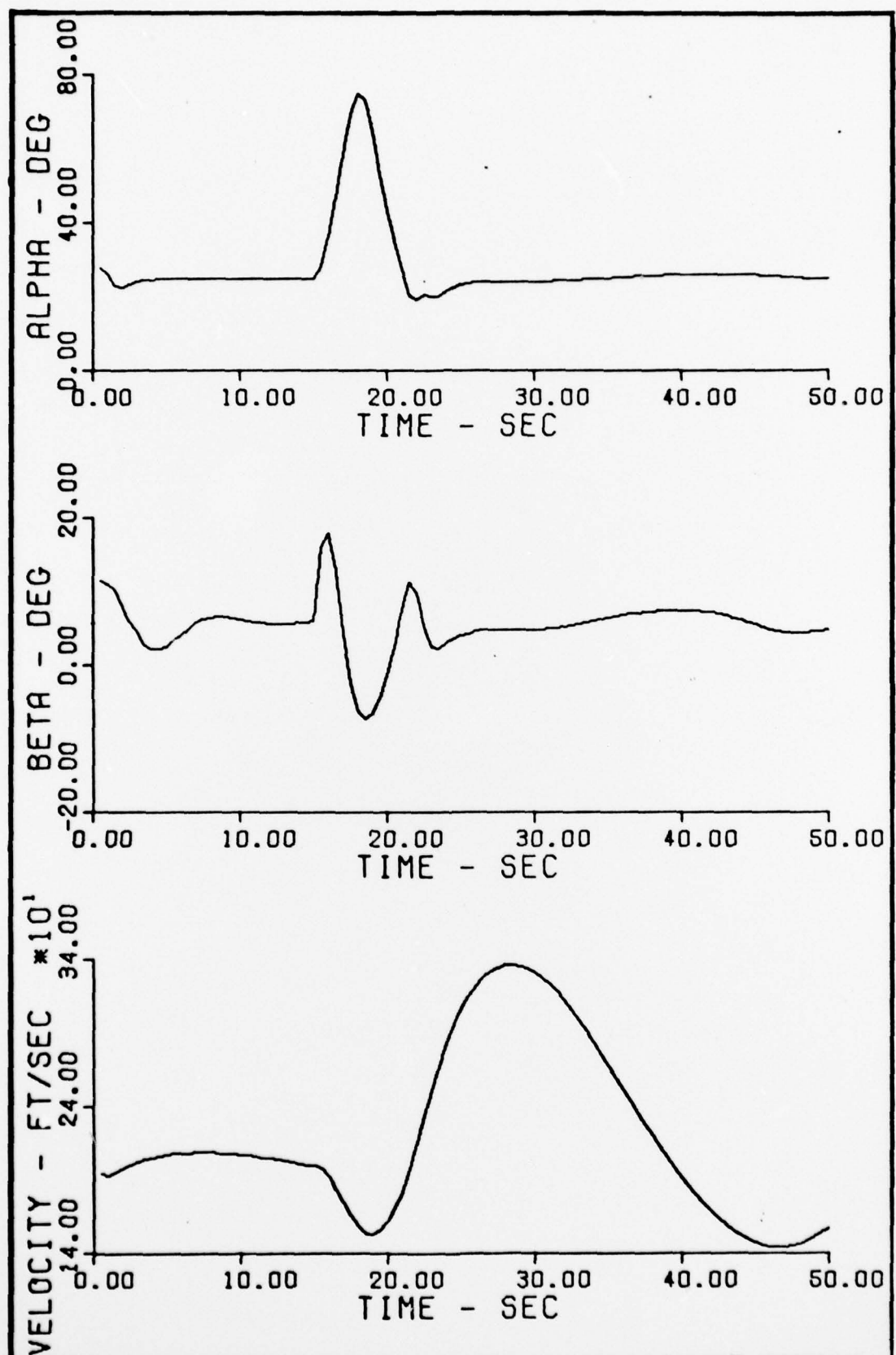


Fig. M-2 α , β , and Velocity vs. time, $\alpha = 25$ deg,
 $\beta = 6$ deg, $r = -30$ deg/sec at $t = 15$ sec

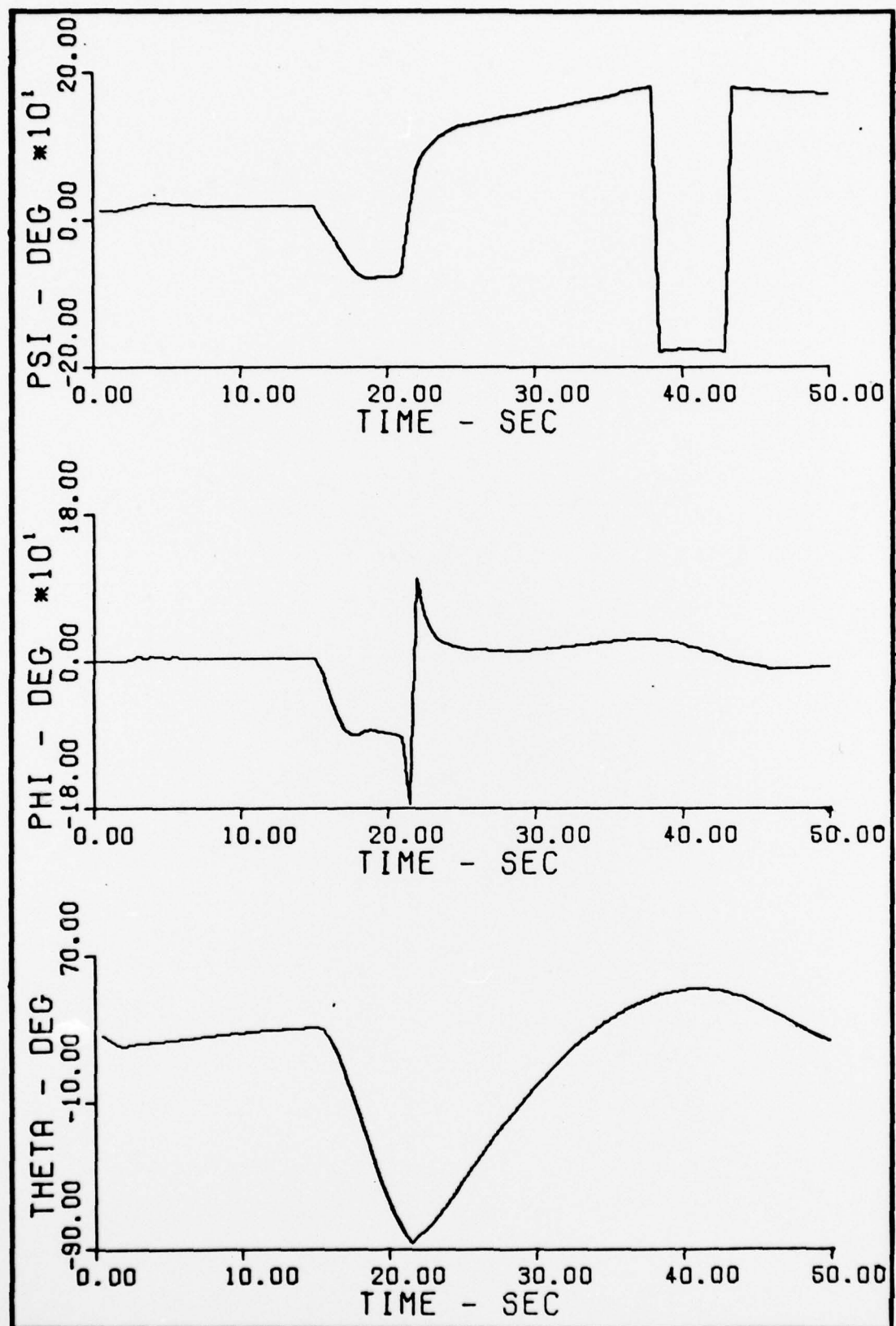


Fig. M-3 θ , ϕ , and ψ vs. time, $\alpha = 25$ deg, $\beta = 6$ deg,
 $r = -30$ deg/sec at $t = 15$ sec

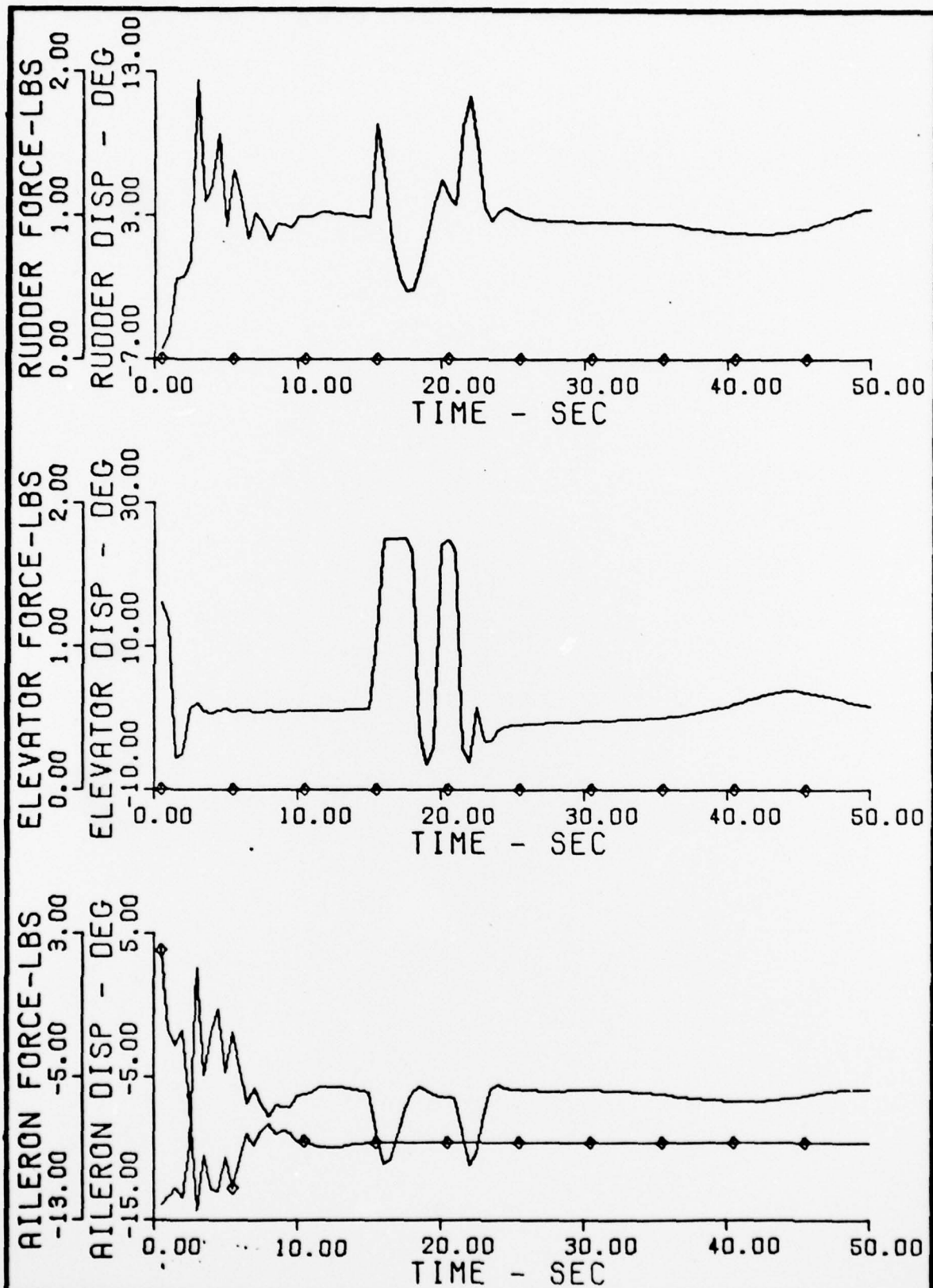


Fig. M-4 Control Forces and Deflections vs. time, $\alpha = 25$ deg,
 $\beta = 6$ deg, $r = -30$ deg/sec at $t = 15$ sec

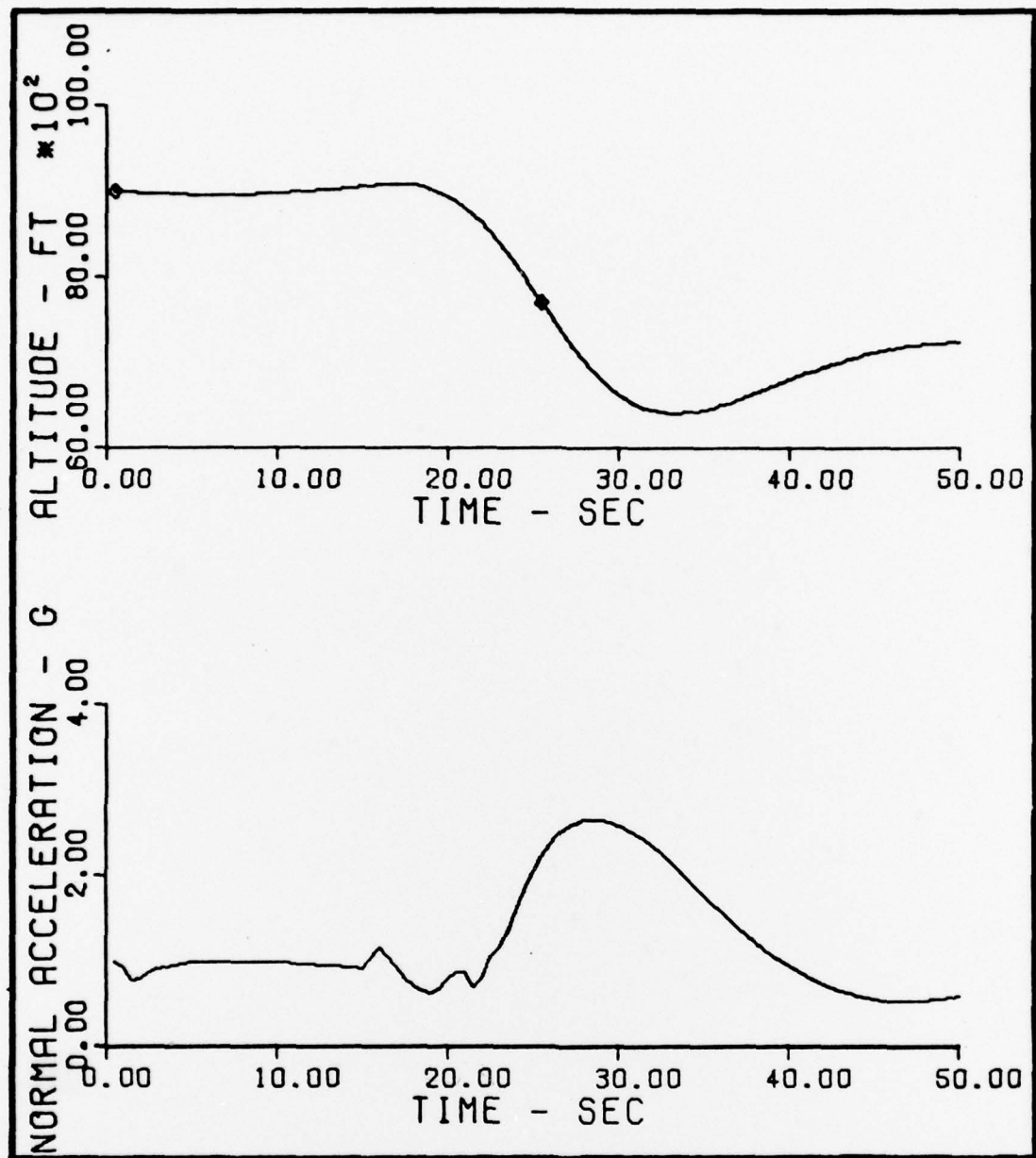


Fig. M-5 N_z and Altitude vs. time, $\alpha = 25$ deg, $\beta = 6$ deg,
 $r_z = -30$ deg/sec at $t = 15$ sec

Appendix N

Effects of Departure Controller

$\alpha = 19$ deg, $\beta = 4$ deg

$r = -30$ deg/sec at $t = 15$ sec

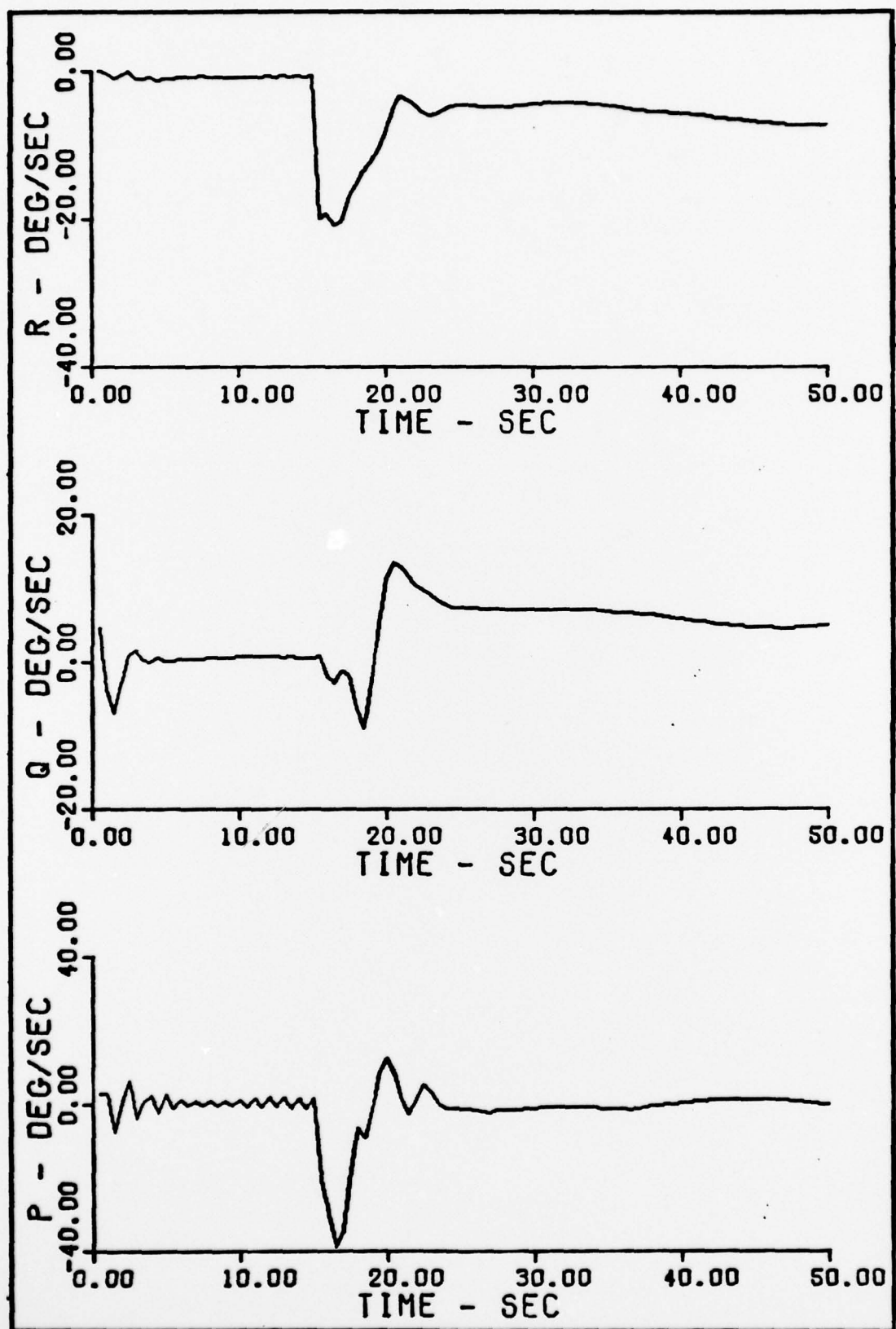


Fig. N-1 p, q, and r vs. time, $\alpha = 19$ deg, $\beta = 4$ deg,
 $r = -30$ deg/sec at $t = 15$ sec

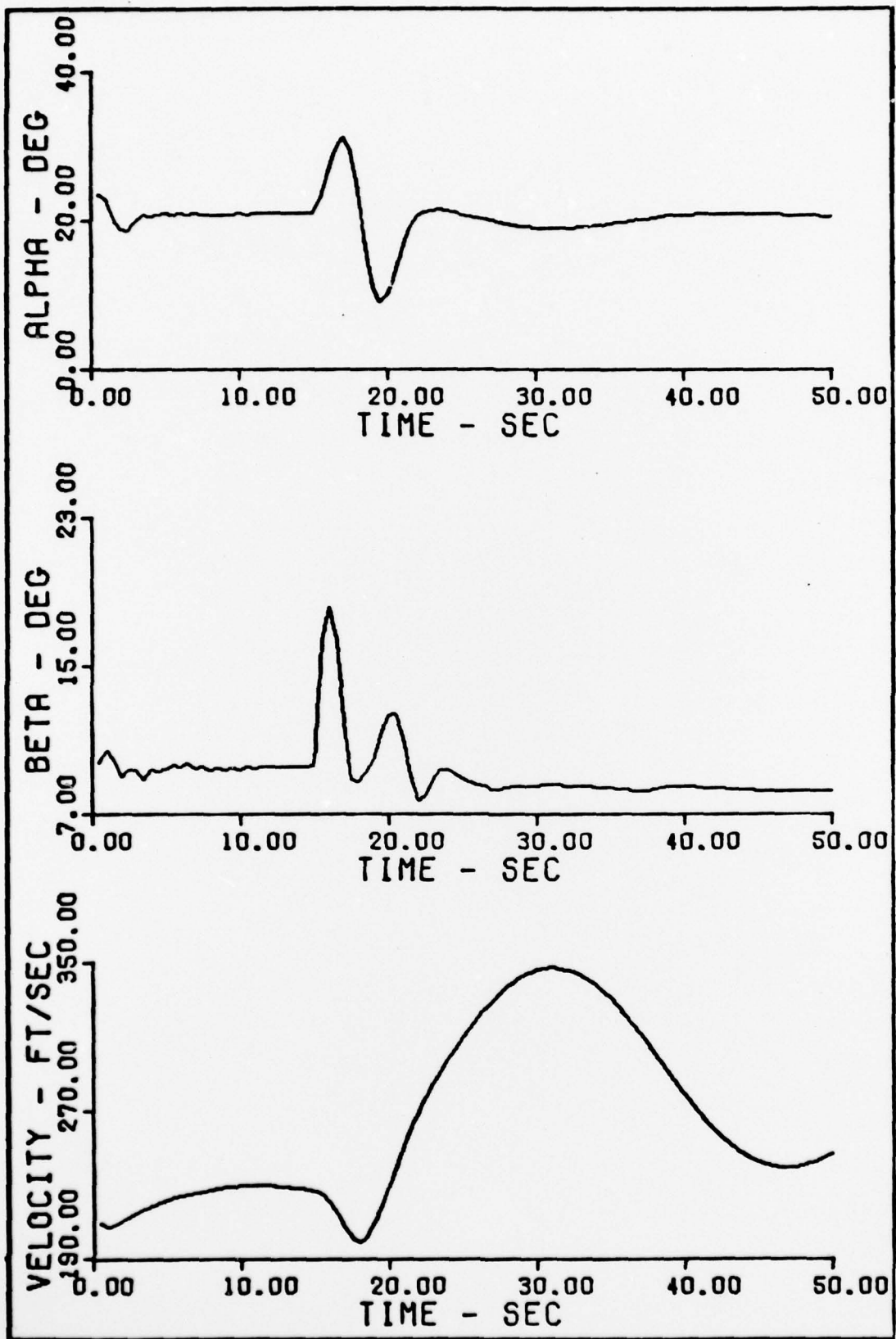


Fig. N-2 α , β , and Velocity vs. time, $\alpha = 19$ deg,
 $\beta = 4$ deg, $r = -30$ deg/sec at $t = 15$ sec

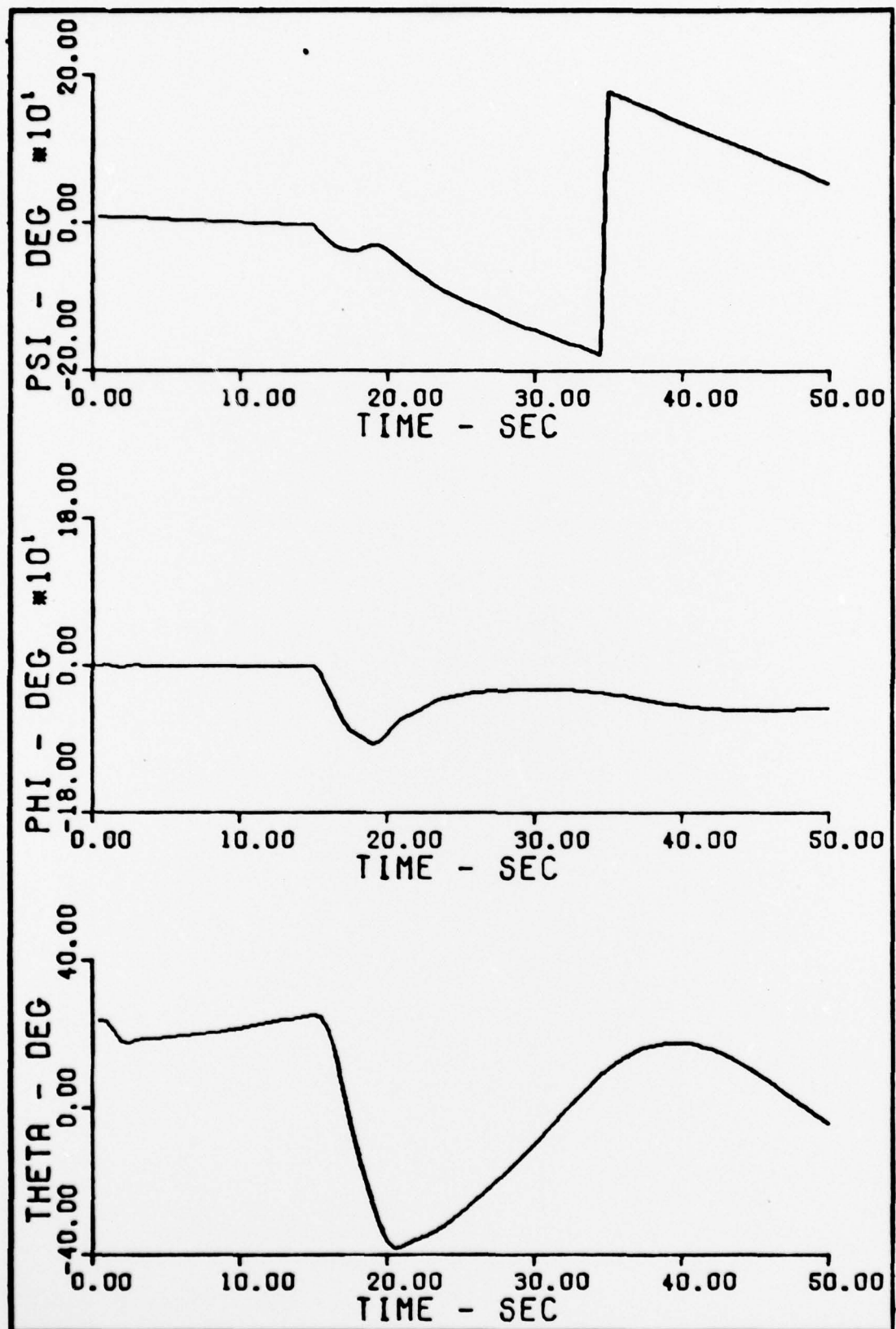


Fig. N-3 θ , ϕ , and ψ vs. time, $\alpha = 19$ deg, $\beta = 4$ deg,
 $r = -30$ deg/sec at $t = 15$ sec

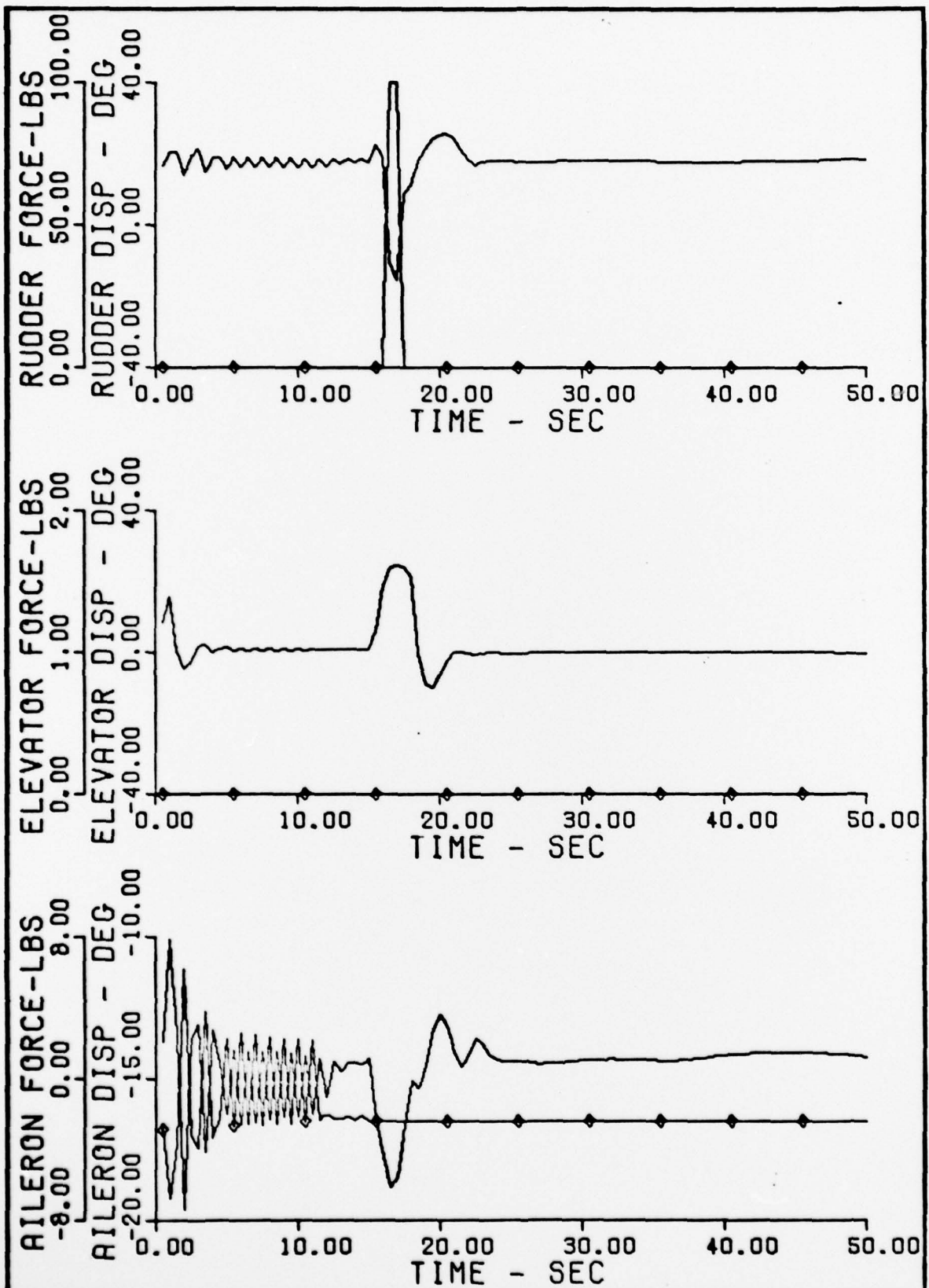


Fig. N-4 Control Forces and Deflections vs. time, $\alpha = 19$ deg,
 $\beta = 4$ deg, $r = -30$ deg/sec at $t = 15$ sec

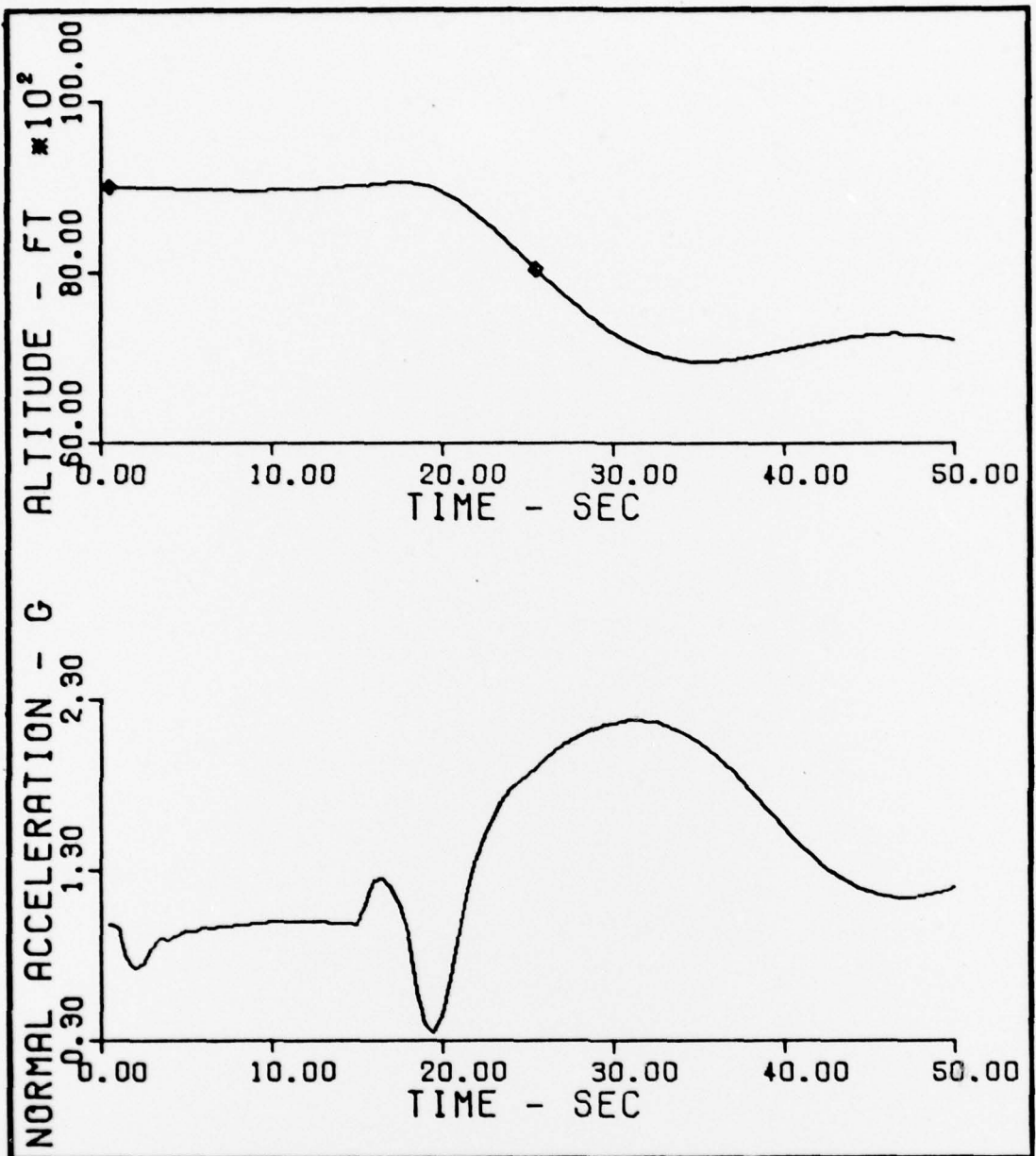


Fig. N-5 N_z and Altitude vs. time, $\alpha = 19$ deg, $\delta = 4$ deg,
 $r_z = -30$ deg/sec at $t = 15$ sec

Vita

Eric B. House II was born in Portland, Maine in November 1947. He graduated from the Georgia Institute of Technology in June 1970 and was awarded the degree of Bachelor of Aerospace Engineering. He was commissioned a 2nd Lt through AFROTC. His initial assignment was to Undergraduate Pilot Training at Laughlin AFB, Texas. He received his wings in November 1971, and was assigned to the 357th Tactical Fighter Squadron, Davis-Monthan AFB, Arizona, where he flew the T-33. His last assignment prior to reporting to AFIT in September 1976 was to Craig AFB, Alabama. While at Craig AFB, he was a T-38 Instructor Pilot, and his duties included Squadron Executive Officer for the 52nd Flying Training Squadron and Wing Flying Safety Officer.

Permanent Address: 4822 Brenda Dr.
Orlando, FL 32806

UNCLASSIFIED

SECURITY CLASSIFICATION OF THIS PAGE (When Data Entered)

REPORT DOCUMENTATION PAGE		READ INSTRUCTIONS BEFORE COMPLETING FORM
1. REPORT NUMBER AFIT/GAE/AA/78-M	2. GOVT ACCESSION NO.	3. RECIPIENT'S CATALOG NUMBER
4. TITLE (and Subtitle) INVESTIGATION OF THE YF-16 IN HIGH ANGLE OF ATTACK ASYMMETRIC FLIGHT		5. TYPE OF REPORT & PERIOD COVERED MS Thesis
7. AUTHOR(s) Eric B. House II Captain USAF		6. PERFORMING ORG. REPORT NUMBER
9. PERFORMING ORGANIZATION NAME AND ADDRESS Air Force Institute of Technology (AFIT-EN) Wright-Patterson AFB, Ohio 45433		10. PROGRAM ELEMENT, PROJECT, TASK AREA & WORK UNIT NUMBERS
11. CONTROLLING OFFICE NAME AND ADDRESS		12. REPORT DATE March 1978
		13. NUMBER OF PAGES 149
14. MONITORING AGENCY NAME & ADDRESS (if different from Controlling Office)		15. SECURITY CLASS. (of this report) Unclassified
		15a. DECLASSIFICATION DOWNGRADING SCHEDULE
16. DISTRIBUTION STATEMENT (of this Report) Approved for public release; distribution unlimited.		
17. DISTRIBUTION STATEMENT (of the abstract entered in Block 20, if different from Report)		
18. SUPPLEMENTARY NOTES Approved for public release; IAW AFM 190-11 <i>Jerral B. Guess</i> Jerral B. Guess, Captain, USAF Director of Information		
19. KEY WORDS (Continue on reverse side if necessary and identify by block number) Stability Asymmetric Flight Departure Modes		
20. ABSTRACT (Continue on reverse side if necessary and identify by block number) A study was made of the theoretical departure modes of the YF-16 due to pitch and yaw perturbations from asymmetrical rectilinear flight. An alpha-beta control boundary was developed, and within that boundary perturbations of 20 deg/sec and 30 deg/sec were introduced. The areas of uncontrolled motions were mapped out and the motions were categorized. Three types of motions were identified: erect spins, inverted spins, and rolling departures. For yaw perturbations only, a simple controller was mod-		

UNCLASSIFIED

SECURITY CLASSIFICATION OF THIS PAGE(*When Data Entered*)

elled which had as its inputs alpha, beta, and yaw rate. The controller prevented the aircraft from departing controlled flight. Time traces of the various departure modes and the effects of including a departure controller are presented in the appendices.

UNCLASSIFIED

SECURITY CLASSIFICATION OF THIS PAGE(*When Data Entered*)